
Doctoral Dissertations

Student Theses and Dissertations

Fall 2019

Investigating the performance of high viscosity friction reducers used for proppant transport during hydraulic fracturing

Mohammed Salem Ba Geri

Follow this and additional works at: https://scholarsmine.mst.edu/doctoral_dissertations

 Part of the [Petroleum Engineering Commons](#)

Department: Geosciences and Geological and Petroleum Engineering

Recommended Citation

Ba Geri, Mohammed Salem, "Investigating the performance of high viscosity friction reducers used for proppant transport during hydraulic fracturing" (2019). *Doctoral Dissertations*. 2827.
https://scholarsmine.mst.edu/doctoral_dissertations/2827

This thesis is brought to you by Scholars' Mine, a service of the Missouri S&T Library and Learning Resources. This work is protected by U. S. Copyright Law. Unauthorized use including reproduction for redistribution requires the permission of the copyright holder. For more information, please contact scholarsmine@mst.edu.

INVESTIGATING THE PERFORMANCE OF HIGH VISCOSITY FRICTION
REDUCERS USED FOR PROPPANT TRANSPORT DURING HYDRAULIC
FRACTURING

by

MOHAMMED SALEM BA GERI

A DISSERTATION

Presented to the Faculty of the Graduate School of the
MISSOURI UNIVERSITY OF SCIENCE AND TECHNOLOGY

In Partial Fulfillment of the Requirements for the Degree

DOCTOR OF PHILOSOPHY

in

PETROLEUM ENGINEERING

2019

Approved by:

Ralph Flori, Advisor
Mingzhen Wei
David Rogers
Kelly Liu
Vamegh Rasouli

© 2019

Mohammed Salem Ba Geri

All Rights Reserved

PUBLICATION DISSERTATION OPTION

This dissertation consists of the following six articles, formatted in the style used by the Missouri University of Science and Technology:

Paper I: Pages 5-34 have been published in SPE OnePetro.

Paper II: Pages 35-64 have been published in SPE OnePetro.

Paper III: Pages 65-92 have been published in SPE OnePetro.

Paper IV: Pages 93-123 have been published in SPE OnePetro.

Paper V: Pages 124-150 have been published in SPE OnePetro.

Paper VI: Pages 151-171 have been published in SPE OnePetro.

ABSTRACT

Over the last few recent years, high viscosity friction reducers (HVFRs) have been successfully used in the oil and gas industry across all premier shale plays in North America including Permian, Bakken, and Eagle Ford. However, selecting the most suitable fracture fluid system plays an essential role in proppant transport and minimizing or eliminating formation damage.

This study investigates the influence of the use of produced water on the rheological behavior of HVFRs compared to a traditional linear guar gel. Experimental rheological characterization was studied to investigate the viscoelastic property of HVFRs on proppant transport. In addition, the successful implication of utilizing HVFRs in the Wolfcamp formation, in the Permian Basin was discussed. This study also provides a full comparative study of viscosity and elastic modulus between HVFRs and among fracturing fluids such as xanthan, polyacrylamide-based emulsion polymer, and guar.

The research findings were analyzed to reach conclusions on how HVFRs can be an alternative fracture fluid system within many unconventional reservoirs. Compared to the traditional hydraulic fracture fluid system, the research shows the many potential advantages that HVFR fluids offer, including superior proppant transport capability, almost 100% retained conductivity, around 30% cost reduction, and logistics such as minimizing chemical usage by 50% and the ability to stoner operation equipment on location. Finally, this comprehensive investigation addresses up-to-date of using HVFRs challenges and emphasizes necessities for using HVFRs in high TDS fluids.

ACKNOWLEDGMENTS

First and foremost, I would like to thank Allah for giving me the strength, and opportunity to undertake this accomplished satisfactorily.

I would like to express my sincere gratitude to my advisor Dr. Ralph Flori for his guidance, patience, encouragement, and support during my Ph.D. study. I would also like to thank Dr. David Rogers, Dr. Mingzhen Wei, Dr. Kelly Liu, Dr. Steven Hilgedick and Dr. Vamegh Rasouli for their great effort, assistant, and serving on my Ph.D. committee.

Equally, I would like to express my appreciation to the police department at Missouri S&T for their unlimited support and creative environment. Million thanks go to Chief Doug Roberts, Assistant Chief Oscar Kemp, Sergeant Bryan Fox and all the Sergeants, officers, guards, and CSOs team.

Many thanks to my sponsor, Al sheikh Eng'r Abdullah Ahmed Bugshan, Chief Executive Officer of Hadramout Establishment for Human Development for sponsoring my Ph.D. I would also like to acknowledge the BJ Services; U.S. Silica and CoilChem LLC that provided all the necessary materials for this research. My further appreciation goes to Jerry. Noles, Sangjoon Kim and CoilChem team for there unaltime assistant during this acadimec journey.

The deepest gratefulness goes to all my friends for encouraging, and propelling me to endeavor to achieve my goals.

Last but not least, my cordial gratitude, my precious and my love goes to my parents, my grandmother my beloved sisters, brothers, nephews, nieces, brother's in-law, sisters' in-law and my sweet heart my wife, thanks all for your continued support.

TABLE OF CONTENTS

	Page
PUBLICATION DISSERTATION OPTION	iii
ABSTRACT	iv
ACKNOWLEDGMENTS	v
LIST OF ILLUSTRATIONS	xv
LIST OF TABLES	xx
NOMENCLATURE	xxii
 SECTION	
1. INTRODUCTION	1
2. RESEARCH OBJECTIVES	3
 PAPER	
I. A CRITICAL REVIEW OF HIGH-VISCOSITY FRICTION REDUCERS APPLICATIONS AS AN ALTERNATIVE HUDRAULIC FRACTURING FLUIDS SYSTEM	5
ABSTRACT	5
1. INTRODUCTION	6
2. DESCRIPTION OF FRICTION REDUCERS AND HIGH-VISCOUS FRICTION REDUCERS	9
3. LABORATORY AND FIELD STUDIES USING HVFR	13
3.1. DATA ANALYSIS OF USING HVFRS AT FIELD AND LAB CONDITIONS	13
3.2. FRICTION REDUCER AS ADDITIVES VS. AS A HVFR FRACTURE FLUID.	14
3.3. SCREENING CRITERIA GUIDELINES FOR HVFRS.	18

4. CONDUCTIVITY PROFILE.....	19
5. BREAKABILITY PROFILE	20
6. PRODUCED WATER WITH HVFRS	23
7. ECONOMIC ANALYSIS	26
8. CONCLUSIONS	29
REFERENCES.....	30
II. INVESTIGATE THE RHEOLOGICAL BEHAVIOR OF HIGH VISCOSITY FRICTION REDUCER FRACTURE FLUID AND ITS IMPACT ON PROPPANT STATIC SETTLING VELOCITY	35
ABSTRACT	35
1. INTRODUCTION.....	37
2. PROPPANT STATIC SETTLING VELOCITY IN HYDRAULIC FRACTURING	39
2.1. PARTICLE SHEAR RATE ($\dot{\gamma}$)	40
2.2. APPARENT SHEAR VISCOSITY (μ_a)	40
2.3. WEISSENBERG NUMBER (Wi).....	40
2.4. ELASTICITY TO VISCOSITY RATIO (λ_e/ν).....	41
2.5. FORCES INFLUENCED PARTICLES SETTLING VELOCITY	41
3. EXPERIMENT DESCRIPTION.....	42
3.1. MATERIALS.....	42
3.1.1. Hydraulic Fracturing Fluids.	42
3.1.2. Preparing Fracturing Fluids.....	43
3.1.3. Proppant Sizes.	43
3.1.4. Rheometer.	43
3.2. SETTLING VELOCITY IN UNCONFINED FRACTURE SETUP	43

3.3. RHEOLOGICAL CHARACTERIZATION OF THE HVFRS	44
3.3.1. Viscosity Profile Measurement.	44
3.3.2. Elasticity Profile Measurement.	44
3.3.3. Thermal Stability Measurement.	44
3.3.4. Static Settling Velocity Measurement.....	44
4. RESULTS AND DISCUSSION	45
4.1. VISCOSITY MEASUREMENT RESULTS	45
4.2. ELASTICITY MEASUREMENT RESULTS.....	48
4.2.1. Normal Stress Measurements.....	50
4.3. THERMAL STABILITY MEASUREMENT RESULTS.....	52
4.4. SETTLING VELOCITY MEASUREMENT RESULTS.....	53
4.4.1. Qualitative Multi-Particle Static Settling Velocity.	53
4.4.2. Quantitative Single Particle Static Settling Velocity.	55
4.4.2.1. Proppant size effect on static settling velocity.....	55
4.4.2.2. Effect of elasticity and viscosity properties on settling velocity.	56
5. COST ANALYSIS	60
6. CONCLUSIONS	61
REFERENCES	62
III. STATIC PROPPANT SETTLING VELOCITY CHARACTERISTICS IN HIGH-VISCOSITY FRICTION REDUCERS FLUIDS FOR UNCONFINED AND CONFINED FRACTURES	65
ABSTRACT	65
1. INTRODUCTION.....	66
2. PROPPANT STATIC SETTLING VELOCITY	69

2.1. WALL EFFECT (F_w)	69
2.2. PARTICLE SHEAR RATE ($\dot{\gamma}$)	69
2.3. ELASTICITY TO VISCOSITY RATIO (λ_e/ν).....	70
2.4. FORCES INFLUENCED PARTICLES SETTLING VELOCITY	71
3. EXPERIMENT DESCRIPTION.....	72
3.1. MATERIALS.....	72
3.1.1. Hydraulic Fracturing Fluids.	72
3.1.2. Preparing Fracturing Fluids.....	72
3.1.3. Proppant Sizes.....	72
3.1.4. Rheometer.	72
3.2. EXPERIMENT SETUP	72
3.2.1 Unconfined Fracture Wall Experiments.....	72
3.2.2 Confined Fracture Wall Experiments.....	73
3.3. EXPERIMENT PROCEDURES	75
3.3.1. Viscosity Rheological Characterization of the HVFRs.....	75
3.3.1.1. Viscosity profile measurement	75
3.3.1.2. Elasticity profile measurement.	75
3.3.1.3. Static settling velocity measurement.	75
3.3.2. Static Settling Velocity Calculations Based on Power Law Parameters (K, n)	76
4. RESULTS AND DISCUSSION	77
4.1. VISCOSITY MEASUREMENT RESULTS.....	77
4.2. ELASTICITY MEASUREMENT RESULTS.....	78
4.3. SETTLING VELOCITY MEASUREMENT RESULTS.....	81

4.4. PROPPANT SETTLING VELOCITY PERFORMANCE IN UNCONFINED FRACTURE WALL.....	81
4.5. PROPPANT SETTLING VELOCITY PERFORMANCE IN CONFINED FRACTURE WALL.....	81
4.6. WALL EFFECT ON STATIC SETTLING VELOCITY.....	84
4.7. EFFECT OF VISCOSITY AND ELASTICITY OF HFVR ON PROPPANT SETTLING VELOCITY	85
4.8. EFFECT OF ELASTICITY TO VISCOSITY RATIO ($\Delta E/Y$).....	87
5. COST ANALYSIS.....	88
REFERENCES.....	90
IV. INVESTIGATE PROPPANT TRANSPORT WITH VARYING PERFORATION DENSITY AND ITS IMPACT ON PROPPANT DUNE DEVELOPMENT INSIDE HYDRAULIC FRACTURES.....	93
ABSTRACT	93
1. INTRODUCTION.....	94
2. EXPERIMENT DESCRIPTION.....	97
2.1. EXPERIMENT MATERIALS	97
2.2. FRACTURE MODEL SETUP	98
2.3. EXPERIMENT PROCEDURE	99
2.4. EXPERIMENT ANALYSIS APPROACHES	101
2.4.1. Equilibrium Dune Level (EDL)	101
2.4.2. Proppant Dune Level Development (PDL)	101
2.4.3. Equilibrium Dune Length (EDX).....	101
2.4.4. Pressure Losses Calculations.....	101
3. RESULTS AND ANALYSIS	102
3.1. NUMBER OF PERFORATION EFFECT	102

3.2. PERFORATION OPENING SIZE EFFECT	105
3.3. SHEAR RATE EFFECT	107
3.4. FRACTURE ORIENTATION EFFECT	110
3.5. PROPPANT SIZE DISTRIBUTION EFFECT	113
4. DISCUSSION	116
4.1. EFFECT OF PRESSURE LOSS ALONG THE FRACTURE SLOT ON PROPPANT TRANSPORT PERFORMANCE.....	116
4.2. MECHANISMS OF PROPPANT TRANSPORT	117
4.2.1. Stage 1: Hindered and Free Settling.....	117
4.2.2. Stage 2: Saltation.....	117
4.2.3. Stage 3: Suspension, Rolling, and Swirl at Inlet	118
4.2.4. Stage 4: Saltation, Rolling, and Swirl at Inlet	118
4.2.5. Thermal Stability Measurement.	119
4.2.6. Static Settling Velocity Measurement.	119
5. CONCLUSIONS	120
REFERENCES.....	121
V. VISCOELASTIC CHARACTERIZATION EFFECT OF HIGH- VISCOSITY FRICTION REDUCERS AND PROPPANT TRANSPORT PERFORMANCE IN HIGH-TDS ENVIRONMENT	124
ABSTRACT	124
1. INTRODUCTION.....	125
1.1. PRODUCED WATER IN USA BASINS	130
2. EXPERIMENT DESCRIPTION.....	131
2.1. EXPERIMENT MATERIALS	131
2.1.1. Fracturing Fluids.	131

2.1.2. Frac Sand and Dosage.....	132
2.2. MEASUREMENTS OF RHEOLOGICAL PROPERTY.....	132
2.2.1. Friction Reducers Preparation for Rheological Property.	132
2.2.2. Fracturing Fluid Viscosity Measurement.	133
2.2.3. Elasticity Characterization (Elastic Modulus, G').	133
2.2.4. Friction Reducers Preparation for Elasticity Property.	133
2.2.5. Elastic Modulus Measurement.	133
2.3. THE SETTLING RATE MEASUREMENT OF FRAC SAND IN HVFR FRACTURING FLUID.....	134
2.3.1. HVFR Fracturing Fluid Preparation.....	134
2.3.2. Test Method on Frac Sand Settlement Rate.	134
3. RESULTS AND ANALYSIS	134
3.1. THE VISCOSITY PROFILES OF VARIOUS FRICTION REDUCERS IN DI WATER, 2 WT% KCL, AND 10 LBS. BRINE (SATURATED NACL SOLUTION (TDS: 347,000 PPM))	134
3.2. THE N' AND K' VALUES OF VARIOUS FRICTION REDUCERS IN DI WATER, 2 WT% KCL, AND 10 LBS. BRINE (SATURATED NACL SOLUTION (TDS: 347,000 PPM))	137
3.3. THE ELASTIC MODULUS COMPARISON OF VARIOUS FRICTION REDUCERS IN DI WATER AND 10 LBS. BRINE SOLUTION (TDS:347,000PPM).....	137
3.4. PROPPANT SETTLING RATE RESULT	139
3.5. HVFR ELASTIC MODULUS CHARACTERISTICS BY AMPLITUDE, FREQUENCY, FLUID TYPE, AND TEMPERATURE	141
3.6. HVFR ELASTIC MODULUS PROFILES IN DI WATER & 10 LBS. BRINE (TDS: 347,000 PPM).....	143
3.7. HVFR ELASTIC MODULUS PROFILES BY TEMPERATURE	144
3.8. FIELD CASE STUDY.....	144

4. DISCUSSION THE POTENTIAL OF FORMATION DAMAGE	145
5. CONCLUSIONS	147
REFERENCES	148
VI. A COMPREHENSIVE REVIEW OF FORMATION DAMAGE CAUSED BY HIGH-VISCOSITY FRICTION REDUCERS: WOLFCAMP CASE STUDY.....	151
ABSTRACT	151
1. INTRODUCTION.....	152
2. FORMATION DAMAGE MECHANISMS	155
3. WHY HIGH VISCOSITY FRICTION REDUCERS?	157
4. EXPERIMENTAL DESCRIPTION	158
4.1. EXPERIMENTAL MATERIALS	158
4.1.1. Experimental Materials.	158
4.1.2. Proppant.....	158
5. MEASUREMENTS OF RHEOLOGICAL PROPERTY	160
5.1. SHEAR VISCOSITY CHARACTERIZATION (K, N)	160
5.2. SHEAR ELASTICITY CHARACTERIZATION (ELASTIC MODULUS, G').....	160
5.3. FRACTURE CONDUCTIVITY EXPERIMENT PROCEDURE	160
6. RESULTS AND ANALYSIS	161
6.1. RHEOLOGICAL CHARACTERIZATION OF THE HVFRS.....	161
6.1.1. Viscosity Profile Measurement.	161
6.1.2. Elasticity Profile Measurment.	162

6.2. CONDUCTIVITY AND PERMEABILITY MEASUREMENT ON BASELINE, 0.5 GPT, AND 2.5 GPT.	163
6.3. CASE STUDY: WOLFCAMP FORMATION, REEVES COUNTY, TX.	165
6.3.1. Geological Background.	165
6.3.2. Fracture Design and Execution.	165
7. CONCLUSIONS	167
REFERENCES	168
SECTION	
3. CONCLUSIONS	172
REFERENCES	173
VITA	174

LIST OF ILLUSTRATIONS

PAPER I	Page
Figure 1. Visualization of proppant transport using friction reducer and high-viscosity friction reducers.....	8
Figure 2 Friction reducers types.	9
Figure 3. Chemical structure of various Friction Reduction (FR) agents and a comparison of friction pressure for water containing only 2% KCl vs. water containing 2% KCl and 2 gallons per 1000 gallons (FR) and 10# Guar pumped down 4 ½” 11.5# 4” ID casing..	11
Figure 4. Field case studies distribution of using HVFRs in North America.	14
Figure 5. Box plots of temperature ranges of HVFRs in the lab measurements and field application.	15
Figure 6. Maximum loading of HVFRs applied in the field.....	15
Figure 7. Box plots of HVFR concentration ranges in the lab measurements and field application.....	16
Figure 8. Box plots of concentration ranges of FR and HVFRs.....	16
Figure 9. Box plots of viscosity ranges of HVFRs at high shear rate 511 S-1.....	17
Figure 10. Box plots of viscosity ranges of HVFRs at low shear rate 70 S-1.....	18
Figure 11. Chemical cost reduction of using HVFRs from different case studies.	27
Figure 12. Production improvement of using HVFRs from different case studies.	28
Figure 13. Chemical cost comparison for standard Bakken system	29
 PAPER II	
Figure 1. Schematic of fracture setup for unconfined fluids.	43
Figure 2. Effect of HVFR (left) and linear gel (right) concentrations as a function of shear rate.....	46
Figure 3. Viscosity as a function of concentration of HVFRs (left) and linear gel (right) at low shear rates.	47

Figure 4. Elastic modulus and storage modulus as a function for HVFR-2 at different concentration.	49
Figure 5. Elastic modulus and storage modulus as a function of angular frequency for linear gel at different concentrations 20ppt and 40ppt.	50
Figure 6. Relaxation time as a function of concentration of HVFR-1, HVFR-2, and HVFR-3 (left) and linear gel (right).	50
Figure 7. Effect of HVFR 2 concentration as a function in normal stress profile.	51
Figure 8. Effect of HVFR 2 concentration as a function in normal stress profile.	51
Figure 9. Thermal stability of viscosity as a function of shear rate of HVFR-2 (left) and linear gel (right).	52
Figure 10. Thermal stability of viscosity as a function of shear rate of HVFR-2 (left) and linear gel (right).	53
Figure 11. Multi-static measurement for proppant settling time using HVFR-2 (2gpt)...	54
Figure 12. Multi-static measurement for proppant settling time using HVFR-2 (4gpt)...	55
Figure 13. Multi-static measurement for proppant settling time using liner gel (20 ppt)..	55
Figure 14. Effect of proppant settling velocity in HVFR-2 gpt vs. linear gel-20 ppt fracture fluids.	56
Figure 15. Viscosity as a function of shear rate for HVFR-2 loading 2 gpt (left) and linear gel loading 20 ppt (right).	57
Figure 16. Calculated elastic/viscous ratio as a function of shear rate for HVFR-2, 2 gpt and linear gel – 20 ppt.....	59
 PAPER III	
Figure 1. Schematic of fracture setup for unconfined fluids.	73
Figure 2. Schematic of fracture setup for confined fluids.	74
Figure 3. Schematic of the experimental fracture cell for measuring inclination angle effect.	75
Figure 4. Effect of HVFR-3 concentration as a function in viscosity shear profile.	78
Figure 5. Elastic modulus G' and storage modulus G'' as a function of HVFR-3 concentrations.	79

Figure 6. Effect of HVFR 3 concentration as a function in Normal stress profile.	80
Figure 7. Effect of proppant settling velocity in HVFR-3 gpt vs. slickwater fracture fluids.	82
Figure 8. Settling velocity of HVFR vs. slickwater in vertical fractures by 90 angle vs. inclined fractures angles 60 and 45 degree in confined fractures of 9 mm fracture width.	83
Figure 9. Settling velocity reduction in slickwater versus HVFR-3 loading 2 in different fracture orientation.	84
Figure 10. Wall factors as a function of particle diameter to wall spacing in the HVFR-3 loading 2 gpt.	85
Figure 11. Viscosity as a function of shear rate for HVFR-3 loading 2gpt.	86
Figure 12. Velocity ratio as a function of proppant diameter in HVFR-3 loading 2 gpt.	87
Figure 13. Calculated elastic/viscous ratio as a function of shear rate for HVFR-3 loading 2 gpt.	88

PAPER IV

Figure 1. Schematic schematic of the experimental proppant transport evaluation system.	99
Figure 2. Effect of number of perforations at first FPV.	103
Figure 3. Effect of number of perforations on EDL.	104
Figure 4. Effect of number of perforations on fracture propped area.	104
Figure 5. Real picture of experiment results shown number of perforation effect on proppant transport, top-perf (left), bottom-perf (middle) and multi-perf. (right).	104
Figure 6. Effect of perforation opening size at first FPV.	105
Figure 7. Effect of perforation opening size on EDL.	106
Figure 8. Real picture of experiment results shown perforation opening size effect on proppant transport, perf opening 100% (left), perf opening 60% (middle) and perf opening 40% (right).	106
Figure 9. Effect of fracture shear rate at first FPV.	107

Figure 10. Real picture of experiment results shown shear rate effect on proppant transport, high shear rate (left) and low shear rate (right).	108
Figure 11. Effect of high (60s – 1) and low (35s – 1) shear rates on EDL.	109
Figure 12. Effect of shear rate on EDL.	109
Figure 13. Effect of shear rate on fracture propped area.	110
Figure 14. Effect of fracture orientation (vertical vs. inclined) at first FPV.	111
Figure 15. Effect of fracture orientation (vertical vs. inclined) on EDL.	111
Figure 16. Effect of fracture orientation (vertical vs. inclined) on fracture propped area.	112
Figure 17. Real picture of experiment results shown perforation opening size effect on proppant transport, inclined fracture (left), and vertical fracture (right).	113
Figure 18. Effect of proppant size at first FPV.	114
Figure 19. Effect of proppant size on EDL.	114
Figure 20. Effect of proppant size on fracture propped area.	115
Figure 21. Real picture of experiment results shown proppant size effect on proppant transport, 100 mesh (left), 40/70 mesh (middle) and 20/40 mesh (right).	115
Figure 22. a and b pressure loss along fracture slot on shear rate (left) and shear rate effect on Fracture propped area (right).	116
 PAPER V	
Figure 1. The viscosity profile of various friction reducers in DI water	136
Figure 2. The viscosity profile of various friction reducers in 2wt% KCl solution.	136
Figure 3. The viscosity profile of various friction reducers in 10 lbs. brine.	136
Figure 4. Frac sand settling rate comparison with various HVFR dosage.	140
Figure 5. The elastic modulus measurement of HVFR, xanthan, emulsion polymer, and guar at 75, 150, and 250 °F in DI water (left) 10 lbs. brine solution (right).	141

Figure 6. The elastic modulus characteristic of HVFR by amplitude and frequency at room ambient.....	142
Figure 7. The elastic modulus characteristic of HVFR by fluids (DI water vs. 10 lbs. brine)	143
Figure 8. The elastic modulus characteristic of HVFR by temperature.	144
Figure 9. Hydraulic fracture treatment plot from Well-C using HVFRs.....	145
Figure 10. Conductivity and permeability on baseline, 0.5 gpt, and 2.5 gpt at 2,000 psi and 24 hr.....	147
 PAPER VI	
Figure 1. Classification of the common formation damage mechanisms	156
Figure 2. HVFR viscosity profile with various dosage in fresh water.....	162
Figure 3. HVFR elastic property with various dosage in fresh water.....	163
Figure 4. Conductivity and permeability on baseline, 0.5 gpt, and 2.5 gpt by pressure and time.....	164
Figure 5. Hydraulic fracture treatment plot from Well-H using HVFRs.....	166
Figure 6. HVFR dosage real time data.....	167

LIST OF TABLES

PAPER I	Page
Table 1. Summary of viscosity data of HVFRs reviewed in this paper.....	19
Table 2. High viscosity friction reducers concentration, gpt	19
Table 3. Fracture conductivity data of HVFRs reported in this paper.....	21
Table 4. Breakability data of HVFRs summarized in this paper.	22
Table 5. Chemical composition of produced water in Delaware basin	24
Table 6. Produced water TDS used with HVFRs.	25
Table 7. Stimulation summary of case study	29
PAPER II	
Table 1. Power law model equations and parameters (n, k) for HVFRs and linear gel. ..	47
Table 2. Weissenberg number calculation as a function of relaxation time and particle shear rate.	58
Table 3. Elastic/Viscous ratio $\lambda e/\nu$ calculations.....	59
Table 4. Stimulation summary of case study	60
PAPER III	
Table 1. Power law model equations and parameters (n, k) for HVFR-3.	78
Table 2. Particles shear rate calculations for HVFR.....	86
Table 3. Elastic/Viscous ratio $\lambda e/\nu$ calculations.....	89
PAPER IV	
Table 1. API/ISO properties of the tested US silica white sand proppants.	98
Table 2. List of experiments and parameters	100
Table 3. shows pressure losses effect at 1st FPV on EDL and Xf.....	117

Table 4. Four proppant transport mechanisms to reach the PDL.....	119
---	-----

PAPER V

Table 1. The molecular weight of friction reducers.....	132
---	-----

Table 2. The n' and K' values with viscosities reading of friction reducers in various fluids.....	138
--	-----

Table 3. The effect of dosage of HVFRs on proppant settling rate.	140
--	-----

PAPER VI

Table 1. Fracture damage categories	156
--	-----

Table 2. Proppant sieve analysis for baseline.	159
---	-----

Table 3. Proppant sieve analysis for 0.5 gpt.	159
--	-----

Table 4. Proppant sieve analysis for 2.5 gpt.	159
--	-----

Table 5. The regain percentage of 0.5 gpt and 2.5 gpt.....	165
--	-----

NOMENCLATURE

Symbol	Description
$\ddot{\gamma}$	particle shear rate
$\eta(\ddot{\gamma})$	Shear viscosity
$N_1(\dot{\gamma})$	First normal stress
μ_a	Apparent shear viscosity
W_i	Weissenberg number
λ	Relaxation time
$\lambda_{e/v}$	Elasticity to viscosity ratio
ρ_p	Particle density
ρ_f	Fluid density
C_D	Drag coefficient

1. INTRODUCTION

Hydraulic fracturing is the most efficient and effective technique enabling greater economic access for oil and gas production in unconventional shale gas plays. Increasing production and reserves from low-permeability hydrocarbon bearing rocks prerequisite stimulation treatment is required to make the fracturing process successfully and economically feasible. Transport of proppant into fractures that either hydraulically created or naturally existed should be fully understood. Proppant transport is influenced by a complex combination of parameters including particle size, density, fracture dimensions, base fluid rheological properties. Different types of fluids are used to enable the transport of proppant into the fractures. An important characteristic of fracturing fluid is to be compatible with reservoir fluids, should be cost effective, environmentally friendly, and cause less damage to formation and fracture conductivity.

Most of the fluids encountered in the industrial applications tend to have both the shear thinning and the viscoelastic properties. A shear-thinning characteristic indicates that the fluid viscosity decreases with the increasing shear rate. A viscoelastic fluid demonstrates both viscous and elastic behavior under deformation. In hydraulic fracturing, for effective proppant transport and to avoid their premature settling, hydraulic fracturing fluids are advised to have viscoelasticity (Acharya, 1988; Adrian, 2005). Therefore, knowledge of the particle settling behavior and the particle settling velocity in viscoelastic shear thinning fluids is indispensable to optimize the properties of these industrial fluids. Essentially, fluid selection and proppant placement play the main key in the hydraulic fracturing process (Ba Geri et al, 2019; Ellafi et al, 2019).

Several types of fracturing fluids have been applied, including the use of slickwater, linear gel, crosslinked in the USA basins. The success of a fluid selection process depends primarily on the length of the fracture and proppant distribution and placement in fracks. Thus, understanding fluid composition, ability to create fractures, the capability to carry and transport proppant deep into the fracture, easy to flow back with minimal damage effect through production from shale formation is the key a crucial successful fracking treatment.

Even though slickwater (water fracturing with few chemical additives) used to be one of the most common fracturing fluids, several concerns are still associated with its use, including usage of freshwater, high-cost operation, and environmental issues. Therefore, current practice in hydraulic fracturing is to use alternative fluid systems that are cost effective and have a less environmental impact, such as fluids which utilize high viscosity friction reducers (HVFRs), which typically are high molecular weight polyacrylamides. Moreover, the recent and rapid success of using HVFRs in hydraulic fracturing treatments is due to several advantages over other fracture fluids (e.g. linear gel), which include better proppant carrying capability, induce more complex fracture system network with higher fracture length, and overall lower costs due to fewer chemicals and less equipment on location.

2. RESEARCH OBJECTIVES

The ultimate goal of this project is to expand the horizon of understanding proppant transport using different fracture fluids in particular HVFRs in complex fracture system. Our new fracture model will be capable of achieving that goal. The new fracture model can be used to evaluate the impact of fracture geometry, half-length, injection pump rate, proppant type, size, & shape, proppant concentration, fluids viscosity, fluids elasticity leak-off, number of perforations, natural fracture angles, particle settling velocity, fracture wall roughness, width heterogeneity, and proppant distribution in the complex fracture network on the transport of the proppant through fractures using different fracture fluids. The specific objectives of this research therefore include:

- To provide a better understanding of the advanced technologies of using high viscosity friction reducer, including the capability of carrying proppant in hydraulic fracturing treatments. The goal also is to statistically analyze the main associated factors with HVFR such as concentration, temperature, viscosity, and breakability.
- This project investigated several major factors affect proppant settling velocity including viscosity measurement profiles, elasticity properties (Normal forces and relaxation time), and thermal stability profile.
- In addition, this work conducted laboratory work intensively to fill the knowledge gap. This study investigated three factors that could affect proppant settling velocity performance: proppant size, wall effect, and fracture orientation.

- This study was deeply investigated five factors that affect proppant transport performance: number of perforations, perforation opening size, slurry shear rate, fracture orientation, and proppant size distribution.
- This work will provide a comprehensive study of the effects of elasticity and shear viscosity on proppant settling velocity using HVFRs and linear gel in fresh water and produced water.
- A proper fracture lab slot will be upscaling to evaluate proppant transport performance using HVFRs to the field implementations.

PAPER**I. A CRITICAL REVIEW OF HIGH-VISCOSITY FRICTION REDUCERS
APPLICATIONS AS AN ALTERNATIVE HYDRAULIC FRACTURING
FLUIDS SYSTEM**

Mohammed Ba Geri, Abdulmohsin Imqam, and Ralph Flori

Department of Petroleum Engineering, Missouri University of Science and Technology,
Rolla, MO 65409

ABSTRACT

The primary purpose of using traditional friction reducers in stimulation treatments is to overcome the tubular drag while pumping at high flow rates. Hydraulic fracturing is the main technology used to produce hydrocarbon from extremely low permeability rock. Even though slickwater (water fracturing with few chemical additives) used to be one of the most common fracturing fluids, several concerns are still associated with its use, including usage of freshwater, high-cost operation, and environmental issues. Therefore, current practice in hydraulic fracturing is to use alternative fluid systems that are cost effective and have less environmental impact, such as fluids that utilize high-viscosity friction reducers (HVFRs), which typically are polyacrylamides with high molecular weight.

This paper carefully reviews and summarizes over 40 published papers, including experimental work, field case studies, and simulation work. This work summarizes the most recent improvements of using HVFRs, including the capability of carrying proppant,

reducing water and chemical requirements, compatibility with produced water, and environmental benefits in hydraulic fracturing treatments. A further goal is to gain insight into the effective design of HVFR-based fluid systems.

The findings of this study are analyzed from over 26 field case studies of many unconventional reservoirs. In comparing HVFRs to the traditional hydraulic fracture fluids system, the paper summarizes many potential advantages offered by HVFR fluids, including superior proppant transport capability, almost 100% retained conductivity, cost reduction, 50% reduction in chemical use by, less operating equipment on location, 30% less water consumption, and fewer environmental concerns. The study also reported that the common HVFR concentration used was 4 gpt. HVFRs were used in the field at temperature ranges from 120°F to 340°F. Finally, this work addresses up-to-date challenges and emphasizes necessities for using HVFRs as alternative fracture fluids.

1. INTRODUCTION

Hydraulic fracturing has been successfully implemented since its inception in 1947. To achieve commercial production from ultra-low permeability formation, development in fracturing fluids is the key factor for stimulation operations. Although a variety of fracturing fluids have been used to increase the productivity of unconventional reservoirs, low viscous (slickwater) and high viscous (crosslinkers/ linear gel) fluids still have some problems in terms of lower capability to carry proppant, creating formation damage, high-cost operation, and environmental concerns.

In recent years, the oil industry has adopted the use of high-viscosity friction reducers (HVFR's) in fracturing fluids due to several operational and economic reasons (Hu et al. 2018; Van Domelen et al. 2017; Motiee et al. 2016). Friction reducers are mostly long-chain polyacrylamide-based (PAM) polymers. Usually friction reducers are added to water-based fracturing fluids to hydrate “on the fly” as water in oil emulsions (Wu et al. 2013; Tomson et al. 2017). Most water-soluble polymeric friction reducers have high molecular weight (normally over 10 M) polymers Sun et al. (2011). The primary function of friction reducers is to change turbulent flow to laminar flow by reducing frictional loss by 70-80% while pumping fracturing fluids (Tomson et al. 2017; Sun et al. 2011; White and Mungal, 2008).

Both academic research and industrial implementation have demonstrated the success of friction reducers within and outside the oil industry Aften et al. (2014). Because of the ability of friction reducers to flocculate solids in liquid phase, PAM polymers have been used extensively in water treatment. In the oil and gas industry PAM has primarily been used in a variety of applications including enhanced oil recovery (EOR), acid gelling agents, clay control during drilling, and hydraulic fracturing. These applications require flexibility and simplicity of PAMs stability under harsh conditions such as high reservoir temperatures and high salinity waters (Ryles et al. 1986; StimLab 2012; Clark et al. 1976).

Research continues developing improved hydraulic fracturing fluids to lessen the problems associated with current fracturing fluids like guar-based gels and slickwater. Slickwater fracturing fluids have low concentrations of friction reducers, falling between 0.5 and 2 gallons per thousand gallon (gpt) (Rodvelt et al. 2015; Ifejika et al. 2017). HVFR fluids can replace slickwater by minimizing proppant pack damage and can carry the same

amount of proppant as linear gel or better with less formation damage. (Ba Geri et al. 2019b, Kunshin et al. 2018). Figure 1 shows that HVFRs can have better proppant transport capability along fractures compared to slickwater with friction reducer additives.

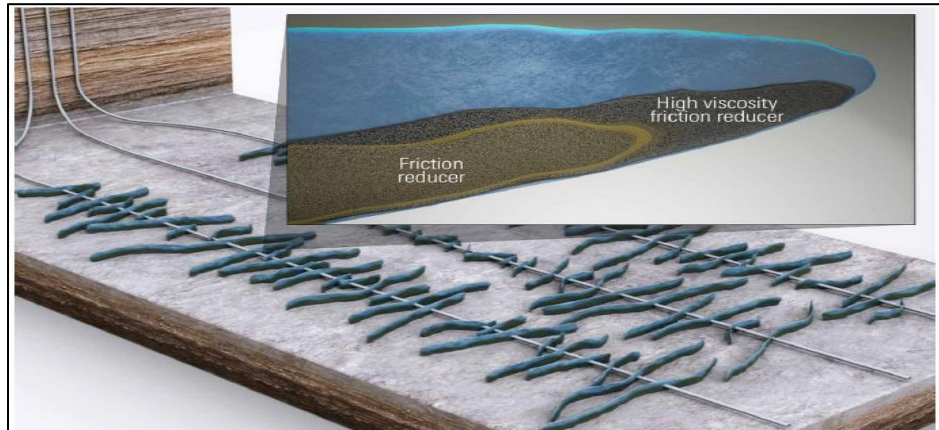


Figure 1. Visualization of proppant transport using friction reducer and high-viscosity friction reducers (slb.com/broadband).

The objectives of this critical review study are to provide better understanding of the advanced technologies of using high-viscosity friction reducers, including capability of carrying proppant, reducing water and chemical requirements, compatibility with produced water, and environmental benefits in hydraulic fracturing treatments. The goal also is to statistically analyze the main associated factors with HVFRs such as concentration, temperature, viscosity, and breakability.

2. DESCRIPTION OF FRICTION REDUCERS AND HIGH-VISCOUS FRICTION REDUCERS

Friction reducers are typically long-chain polyacrylamides (PAM) in dry powder and liquid forms that can be added in the concentration range from 0.5 to 2 gpt to water to make slickwater. PAMs for unconventional reservoirs can be classified into three main categories (see Figure 2): anionic, nonionic, and cationic Hashmi et al. (2014). They may also be classified as hydrophobic and amphoteric Tomson et al. (2017). An anionic nature for most friction reducers is obtained from 30% mole acrylic acid co-polymers. The maximum reduction of friction reducers can be obtained by dissolving the polymer into aqueous solution to become fully inverted before injected as fracturing fluid. Friction reducers have high dissolvability level in water, a high viscosity, and sufficient energy loss reduction.

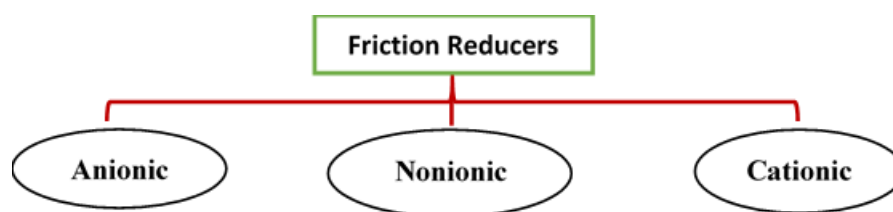


Figure 2. Friction reducers types.

The most common friction reducer is anionic due to its lower cost and better drag reduction. Chung et al. (2014). Water salinity and quality are the two main factors that determine the effectiveness of friction reducers. Drag reduction of friction reducers rely on their backbone flexibility and radius of gyration (molecular size). Drag reduction decreases by increasing the molecular weight or size. In freshwater, the friction reducers have large

radius of gyration, which increases in the friction reducers performance. The same amount of friction reducers in produced water has small gyration radius, so increased FR concentration is needed to attain the same drag reduction level in high TDS water (Chung et al. 2014, Rimassa et al. 2009; Shah et al. 2018). Lastly, less friction reduction can be provided by uncharged (non-ionic) friction reducers than charged ones (Ozuruigbo et al. 2014; Chung et al. 2014).

Using polymers in oil field applications has evolved and expanded from acid gelling agents, drilling operations, and EOR applications to fracturing fluid systems that are carefully designed to have optimum characteristics. To achieve these characteristics, different chemical structure forms have been developed to fit the designed purpose of each case. In addition, the chemistry of the water that is used in hydraulic fracturing treatments—and particularly its salinity—are two main factors considered during friction reducer selection. As presented in Figure 3, the most prevalent friction reducers used in the oil and gas industry are polyacrylamide- (PAM-) based polymers, acrylamido-methylpropane sulfonate polymer (AMPS), polyacrylic acid (PAAc), and hydrolyzed polyacrylamide (PHPA) Montgomery, (2013). Their structural forms are as shown in Figure 3.

There are also many forms of the friction reducer that can be delivered to the field application. The most popular forms are the liquid inverse emulsion and dried. In addition to these polymers, other types of friction reducers are viscoelastic surfactants, dispersion polymers, fibers, metal complexed surfactants, and various microscopic structures Aften et al. (2014).

The inclusion of a friction reducer is one of the main components of slickwater fracture fluids and other stimulation fluids. The primary function of friction reducers is changing turbulent flow to laminar flow, which can reduce frictional loss during pumping fracturing fluids up to 80%. Recently, high-viscosity friction reducers (HVFRs) have gaining popularity as drilling and hydraulic fracturing fluids because the HVFRs exhibit numerous advantages such as the following:

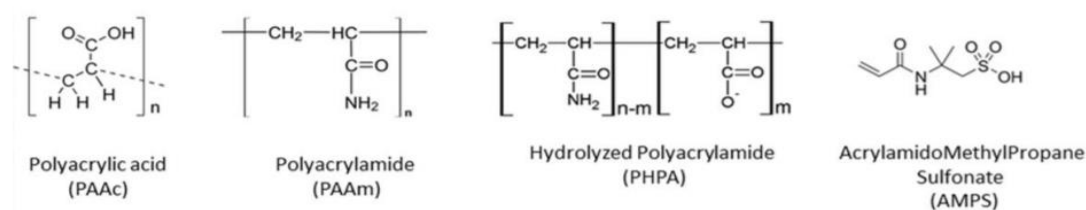


Figure 3. Chemical structure of various friction reduction (FR) agents and a comparison of friction pressure for water containing only 2% KCl vs. water containing 2% KCl and 2 gallons per 1000 gallons (FR) and 10# Guar pumped down 4 ½” 11.5# 4” ID casing (Montgomery, 2013).

- Reduced pipe friction during fracturing treatments
- High regain conductivities compared to linear and crosslinked gels
- Lower operational cost
 - Uses less water compared to conventional slickwater treatments,
 - Consumes 33-48% less chemicals
 - Requires less equipment on location
 - Requires less number of tanks trucks in the field
- More fracture complexity using a less viscous fluid system
- Better hydrocarbon production results compare to or greater than other fluids.

- Improved flexibility to design treatments that balance technical, economic, and operational goals
- Reduced freshwater, proppant, and equipment requirements compared with conventional fluid systems
- Minimized environmental footprint with selection of engineered additives
- Simplified operations by reduced screen out risks

In order to make a successful hydraulic fracturing treatment, the fracking fluid selection process is a significant step in these ultra-low permeability reservoirs. The ultimate purpose of the fracturing fluid is to induce a complex network fracture system and to have the capability of carrying proper amount of proppant deeply into the fractures. Essentially, fluid selection and proppant placement are key to the hydraulic fracturing process. The ultimate success of the fluid selection process depends primarily on the length of the fracture achieved and proppant distribution and placement in fracks. Thus, understanding fluid properties and performance such as its composition, ability to create fractures, ability to carry and transport proppant deep into the fracture, and ease to flowback with minimal damage through production from shale formations is the key to a crucial successful fracking fluid and treatment. Ideally, the HVFRs should have the following physical characterization to achieve the ultimate performance as fracturing fluids (Sareen et al. 2014; Ke et al. 2006; Carman et al. 2007; Aften et al. 2010):

1. The polymer should have good dispersion or solubility in various aqueous phases;
2. Compatible with other fracturing fluids additives e.g. clay stabilizer;
3. Should be less shear sensitive;

4. Quick to hydrate in fluid “on-the-fly”;
5. Compatible with high TDS and hardness;
6. Easy to break and clean up;
7. Good thermal stability; and
8. Low environmental impact.

3. LABORATORY AND FIELD STUDIES USING HVFR

This work analyzes data collected from more than 26 field case studies that implemented High-viscosity friction reducers in unconventional reservoirs. For example, in the Permian basin four different case studies were applied using HVFR successfully which represent 16% of case study distribution of using HVFRs in North America. The main findings of each case are highlighted in Figure 4.

3.1. DATA ANALYSIS OF USING HVFRS AT FIELD AND LAB CONDITIONS

Figure 5 shows the temperature ranges for lab and field conditions. HVFR’s were tested at minimum temperatures of 70°F in the lab and 140°F at field conditions. The reported data also showed that HVFR’s were tested at maximum temperature of 180°F in the lab and 335°F in field studies.

Figure 6 shows the HVFR concentration range used in hydraulic fracture treatment in different US basins (Van Domelen et al. 2017; Hu, et al. 2018). The collected data show that HVFR concentration ranged were from 2.5 gpt to 3.5 gpt.

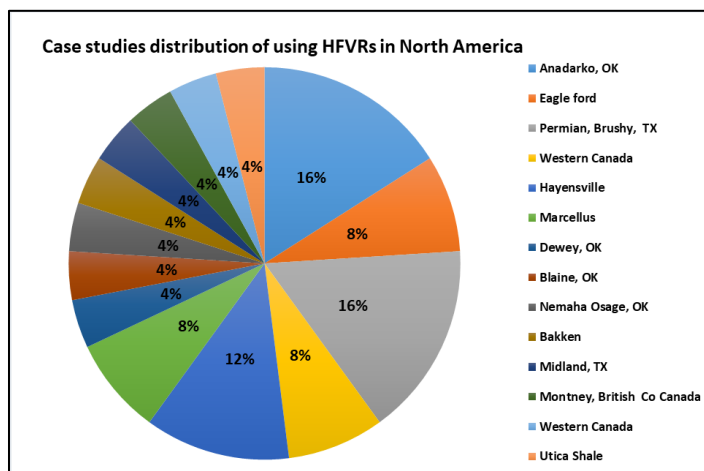


Figure 4. Field case studies distribution of using HFVRs in North America.

Figure 7 reports the concentration distributions of HFVRs in lab evaluation and field application. The lab test covers a wide HFVR concentration ranges from 1gpt to 10gpt, while the field applications have an HFVR concentration range between 0.5 gpt and 4 gpt.

3.2. FRICTION REDUCER AS ADDITIVES VS. AS A HFVR FRACTURE FLUID

Figure 8 presents the low concentrations of friction reducers used only as fluid additives versus their higher concentration used as a key ingredient in HFVR-based fracture fluids. Friction reducers as an additive cover a small range from 0.5 gpt to 2 gpt, while as HFVRs covered a large range from 1 gpt to 10 gpt.

Figure 9 reveals the viscosity ranges of HFVR fluids at high shear rate ($511s^{-1}$) corresponding to various concentrations of HFVR in the fluids. HFVR's at 8 gpt can have viscosities as high as 54 cp; whereas at low concentrations such as 2gpt of HFVR, the typical viscosity ranges were from 7 to 15 cp.

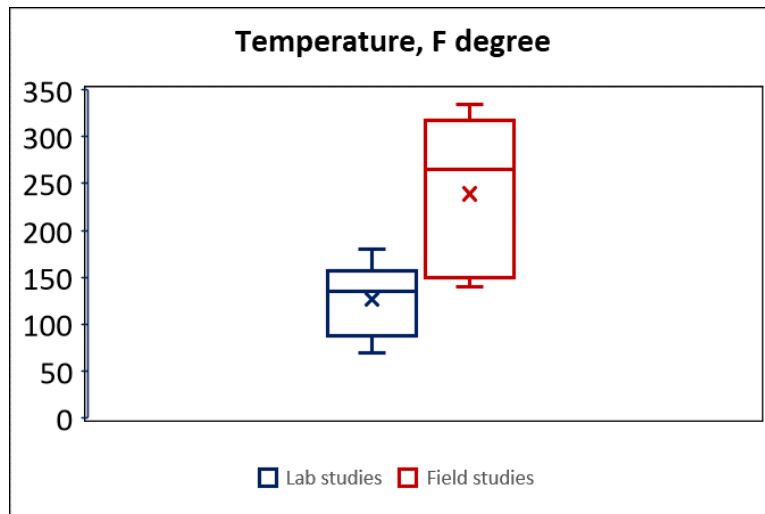


Figure 5. Box plots of temperature ranges of HVFRs in the lab measurements and field application.

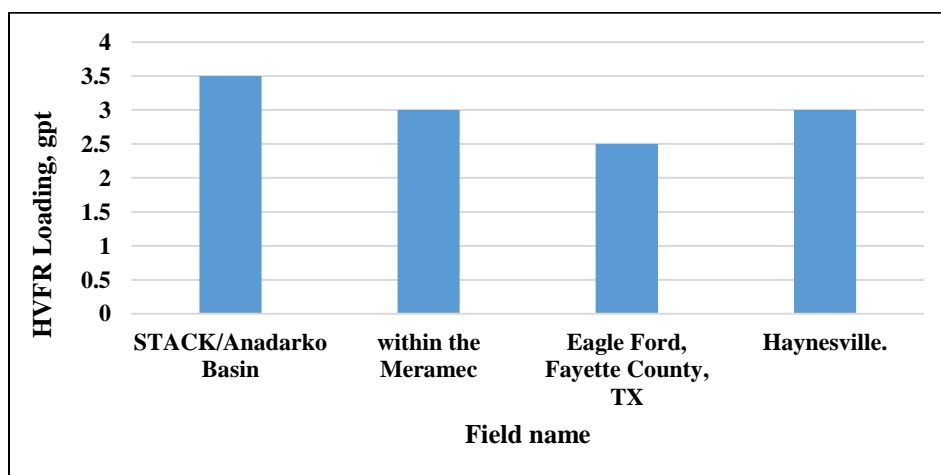


Figure 6. Maximum loading of HVFRs applied in the field.

Figure 10 illustrates the viscosity ranges of HVFR fluids at low shear rate (70 s^{-1}) corresponding to various concentrations of HVFR in the fluids. Since the shear rate inside the fractures is between 100 s^{-1} and 10 s^{-1} , the selected viscosity profile for data analysis was at 70 s^{-1} Ba Geri et al. (2019a).

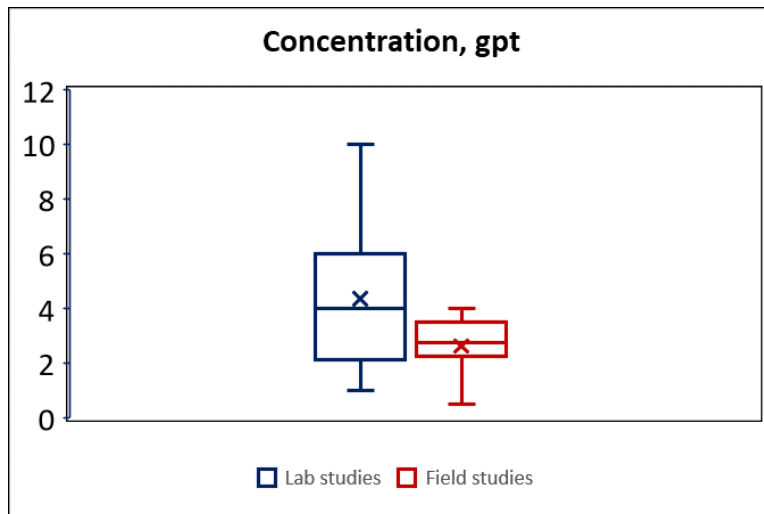


Figure 7. Box plots of HVFR concentration ranges in the lab measurements and field application.

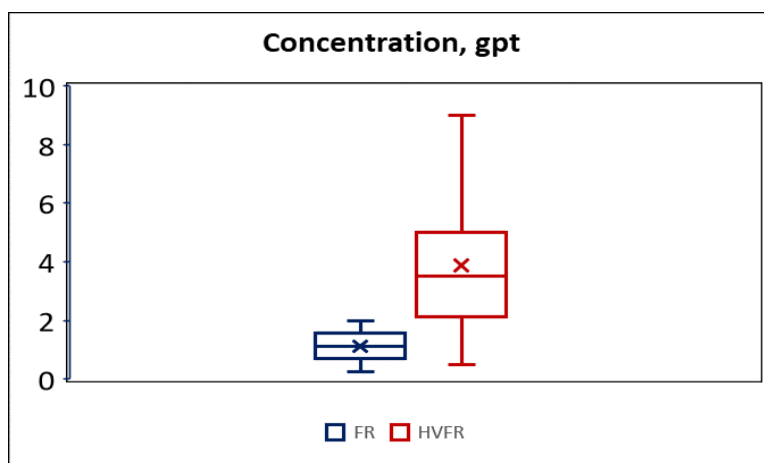


Figure 8. Box plots of concentration ranges of FR and HVFRs.

The rapid increase in viscosity as shear rate decreases helps in carrying proppant farther through the fractures. For example, the window range of 4 gpt HVFRs for the viscosity was from 20 cp to 80 cp.

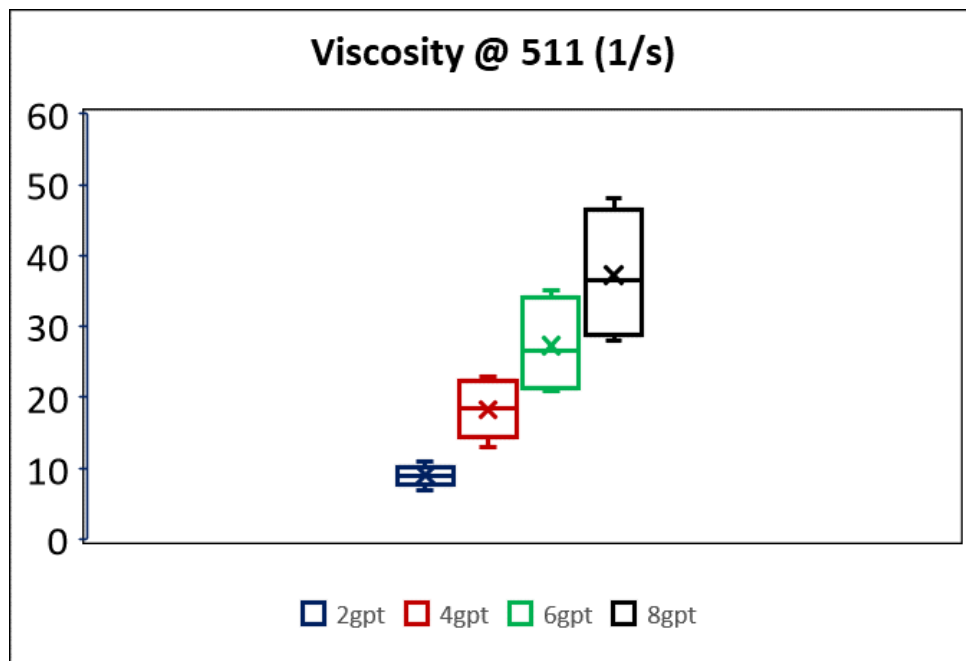


Figure 9. Box plots of viscosity ranges of HVFRs at high shear rate 511 s^{-1} .

Table 1 summarizes the extracted viscosity data of HVFRs. The viscosity profile of HVFRs depends on many factors including polymer concentration, shear rate, time, solvent properties, and temperature Aften et al. (2014). Increasing temperature from 70°F to 180°F decreases the viscosity from 40 cp to 30 cp Motiee et al. (2016). Decreasing HVFR concentration from 8 gpt to 2 gpt can reduce the viscosity by 75% (from 40 cp to 10 cp, at the same shear rate and temperature conditions) Kunshin et al. (2018). A thermal study of high concentration 8 gpt of HVFRs was studied by Ba Geri et al. (2019). The study observed that increase HFVR temperature from 77°F to 176°F decreased the HVFR viscosity profile from 33 cp to 13 cp, respectively.

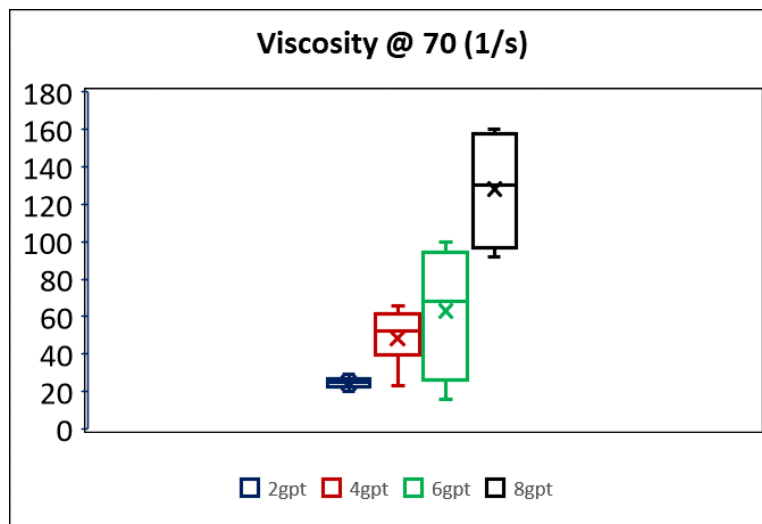


Figure 10. Box plots of viscosity ranges of HVFRs at low shear rate 70 s^{-1} .

3.3. SCREENING CRITERIA GUIDELINES FOR HVFRS

Table 2 provides screening guidelines for HVFRs in terms of fluid concentration and viscosity. The range of each property used in the lab measurements and field application is reported for more successful treatment. The concentration of HVFRs is a significant parameter for the selection process. The maximum concentration of HVFRs was 10 gpt and 4 gpt in the laboratory and field application, respectively. Several factors control the concentration selection such as water source, high TDS, and formation damage so in the field trials 4 gpt was the maximum. In addition, the temperature effect was also investigated in this paper. The maximum temperature was 180°F and 335°F in laboratory and field application, respectively. Increasing the temperature lowered the HVFR viscosity profile due to the thermal degradation of the fluid.

Table 1. Summary of viscosity data of HVFRs reviewed in this paper.

HVFRs	Measurement Conditions				Reference
	Concentration (gpt)	Temperature [°F]	Shear Rate (sec^{-1})	Viscosity (cp)	
HCFR	10	70	511	40	Motiee et al. 2016
HCFR	2	70	511	7	Motiee et al. 2016
HCFR	6	70	150	40	Motiee et al. 2016
HCFR	6	180	150	30	Motiee et al. 2016
HVFR	4.5	N/A	511	16.5	Hu et al. 2018
HVFR	2.25	N/A	511	10.2	Dahlgren et al. 2018
HVFR	4	200	50	17	Dahlgren et al. 2018
HVFR	2	200	50	5	Dahlgren et al. 2018
HVFR	8	70	511	40	Kunshin et al. 2018
HVFR	2	70	511	10	Kunshin et al. 2018
HVFR	8	77	511	33	Ba Geri et al. 2019b
HVFR	8	176	511	13	Ba Geri et al. 2019b

Table 2. High viscosity friction reducers concentration, gpt.

	Minimum	Maximum	Mean	Median	Standard Deviation
Laboratory	1	10	4.36	4	2.25
Field	0.5	4	2.63	2.75	0.87

High Viscosity Friction Reducers Temperature, °F					
	Minimum	Maximum	Mean	Median	Standard Deviation
Laboratory	70	180	126.7	135	27.5
Field	140	335	239.3	158	48.7

4. CONDUCTIVITY PROFILE

Achieving high fracture conductivity is a primary goal of hydraulic fracturing treatment because these conductive channels enable flow of oil and gas from the formation

to the wellbore. Many factors influence the fracture conductivity such as proppant size and type, fracture closure stress, and fracturing fluid type. HVFR fracturing fluids are rapidly gaining in popularity because of their numerous advantages. Table 3 summarizes the regained conductivity using HVFR fracture fluids. Motiee et al. (2016) used high concentrations of friction reducers (HCFR) of 14 gpt. They conducted conductivity experiments under high temperature system 220°F for 25 hours; and concluded that using 14gpt of HCFR gives 72% of regained conductivity while by adding 1ppt of breaker the regained conductivity increased up to 80%.

Moreover, Van Domelen et al. (2017) evaluated the viscosity-building friction reducers experimentally and in the field application. The experiment conditions were 2 lb/sqft 30/50 sand at 180 °F using 1gpt of breaker. The study presented that the regained permeability was 96% at time zero; then, the regained permeability increased to 93% and 106% by increasing test time from 24 hours to 50 hours. Huang et al. (2018) presented an engineered low-polymer-loading non-cross-linked (ELN) fluid. A conductivity test was performed using carbonate core and sandstone core under closure pressure 1800 psi at 250°F. Promising results concluded that 89% and 91% regained permeability was observed for sandstone and carbonate core, respectively.

5. BREAKABILITY PROFILE

Currently, HVFRs as a completion fluid have been successfully used in unconventional formations. However, some concerns remain of the potential formation damage that might occur by using these high molecular weight polyacrylamide-based

fluids. Therefore, to address these concerns, different types of breaker system are required to eliminate or minimize the possible damage to fracturing treatment (Kern 1962; Brannon and Ault 1991; Economides and Nolte 2000).

Table 3. Fracture conductivity data of HVFRs reported in this paper.

HVFRs Type	Concentration (gpt)	Breaker (gpt)	Closure Stress (psi)	Shut-in Time (hrs)	Temperature [°F]	Regained Conductivity (%)	Reference
HCFR	14	NB	2000	25	220	72	Motiee et al. 2016
HCFR	14	1	2000	25	220	80	Van Domelen et al. 2017
VFR	3	1	2000	24	180	93	
VFR	3	1	2000	50	180	106	
ELN	N/A	N/A	1800	N/A	250	91	Huang et al. 2018

Degradation of polyacrylamide can occur biologically and chemically. Various types of breakers such as oxidative breakers are commonly used to break the polymers and reduce their viscosity. The chemical reaction of the breaker is controlled by several factors such as breaker dosage, temperature, and composition of the fluid, breaker chemistry, polymer concentration, and pH. Table 4. summarizes the work that has been performed for evaluating the breakability profile after using HVFR fracture fluids. Stim-Lab (2012) investigated using high loading (14 gpt) of HVFRs with and without breaker on retained conductivity compared to linear gel 30 ppt. At the same lab conditions temperature 220°F, closure pressure 2000 psi, and test time 25 hours, retained conductivity present was 72%

without breaker while with using 1 ppt of ammonium persulfate, the retained conductivity increased up to 80%.

Table 4. Breakability data of HVFRs summarized in this paper.

Breaker Type	Concentration (gpt) FR	Breaker (ppt)	Time (hrs)	Temperature [°F]	Breaker Released (%)	Reference
AP	14	1	25	220	80	Stim-Lab2012
N/A	3	1	24	180	93	Van Domelen et al. 2017
Ammonium Persulfate	3	1	2	180	33	Sun et al. 2010
Live oxidizer	3	0.1	2	180	83	Sun et al. 2010
Live oxidizer	3	0.5	2	180	92	Sun et al. 2010

Van Domelen et al. (2017) conducted a conductivity test to compare the crosslinked and Viscous FR (VFR) with 1ppt breaker. The measurements were performed at the same conditions of temperature 180°F and 2lb/sq. of 30/50 of proppant. After 24 hours of testing, the regained conductivity was 33% and 93% of 15 lb/Mgal crosslinked and 3 gpt of VFR, correspondingly. Sun et al. (2010) studied breaker behavior on viscous slickwater in unconventional reservoirs. Adding 1ppt of encapsulated oxidizer breaker to 8 gpt HVFR at 180°F for 2 hours began break down viscosity profile. After two hours the viscosity decreases from 120 cp to 80 cp at shear rate 40 s^{-1} . At the same experiment conditions, they tried to use another breaker live oxidizer breaker with different concentration 0.1 ppt and 0.5 ppt. The viscosity profile of 8 gpt HVFR rapidly dropped out from 120 cp to 20 cp when the 0.1 of live oxidizer breaker was used. They also compared solid residue from 20 ppt of linear gel and from 40 gpt HVFR at 150°F for two hours. The observation of the test was that HVFR had only little residue while liner gel had a large amount of residue.

6. PRODUCED WATER WITH HVFRS

Slickwater fracture fluid has been proven as one of the best fracture fluids in terms of high fracture length and low cost. However, government regulations have increased due to large amounts of water consumption in hydraulic fracturing techniques to increase the productivity of shale rocks. According to the US Environmental Protection Agency (EPA), the hydraulic fracturing operations require between 70 and 140 billion gallons of water annually in the United States alone (API, 2017). Therefore, using produced water instead of fresh water is gaining traction to minimize water usage, reduce environmental impacts, and increase hydrocarbon recovery from unconventional formations. However, generally polymer friction reducers perform more poorly in high salinity waters. High salinity produced waters are more common in the Marcellus and the Bakken basins with high TDS ranging from 30,000 to 50,000 ppm and over 225,000 mg/l, respectively. Almutashri (2014) noted that produced water contains solid suspension and bacteria; these bacteria generate enzymes that degrade the polymer viscosity significantly.

Sareen et al. (2014) developed a friction reducer (Table 5) compatible with high-salinity produced water used with slickwater in hydraulic fracturing treatments. The case study in Delaware basin reported that the friction reducer was compatible with produced water containing over 250,000 ppm TDS and 90,000 ppm total hardness. The maximum concentration of friction reducer was 1.5 gpt and the bottomhole temperature was 136°F. The application was implemented in 17-stages with significant 40% reduction on the amount of proppant, increasing the oil production by 50%, and 20% increase of gas production compared to conventional friction reducer.

Table 5. Chemical composition of produced water in Delaware basin (Sareen et al. 2014).

Specific gravity	1.2	pH	6.02
Temperature	70°F		
Cations	ppm	Anions	ppm
Sodium	73,978	Chloride	149,750
Calcium	12,313	Sulfates	250
Soluble Iron (Fe)	10	Bicarbonates	61
Magnesium	4,992		
Total Hardness	51,781 ppm (CaCO ₃)		
Total Dissolved Solids	241,354 ppm		
Calcium Carbonate Index	1,083,360		
Calcium Sulfate Index	4,440,000		

Table 6 summarizes the work that has been performed to evaluate using produced water with HVFRs. Sareen et al. (2014) presented an experimental study on HFVRs in fresh water and salt water with HVFR varying from 1 to 6 gpt. A variety of HVFR systems were tested, including both anionic, and cationic HVFRs with surfactants. They examined their viscosity profile and settling velocity measurements. The study concluded that surfactant and polymer type systems play a key role in the viscosity-shear rate profile. Sanders et al. (2016) presented field trials using dry friction reducer (DFR) in the Fayetteville shale, with produced water having approximately 10,000 ppm TDS. The DFR provided a better placement of proppant and has more advantages compared to gel-based systems in terms of environmental effect and logistical costs. Johnson et al. (2018) reported successful case studies implemented in Marcellus and Bakken shale using high-brine viscosity-building friction reducer (HBVB) in high brine produced water. The TDS in Marcellus formation was in the range of 30,000 to 50,000 ppm. Lab measurements were performed to HBVB at shear rate 50 s^{-1} . The viscosity profile of HBVB loading 5 gpt at 50 s^{-1} was 45 cp and decreased to 12 cp in fresh water and produced water,

correspondingly. In Marcellus shale HBVB is used in the field to replace guar-based systems; HBVB has better performance results in lab measurements and field applications. Moreover, seven different types of friction reducers were selected to apply in the Bakken field in North Dakota; six of them did not work well because they were not compatible with the produced water. The seventh one was successfully used with loading from 1.5 gpt to 3.6 gpt HBVB. Six stages of that well were treated by HBVB product with effective carrying proppant concentration up to 3 ppa.

To conclude, utilizing produced water for hydraulic fracturing in the oil and gas industry is gaining popularity because using produced water leads to operational cost savings and has environmental benefits. However, compatibility of the friction reducers with the various types of produced water requires different test protocols.

Table 6. Produced water TDS used with HVFRs.

HVFRs Loading (gpt)	Temperature (°F)	Produced water TDS (ppm)	Produced water total hardness (ppm)	Findings	References
1.5	136	240,000	50,000	50% oil production increase, 40% less proppant	Sareen et al. 2014
0.75	175	10,000	N/A	Better placement of proppant	Sanders et al. 2016
3.58	N/A	50,000	N/A	Significant cost reduction	Johnson et al. 2018

7. ECONOMIC ANALYSIS

Several successful field case studies were adopted using HVFRs as an alternative for conventional hydraulic fracturing fluids. They addressed clearly the main concern of the HVFR systems, which is its capability to carry a sufficient amount of proppant with less formation damage Hu et al. (2018). In 2012, Stim-Lab performed an extensive investigation about regained conductivity using high concentration (14 gpt) of HVFRs compared to 30 ppt linear gel fluid. Superior results from the evaluation test shows that 14 gpt can regain conductivity up to 80%. Dahlgren et al. (2018) reported economics cost evolution in the STACK play using three case studies. In cases 1 and 2, the fracturing fluid system was changed from a hybrid system to HVFR with max proppant concentration of 5 ppg. Moreover, in Case 3, HVFR was used for around 32 stages with successful chemical cost reduction about 38%. Due to the fast hydration process and fewer chemicals used, the chemical cost savings that used on case 1, 2, and 3 were 32%, 33%, and 38%, respectively. Figure 11 presents the chemical cost reduction of using HVFRs during hydraulic fracturing applications. In the Utica plays, the cost reduction reached almost 80% compared with previous hydraulic fluids.

Furthermore, using HVFRs provided promising results in production improvements as shown in Figure 12. The Eagle Ford, Haynesville, and Utica reported over 60% improvement in hydrocarbon production while around 30% increasing in oil production occurred in the STACK play.

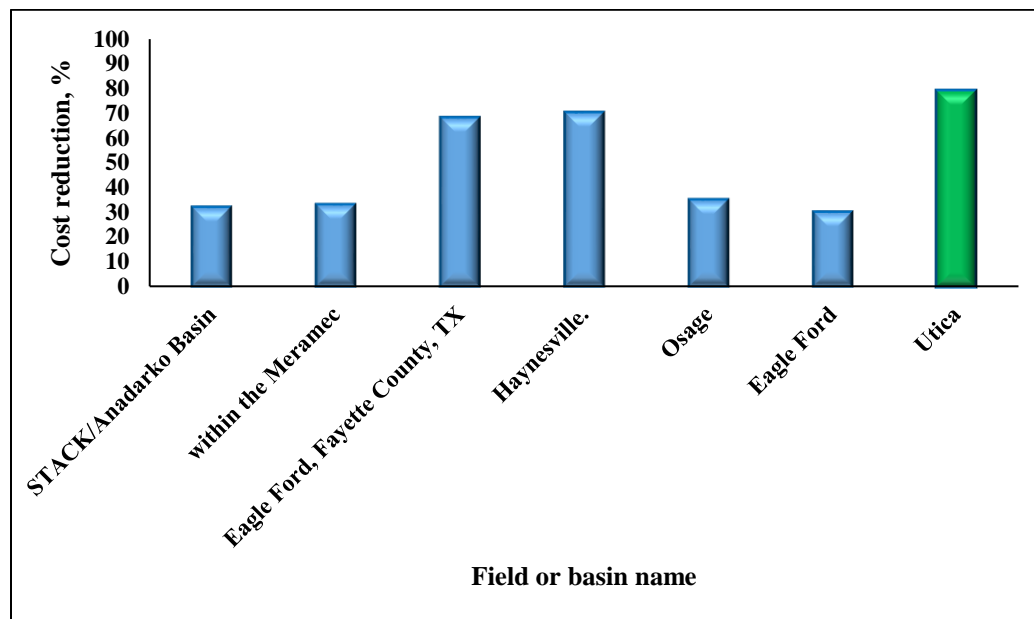


Figure 11. Chemical cost reduction of using HVFRs from different case studies.

Dahlgren et al. (2018) showed case studies of using HVFRs in the STACK play. Interestingly, one of these two compared wells completed identically in fracturing design. Well 1 was treated with hybrid guar-based fluid system consisting of 18# linear gel and 18# crosslinked. Well 2 used HVFR starting with 5 gpt and end up the fracture treatment by 3 gpt of HVFR. All the other parameters were the same in both stimulation process in Well 1 and Well 2 as shown in Table 8. The field results showed over 30% improvement in production, and 32% reduction of chemical cost in Well 2 where HVFR was used compared to using guar-based fluids in Well 1.

Using fewer chemicals during hydraulic fracturing treatment improves well economics. Motiee et al. (2016) present a case study about the operational cost reduction using HVFR's compared to crosslinked fluid systems.

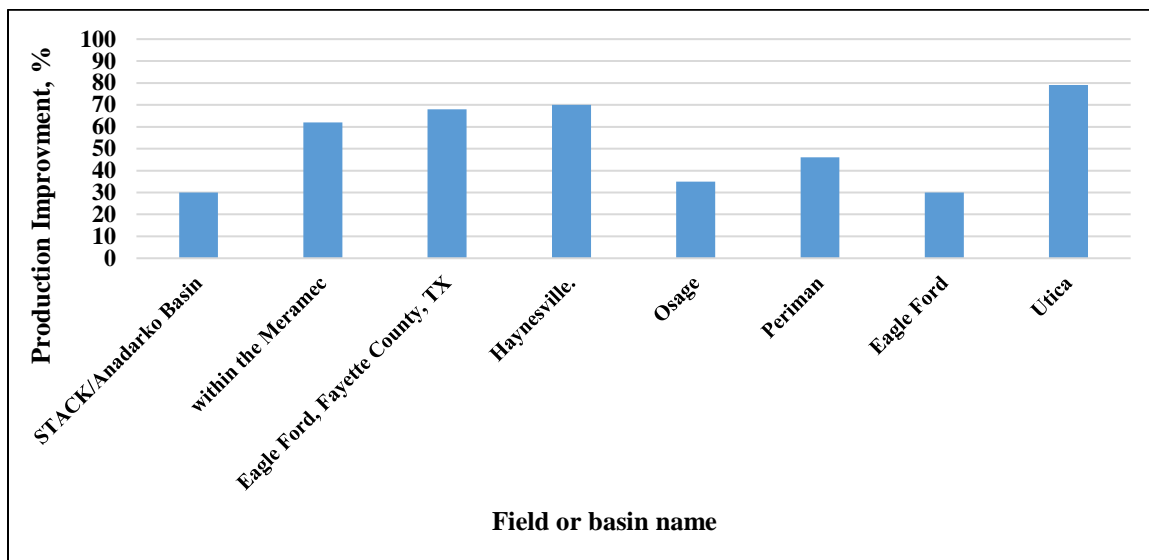


Figure 12. Production improvement of using HVFRs from different case studies.

The data results reported that the average reduction ranged from 33% to 48% of the chemical volume used in fracturing treatment as well as 22% average reduction on fluid cost as shown in Figure 13.

Another logistic of cost reduction is the fracturing fluids material themselves. Earthstone Energy, Inc. reported several case studies replacing crosslinked or hybrid system with HVFRs, where the average completion cost was reduced by 35%, and the charge in pump pressure decreased by 17%. Since the characterization nature of HVFRs has rapid solubility on water, HVFRs hydrate quickly “on-the-fly.” Therefore, hydration unit is not required in the field which helps to save cost as well Van Domelen et al. (2017).

Table 7. Stimulation summary of case study (Dahlgren et al, 2018).

	SW MBL	HVFR MBL	18# LIN MBL	18# XL MBL	TOTAL FLUID MBL	100 MESH MM#	40/70 MM#	TOTAL PROP MM#
Well 1	243	0	21	41	305.4	4.7	7.6	12.3
Well 2	251	56	0	0	307.3	4.7	7.6	12.3

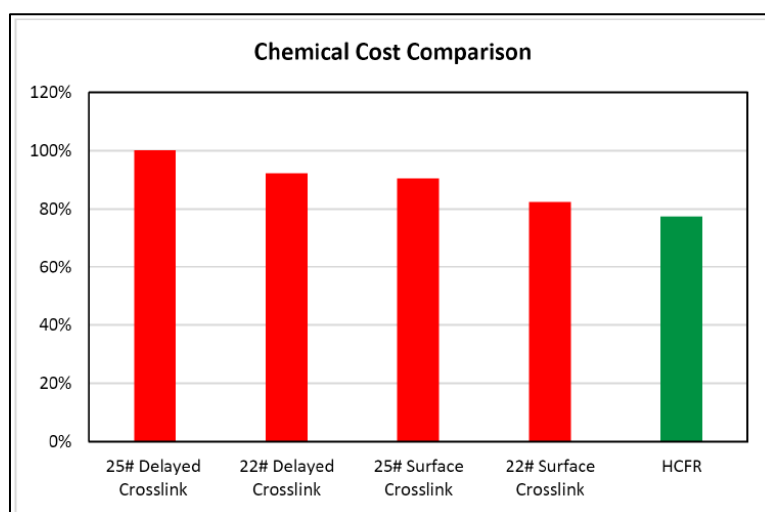


Figure 13. Chemical cost comparison for standard Bakken system (Motiee et al. 2016).

8. CONCLUSIONS

This study provides a comprehensive review on using high viscous friction reducers as a potential alternative for conventional fracture fluid. Potential advantages of using HVFRs over other fracture fluids were discussed. Results for laboratory and successful field studies that used HVFR were also analyzed and presented. The following conclusions can be drawn from this work:

- Screening criteria for using HVFRs were presented to understand the optimum selection of HVFRs. HVFR concentration and temperature are the main factors that influence the viscosity profile of HVFRs. The median used of these factors in the field application was 2.75 gpt and 158 °F for the HVFR concentration and temperature, respectively.
- Successful field case studies and lab measurements discussed the use of HVFRs as an alternative fracturing fluid system to the conventional fracturing fluids (e.g., linear gel system).
- Numerous advantages of using HVFRs are reported including the ability of carrying proppant, less formation damage, and reduction in chemical cost and water usage.
- High viscous friction reducers using produced water showed promising results but more investigation with different produced water composition is still required.
- High viscous friction reducers showed improvement on the hydrocarbon production in many filed case studies reaching over 70% improvement.

REFERENCES

- Aften, C. W. (2010, January 1). Study of Friction Reducers For Recycled Stimulation Fluids In Environmentally Sensitive Regions. Society of Petroleum Engineers. <https://doi:10.2118/138984-MS>
- Aften, C. W. (2014, October 21). Friction Reducers Fresh Rheological Insights Married to Performance. Society of Petroleum Engineers. <https://doi:10.2118/171025-MS>
- Al-Khaldy, M. D., Dutta, A., Goswami, B., Al-Rashidi, A., Rondon, L. J., Warrakey, M., & Abdel Samie, M. A. (2014, November 10). First-Ever Level 4 Multilateral Well in North Kuwait Successfully Completed, Improves Oil Production. Society of Petroleum Engineers. <https://doi:10.2118/171792-MS>

- Al-Muntasheri, G. A. (2014, April 17). A Critical Review of Hydraulic Fracturing Fluids over the Last Decade. Society of Petroleum Engineers. <https://doi:10.2118/169552-MS>
- API, A. P. (n.d.). Energy and Opportunity. Retrieved April 10, 2017, from <http://www.hydraulicfracturing.com/#/?section=energy-and-opportunity>
- Ba Geri, M., Imqam, A., & Suhail, M. (2019a, March 19). Investigate Proppant Transport with Varying Perforation Density and Its Impact on Proppant Dune Development Inside Hydraulic Fractures. Society of Petroleum Engineers. <https://doi:10.2118/195018-MS>
- Ba Geri, M., Imqam, A., Bogdan, A., Shen, L. (2019b, April 9). Investigate the Rheological Behavior of High Viscosity Friction Reducer Fracture Fluid and Its impact on Proppant Static Settling Velocity. Society of Petroleum Engineers. <https://doi:10.2118/195227-MS>
- Brannon, H. D., & Ault, M. G. (1991, January 1). New, Delayed Borate-Crosslinked Fluid Provides Improved Fracture Conductivity in High-Temperature Applications.
- Carman, P. S., & Cawiezel, K. (2007, January 1). Successful Breaker Optimization for Polyacrylamide Friction Reducers Used in Slickwater Fracturing. Society of Petroleum Engineers. <https://doi:10.2118/106162-MS>
- Castro-Vera, E., Chuc, E. A., Gutierrez, L., & Sanchez, A. (2015, October 26). Implementation of Low-Residue Polysaccharide Fracturing Fluid System Aids Flowback Recovery at Chicotepec Basin: Field Experiences on Sandstone Tight-Oil Wells. Society of Petroleum Engineers. <https://doi:10.2118/176722-MS>
- Chung, H. C., Hu, T., Ye, X., & Maxey, J. E. (2014, October 27). A Friction Reducer: Self-Cleaning to Enhance Conductivity for Hydraulic Fracturing. Society of Petroleum Engineers. <https://doi:10.2118/170602-MS>
- Clark, R. K., Scheuerman, R. F., Rath, H., & Van Laar, H. G. (1976, June 1). Polyacrylamide/Potassium-Chloride Mud for Drilling Water-Sensitive Shales. Society of Petroleum Engineers. <https://doi:10.2118/5514-PA>
- Cooke, C. E. (1975, October 1). Effect of Fracturing Fluids on Fracture Conductivity. Society of Petroleum Engineers. <https://doi:10.2118/5114-PA>
- Dahlgren, K., Green, B., Williams, B., Inscore, J., Domelen, M. V., & Fenton, A. (2018, January 23). Case Studies of High Viscosity Friction Reducers HVFR in the STACK Play. Society of Petroleum Engineers. <https://doi:10.2118/189893-MS>

- Economides, M.J. and Nolte K.G. 2000. *Reservoir Stimulation*, Third Edition. John Wiley & Sons.
- Hashmi, G., Kabir, C. S., & Hasan, A. R. (2014, October 27). Interpretation of Cleanup Data in Gas-Well Testing From Derived Rates. Society of Petroleum Engineers. <https://doi:10.2118/170603-MS>
- <https://www.slb.com/-/media/Files/stimulation/.../engineered-fracturing-fluids.pdf>
- Hu, Y. T., Fisher, D., Kurian, P., & Calaway, R. (2018, January 23). Proppant Transport by a High Viscosity Friction Reducer. Society of Petroleum Engineers. <https://doi:10.2118/189841-MS>
- Huang, J., Perez, O., Huang, T., Safari, R., & Fragachan, F. E. (2018, October 16). Using Engineered Low Viscosity Fluid in Hydraulic Fracturing to Enhance Proppant Placement. Society of Petroleum Engineers. <https://doi:10.2118/191395-18IHFT-MS>
- Ifejika, E., De Cumont, B., & Kashani, N. (2017, January 24). Optimum Production Metrics to Predict Unconventional Well's Long-term Performance. Society of Petroleum Engineers. <https://doi:10.2118/184817-MS>
- Johnson, M., Winkler, A., Aften, C., Sullivan, P., Hill, W. A., & VanGilder, C. (2018, October 5). Successful Implementation of High Viscosity Friction Reducer in Marcellus Shale Stimulation. Society of Petroleum Engineers. <https://doi:10.2118/191774-18ERM-MS>
- Ke, M., Qu, Q., Stevens, R. F., Bracksieck, N. E., Price, C. R., & Copeland, D. L. (2006, January 1). Evaluation of Friction Reducers for High-Density Brines and Their Application in Coiled Tubing at High Temperatures. Society of Petroleum Engineers. <https://doi:10.2118/103037-MS>
- Kern, L.R. 1962. Method and Composition for Formation Fracturing. US Patent No. 3, 058, 909.
- Kunshin, A., & Dvoynikov, M. (2018, October 15). Design and Process Engineering of Slotted Liner Running in Extended Reach Drilling Wells. Society of Petroleum Engineers. <https://doi:10.2118/191520-18RPTC-MS>
- Li, L., Saini, R., & Mai, N. (2018, September 24). High-TDS Produced Water-Based, Low-Damaging Fracturing Fluids for Applications at 300°F or Higher. Society of Petroleum Engineers. <https://doi:10.2118/191749-MS>

- Li, L., Sun, H., Qu, Q., Le, H. V., Ault, M., Zhou, J., ... Smith, D. (2014, October 27). High-Temperature Fracturing Fluids Prepared with Extremely High-TDS and Hard Produced Water. Society of Petroleum Engineers. <https://doi:10.2118/170607-MS>
- Montgomery, C. (2013, May 20). Fracturing Fluid Components. International Society for Rock Mechanics and Rock Engineering.
- Motiee, M., Johnson, M., Ward, B., Gradl, C., McKimmy, M., & Meeheib, J. (2016, February 1). High Concentration Polyacrylamide-Based Friction Reducer Used as a Direct Substitute for Guar-Based Borate Crosslinked Fluid in Fracturing Operations. Society of Petroleum Engineers. <https://doi:10.2118/179154-MS>
- Ozuruigbo, C. Q., & Fan, C. (2014, September 30). Influence of Friction Reducer on Scale Inhibitor Performance and Scaling Tendency in Slickwater Fracturing. Society of Petroleum Engineers. <https://doi:10.2118/171661-MS>
- Rimassa, S. M., Howard, P., & Arnold, M. O. (2009, January 1). Are You Buying Too Much Friction Reducer Because of Your Biocide? Society of Petroleum Engineers. <https://doi:10.2118/119569-MS>
- Reddy, B. R. (2013, April 8). Laboratory Characterization of Gel Filter Cake and Development of Non-Oxidizing Gel Breakers for Zirconium Crosslinked Fracturing Fluids. Society of Petroleum Engineers. <https://doi:10.2118/164116-MS>
- Rodvelt, G., Yuyi, S., & VanGilder, C. (2015, October 13). Use of a Salt-Tolerant Friction Reducer Improves Production in Utica Completions. Society of Petroleum Engineers. <https://doi:10.2118/177296-MS>
- Sanders, M., Felling, K., Thomson, S., Wright, S., & Thorpe, R. (2016, February 1). Dry Polyacrylamide Friction Reducer: Not Just for Slick Water. Society of Petroleum Engineers. <https://doi:10.2118/179146-MS>
- Sareen, A., Zhou, M. J., Zaghmoot, I., Cruz, C., Sun, H., Qu, Q., & Li, L. (2014, December 10). Successful Slickwater Fracturing in Ultrahigh TDS Produced Water by Novel Environmentally Preferred Friction Reducer. International Petroleum Technology Conference. <https://doi:10.2523/IPTC-17824-MS>
- Shah, S., Asadi, M., Wheeler, R., Brannon, H., Kakadjian, S., Ainley, B., ... Archacki, D. (2018, February 7). Methodology for Evaluating Drag Reduction Characteristics of Friction Reducer. Society of Petroleum Engineers. <https://doi:10.2118/189537-MS>
- STIM-LAB Proppant Consortium, Report July 2012, Section 3.1 Friction Reducers used in Slickwater Applications.

- Sun, H., Wood, B., Stevens, R. F., Cutler, J., Qu, Q., & Lu, M. (2011, January 1). A Nondamaging Friction Reducer for Slickwater Frac Applications. Society of Petroleum Engineers. <https://doi:10.2118/139480-MS>
- Sun, H., Wood, B., Stevens, R. F., Cutler, J., Qu, Q., & Lu, M. (2011, January 1). A Nondamaging Friction Reducer for Slickwater Frac Applications. Society of Petroleum Engineers. <https://doi:10.2118/139480-MS>
- Sun, H., Stevens, R. F., Cutler, J. L., Wood, B., Wheeler, R. S., & Qu, Q. (2010, January 1). A Novel Nondamaging Friction Reducer: Development and Successful Slickwater Frac Applications. Society of Petroleum Engineers. <https://doi:10.2118/136806-MS>
- Tomson, R. C., Guraieb, P., Graham, S., Yan, C., Ghorbani, N., Hanna, T., & Cooper, C. (2017, January 24). Development of a Universal Ranking for Friction Reducer Performance. Society of Petroleum Engineers. <https://doi:10.2118/184815-MS>
- Van Domelen, M., Cutrer, W., Collins, S., & Ruegamer, M. (2017, March 27). Applications of Viscosity-Building Friction Reducers as Fracturing Fluids. Society of Petroleum Engineers. <https://doi:10.2118/185084-MS>
- White, C. M., and Mungal, M. G. 2008. Mechanics and Prediction of Turbulent Drag Reduction with Polymers. *Ann. Rev Fluid Mech.* 40:235-256
- Wu, Q., Ma, Y., Sun, Y., & Bai, B. (2013, March 23). The Flow Behavior of Friction Reducer in Microchannels During Slickwater Fracturing. Society of Petroleum Engineers. <https://doi:10.2118/164476-MS>

II. INVESTIGATE THE RHEOLOGICAL BEHAVIOR OF HIGH VISCOSITY FRICTION REDUCER FRACTURE FLUID AND ITS IMPACT ON PROPPANT STATIC SETTLING VELOCITY

Mohammed Ba Geri¹, Abdulmohsin Imqam¹, Andrey Bogdan², and Lingjuan Shen²

1: Department of Petroleum Engineering, Missouri University of Science and Technology, Rolla, MO 65409

2: BJ Services, Tomball, TX

ABSTRACT

The recent and rapid success of using high viscosity friction reducers (HVFRs) in hydraulic fracturing treatments is due to several advantages over other fracture fluids (e.g. linear gel), which include better proppant carrying capability, induce more complex fracture system network with higher fracture length, and overall lower costs due to fewer chemicals and less equipment on location. However, some concerns remain, like how HVFRs rheological properties can have impact on proppant transport into fractures. The objective of this study is to provide a comprehensive understanding of the influence the rheological characterization of HVFRs have on proppant static settling velocity within hydraulic fracturing process.

To address these concerns, comprehensive rheological tests including viscosity profile, elasticity profile, and thermal stability were conducted for both HVFR and linear gel. In the steady shear-viscosity measurement, viscosity behavior versus a wide range of shear rates was studied. Moreover, the influence of elasticity was examined by performing oscillatory-shear tests over the range of frequencies. Normal stress was the other elasticity

factor examined to evaluate elastic properties. Also, the Weissenberg number was calculated to determine the elastic to viscous forces. Lastly, quantitative and qualitative measurements were carried out to study proppant settling velocity in the fluids made from HVFRs and linear gel.

The results of rheological measurement reveal that a lower concentration of HVFR-2 loading at 2gpt has approximately more than 8 times the viscosity of linear gel loading at 20ppt. Elastic measurement exposes that generally HVFRs have a much higher relaxation time compared to linear gel. Interestingly, the normal stress N_1 of HVFR-2, 2gpt was over 3 times that of linear gel loading 20ppt. This could conclude that linear gel fracture fluids have weak elastic characterization compared to HVFR. The results also concluded that at 80 Co linear gel has a weak thermal stability while HVFR-2 loses its properties only slightly with increasing temperature. HVFR-2 showed better proppant settling velocity relative to guar-based fluids. The reduction on proppant settling velocity exceed 75% when HVFR-2 loading at 2gpt was used compared to 20ppt of linear gel. Even though much work was performed to understand the proppant settling velocity, not much experimental work has investigated the HVFR behavior on the static proppant settling velocity measurements. This paper will provide a better understanding of the distinct changes of the mechanical characterization on the HVFRs which could be used as guidance for fracture engineers to design and select better high viscous friction reducers.

1. INTRODUCTION

Over the last few recent years high viscosity friction reducers (HVFRs) have been successfully used in the oil and gas industry across all premier shale plays in North America including Permian, Bakken, and Eagle Ford (Van Domenlen et al. 2017; Dahlgren, et al., 2018). Besides reducing friction, HVFRs have also been used to suspend and carry proppants farther into the fracture's networks. Very recently, the popularity of using HVFRs in frac fluid has increased.

A friction reducer is the main component of slick water fracture fluids and stimulation technology packages. The primary function of friction reducers is changing turbulent flow to laminar flow by reducing friction by 70-80% while pumping fracturing fluids (Schein, 2005). Recently, the oil industry started to use high viscosity friction reducers (HVFRs) as a direct replacement for linear and crosslinked gels due to several operational and economic reasons (Motiee et al 2016). High viscosity friction reducers (HVFRs) have been used as fracturing fluids because of the advantages such as reducing pipe friction during the fracturing process, the high potential of placing more proppant volumes compared to conventional hydraulic fluids system such as hybrid and crosslinked, creating complex fracture networks due to a less viscous system, possible higher fracture conductivity, improved production results comparable as using liner gel or crosslinked designs, potentially lower costs due to fewer chemicals and less equipment on location, less environmental footprint, and simplified hydraulic fracturing treatments by minimizing screen out risks (Motiee et al 2016; Van Domenlen et al. 2017; Dahlgren, et al., 2018; Ba Geri et al. 2019).

Both academic research and oil industrial implementation have shown promising results of using high viscosity friction reducers. Motiee et al. 2016 studied high concentration friction reducers (HCFR) as a direct substitute for guar-based crosslinked fluid. Different concentration of HCFR (2, 4, 6, and 8 gpt) were compared with 25 ppt linear gel to study proppant settling velocity. HCFR showed better proppant settling velocity relative to guar-based fluids. The results also concluded that at 180 °F 25 ppt linear gel has a weak thermal stability while HCFR only slight loses its properties. Shen et al. 2018 investigated rheological characterization of HVFRs and measured the settling velocity of multi-particle proppant. The results concluded that both the viscosity and elasticity of HVFRs can affect the proppant carrying capacity during hydraulic fracturing treatments.

Hu et al. 2018 addressed some concerns related to proppant transport capability using HVFRs and linear gel. Viscosity and elasticity measurements were examined to compare HVFRs with linear gel. They observed that at low shear rates HVFRs had higher viscosity. Also, normal forces for linear gels are much lower than HVFRs with increased shear rate. Dahlgren et al. 2018 identified three case studies in which STACK play replaced traditional fracturing fluid with HVFR. Viscosity-shear measurements were performed at 2, 3, and 4 gpt HVFRs concentration with and without a breaker. The study noticed that the viscosity profile was negatively affected by breaker.

Johnson et al. 2018 presented a successful implementation of high brine friction reducers (HBFRs) in high TDS water exceeding 60,000TDS. They observed that the viscosity of HBFRs decreased with increased brines ranges. Drylie et al. 2018 conducted viscosity measurements at a high shear rate of $511s^{-1}$ and a low shear rate $0.01s^{-1}$ for 1

and 6 gpt of HVFR and 24 ppt of guar. The study noticed that at 1gpt of HVFR there was no change in viscosity profile; in contrast, at a low shear rate HVFRs have a much higher viscosity than guar. Most previous work investigated the rheological characterization of HFVRs in low temperature conditions and did not consider that changes in rheological that could happen at high pressure environment. In addition, there was not serious effort to relate the effect of HVFR rheology on proppant settling velocity.

This work presents a comprehensive investigation performed to compare linear gel fracturing fluids with high viscosity friction reducers. This paper investigated several major factors including viscosity measurement profiles, elasticity properties (Normal forces and relaxation time), thermal stability profile, and static settling velocities. The question which is the key factor, the shear-viscosity or the elasticity of HVFRS, governing the settling velocity were also investigated by performing qualitative and quantitative of settling velocity measurements of multi-particles and single particle proppant.

2. PROPPANT STATIC SETTLING VELOCITY IN HYDRAULIC FRACTURING

This study provides insights on the elastic and viscous properties of HVFR and liner gel fluids. Weissenberg number and elasticity to viscosity ratio are calculated to measure the elastic properties of the fluids and to identify which rheological properties has significant contribution to the proppant settling velocity (Broadbent and Mena, 1974; Acharya et al., 1981; Malhotra and Sharma, 2012).

2.1. PARTICLE SHEAR RATE ($\dot{\gamma}$)

Calculating apparent particle shear rate leads to overestimate or underestimate the particle shear rate; therefore, determining the particle shear rate range within the Power law model (K, n) is an essential step to describe the shear thinning effect of the HVFRs and linear gel fluids. Equation 1 can be used to estimate the particle shear rate (Uhlherr et al., 1976; Shah et al., 2007):

$$\dot{\gamma} = 2 * V_s d_p \quad (1)$$

where $\dot{\gamma}$ is the particle shear rate; V_s is the terminal settling velocity; d_p is the particle diameter.

2.2. APPARENT SHEAR VISCOSITY (μ_a)

Lali et al. 1989 introduced Equation 2 to estimate the apparent shear viscosity.

$$\mu_a = K \dot{\gamma}^{n-1} \quad (2)$$

where μ_a is the apparent shear viscosity, K is the Consistency index; n is the flow behavior index

2.3. WEISSENBERG NUMBER (W_i)

To study viscoelastic fluid properties and fluid deformation degree, Weissenberg number should be measured. Weissenberg dimensionless number can be defined as follows:

$$W_i = \frac{\text{Elastic forces}}{\text{Viscous forces}} = \lambda \cdot \dot{\gamma} \quad (3)$$

where W_i is the Weissenberg number; λ is the relaxation time; $\dot{\gamma}$ is the particle shear rate

2.4. ELASTICITY TO VISCOSITY RATIO ($\lambda_{e/v}$)

Viscoelastic fluids consist of two main properties (viscosity and elasticity). To evaluate which property gives the greatest contribution during proppant transport. Equation 4 was used to measure the elasticity to viscosity ratio ($\lambda_{e/v}$) (Shen et al., 2018):

$$\lambda_{e/v} = \frac{0.5\tau N_1(\dot{\gamma})}{\eta(\dot{\gamma})} \quad (4)$$

where, $\lambda_{e/v}$ is the elasticity to viscosity ratio $N_1(\dot{\gamma})$ is the first normal stress, τ is relaxation time, and $\eta(\dot{\gamma})$ is the shear viscosity.

The numerator consists of the elasticity portion (relaxation time τ and first normal stress $N_1(\dot{\gamma})$) and the denominator is a function of only the viscosity profile ($\eta(\dot{\gamma})$). The elastic/viscous ratio demonstrated by elasticity once their value more than one while if the elastic/viscous ratio less than one that indicates is the viscosity play main role during proppant transport.

2.5. FORCES INFLUENCED PARTICLES SETTLING VELOCITY

In a Newtonian fluid, settling velocity of single particle can be calculated from the Stokes model, which is usually referred as Stokes Equation 7 in the creeping flow regime ($Re_p < 1$). Because the settling velocity is a function of Reynolds number and drag forces, it's important to calculate all parameters related to the settling velocity Khan and Richardson, 1987. Several studies developed theoretical expressions that can be used to calculate drag coefficient Renaud et al. (2004) and of Tripathi et al. (1994). The most common correlation was derived by Stokes which can be used to calculate settling velocity (V_s) are shown in Equation 5 – 7 (Arnipally, 2018):

$Re_p < 1$ (creeping flow regime)

$$Re_p = \frac{D_p V_s \rho_f}{\mu_f} \quad (5)$$

$$C_D = \frac{24}{Re_p} \quad (6)$$

$$V_s = \frac{(\rho_s - \rho_f) g D_s^2}{18 \mu_f} \quad (7)$$

Three main forces dominate the vertical motion of solid particles in a fluid: gravitational force; F_G , buoyancy force F_B ; and drag force; F_D (Arnipally, 2018).

$$F_g = \rho_p v_p g \quad (8)$$

$$v_p = \pi d_p^3 / 6 \quad (9)$$

$$F_b = \rho v_p g \quad (10)$$

$$F_D = \frac{C_D A \rho_f V^2}{2} \quad (11)$$

where ρ_p is the particle density, v_p is the volume of the particle, ρ_f is the fluid density, d_p is the particle diameter, g is the acceleration due to gravity (9.81 ms^{-2}). C_D is the drag coefficient, A is the projected area, and V is the settling velocity.

3. EXPERIMENT DESCRIPTION

3.1. MATERIALS

3.1.1. Hydraulic Fracturing Fluids. Two fracture fluid samples were used in this study: 1) HVFRs with different compositions (HVFR-1, HVFR-2, HVFR-3), 2) linear gel (GW-3d). All fracture fluid samples were provided by BJ Services Company.

3.1.2. Preparing Fracturing Fluids. According to standard industry practice for using HVFRs, four different concentrations 1, 2, 4, 8 gallons per thousand gallons (gpt) of each sample were mixed with deionized (DI) water. Linear gel (GW-3d) fluid was tested with three different concentrations 10, 20, 40 pounds per thousand gallons (ppt).

3.1.3. Proppant Sizes. Proppant US silica sand size of 30/60 mesh and glass bead sizes of 2, 4, and 6mm were used to measure terminal settling velocity in HVFRs.

3.1.4. Rheometer. A high accuracy advanced rheometer with a parallel-plate system was used to measure viscosity-shear profile, normal forces, and the dynamic oscillatory-shear measurements at lab and high temperature ranges.

3.2. SETTLING VELOCITY IN UNCONFINED FRACTURE SETUP

Figure 1 shows the setup of an unconfined settling velocity measurement. The experiment was performed in a 1000 ml transparent graduated glass cylinder with a diameter at least 25 times the proppant diameter to ensure proppant settling velocity was not influenced by the walls of the glass container. In addition, alongside the glass container a foot ruler was placed to measure the fluid level inside the model as shown in the setup.

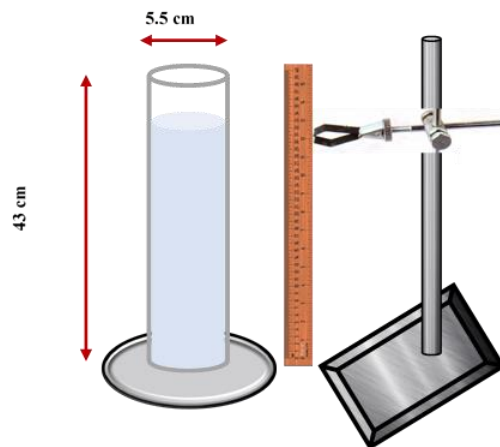


Figure 1. Schematic of fracture setup for unconfined fluids.

3.3. RHEOLOGICAL CHARACTERIZATION OF THE HVFRS

3.3.1. Viscosity Profile Measurement. Two different rheological tests were performed including steady shear-viscosity and time dependency using an advanced rheometer with a parallel-plate system (PP50/TG using a 0.30 mm gap). To investigate the viscous behavior, tests were implemented under varying shear rate from $0.1-1000\text{ s}^{-1}$ with measurements at 21 point/decade.

3.3.2. Elasticity Profile Measurement. The dynamic oscillatory-shear measurements were conducted to measure the elasticity profile characterizations and first normal stress N1. The oscillatory test was implemented over a range of frequencies from 0.01-100Hz. All rheological properties measurements were conducted at lab and high temperature ranges.

3.3.3. Thermal Stability Measurement. The influence of temperature during fracturing operations has not been fully understood in shale oil reservoirs. This paper investigated the effect of thermal stability of rheology characterizations of HVFRs, which tends to alter parameters such as time dependency, fluid elasticity, viscosity and first normal stress. To better mimic the real fracturing process, the experiments were performed under elevated temperatures by using an advanced rheometer. Viscosity-shear profile measurements for three different temperatures of 77°F, 122°F, 176 °F have been conducted for both HVFRs and linear gel fracture fluids.

3.3.4. Static Settling Velocity Measurement. At this point, the graduated cylinder is filled with HVFR and the cell is positioned vertically. To measure proppant settling velocity in unconfined fluids, high-resolution video camera is used to record the settling process. In this setup, proppant diameter ranged from 0.453 mm to 6 mm. A single proppant

was dropped in the HVFR and allowed to settle. A high-resolution video camera has been used to capture the process of free proppant settling. An image analysis tool called “Tracker” (<http://www.cabrillo.edu/~dbrown/tracker/>) was applied to get accurate measurements of vertical position of the proppant at different time steps (Ba Geri et al 2018). The slope of relationship between proppant vertical positions to steps time step is called terminal settling velocity. For more accurate results, settling velocity of each particle were repeated three times.

4. RESULTS AND DISCUSSION

4.1. VISCOSITY MEASUREMENT RESULTS

In Figure 2, a viscosity measurement profile is presented. In order to understand the HVFRs characterizations, three different HVFRs fracture fluids with a wide range of concentrations (1, 2, 4, 8gpt), along with several linear gel concentrations (10, 20, 40ppt), were measured using an advanced rheometer at 25°C in a wide range of shear rates from 0.1 to 1000 s^{-1} . All the results exhibit that the HVFRs fluids follow a shear thinning behavior that as shear rate increases the viscosity decreases. At a loading of 8gpt, results for HVFR-2 showed that HVFRs have high viscosity (20,000cp) at a lower shear rate of 0.1 s^{-1} compared to HVFR-1 and HVFR-3 with 9,000cp and 10,000cp, respectively. Linear gel with a loading of 40ppt at the same low shear rate of 0.1 s^{-1} showed a much lower viscosity of around 1200 cp.

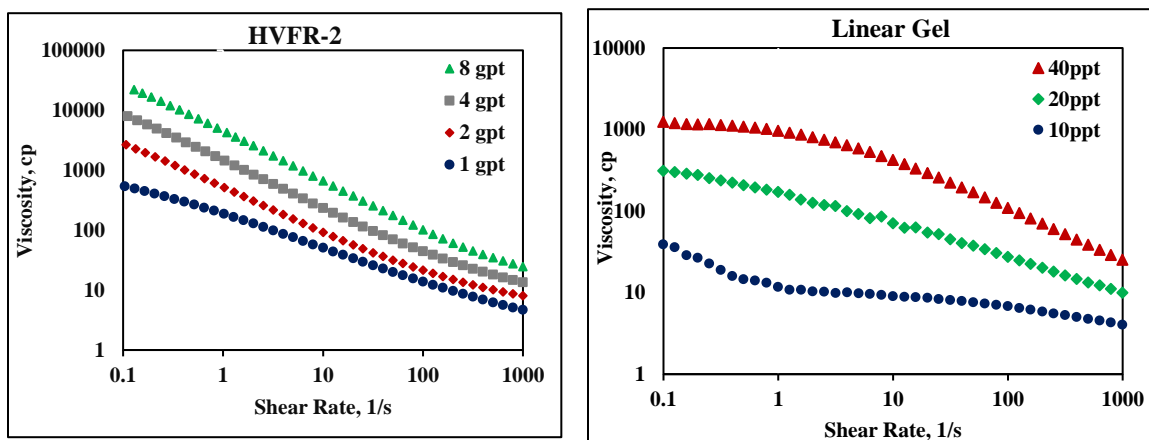


Figure 2. Effect of HVFR (left) and linear gel (right) concentrations as a function of shear rate.

Table 1 shows the Power law model equations fitting for all HVFRs and linear gel samples at different concentrations. The Power law model is clearly best fit of the experiments results of HVFRs and linear gel fluids whereas the R-square values of the equation are close to the unit. The results also observed that by increasing HVFRs or linear gel concentration, the K and n values increased.

Figure 3 shows that HVFR-2 has highest viscosity profile at a low shear rate of 0.1 s^{-1} . For instance, at a loading of 8 gpt HVFR-2 had a viscosity of almost 23,000 cp, which is around double the viscosity of HVFR 1 & 3 at the same loading. Moreover, HVFR-2 loading 2 has higher viscosity profile up to 2670cp while linear gel loading 20ppt has less viscosity around 311cp which represent almost 9 time increasing in viscosity profile of HVFR-2 loading 2gpt.

To conclude, HVFRs have higher viscosity profile along all the shear rate ranges compared to linear gel. HVFR-2 viscosity increased substantially from 176 cp to 22,724 cp as the concentration increased from 1gpt to 8gpt, however, linear gels have much lower

viscosity ranges and their viscosity could increase from 39 cp to 1242 cp as the concentration increased from 10 ppt to 40 ppt.

Table 1. Power law model equations and parameters (n, k) for HVFRs and linear gel.

HVFR Concentration, gpt				
Fluid Name	1	2	4	8
HVFR-1	$\mu = 186.03\gamma^{-0.56}$	$\mu = 378.98\gamma^{-0.59}$	$\mu = 969.33\gamma^{-0.64}$	$\mu = 2634.25\gamma^{-0.69}$
R-square	0.9996	0.9997	0.9998	0.9997
HVFR-2	$\mu = 192.87\gamma^{-0.70}$	$\mu = 552.64\gamma^{-0.73}$	$\mu = 1471.63\gamma^{-0.78}$	$\mu = 4478.22\gamma^{-0.82}$
R-square	0.9994	0.9996	0.9997	0.9998
HVFR-3	$\mu = 61.52\gamma^{-0.43}$	$\mu = 195\gamma^{-0.540}$	$\mu = 607.08\gamma^{-0.63}$	$\mu = 1815.35\gamma^{-0.69}$
R-square	0.9984	0.9987	0.9992	0.9994
Linear Gel Concentration, ppt				
Fluid name	10	20	40	
Linear Gel	$\mu = 11.44\gamma^{-0.10}$	$\mu = 172.98\gamma^{-0.38}$	$\mu = 1163.22\gamma^{-0.48}$	
R-square	0.9786	0.9955	0.9830	

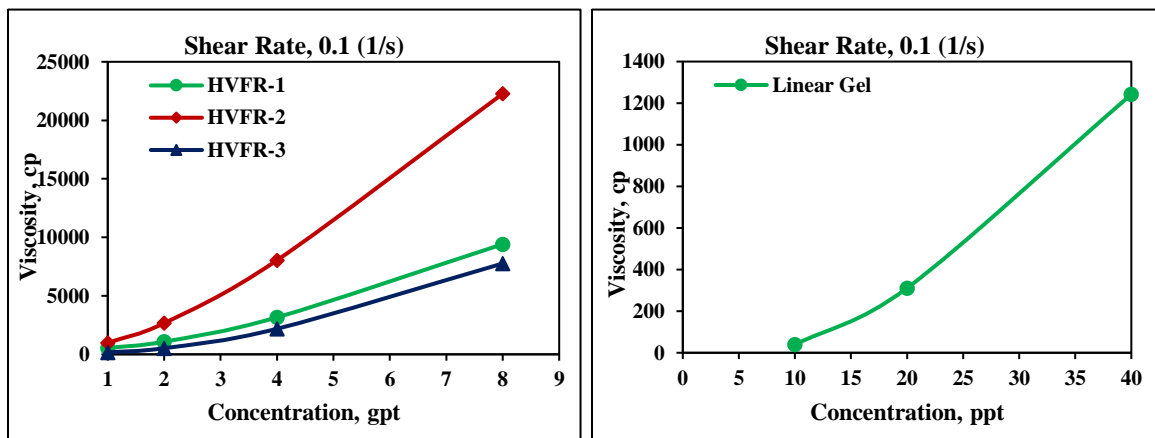


Figure 3. Viscosity as a function of concentration of HVFRs (left) and Linear gel (right) at low shear rates.

4.2. ELASTICITY MEASUREMENT RESULTS

The time associated with changing the structure of the polymer fluids is the relaxation time τ and it can be used to quantify the elasticity of the fluid. Since the HVFRs have a high molecular weight, understanding the elasticity is very important. To evaluate the viscoelastic characterizations of HVFRs, a small amplitude oscillatory shear test was carried out in the fluid solution's linear viscoelastic regime using an advanced rheometer with a parallel-plate system. Storage moduli (G') represents elastic responses and loss moduli (G'') represents viscous responses. Relaxation time is referred to as the inverse of the cross over point ($t = 1/\omega$) where G' is equal to G'' . The longer relaxation time of the fluid means has more elastic properties while the shorter relaxation time means the fluid carries less elastic properties. Figure 4 shows the G' and G'' of HVFR as a function angular frequency. All HVFR-2 concentrations were showing a good elastic property with high relaxation time ranges. The relaxation time increased with increasing the concentrations of HVFR.

In contrast, Figure 5 shows the storage modulus and loss modulus as a function of angular frequency for linear gel with very low elastic properties. At higher concentration of linear gel 40ppt, the elastic properties are much lower around 0.1 sec. Therefore, the linear gel might depend only on viscous properties to carry and place the proppant during hydraulic fracturing treatment.

Figure 6 showed the relaxation time was increased by increasing the fracturing fluid concentration for both fluids. In HVFR2, concentration of 4 gpt has a relaxation time of approximately 17 second, and it increased to 37 second at 8 gpt. The results show that HVFR-2 has a better elastic property than HVFR-1 and HVFR-3. Also, at similar

equivalent loading concentrations, results indicated that HVFRs have better elastic properties compare to liner gel. Even though concentration of linear gel increased to 40 ppt, it still has a very small relaxation time with around 0.1s.

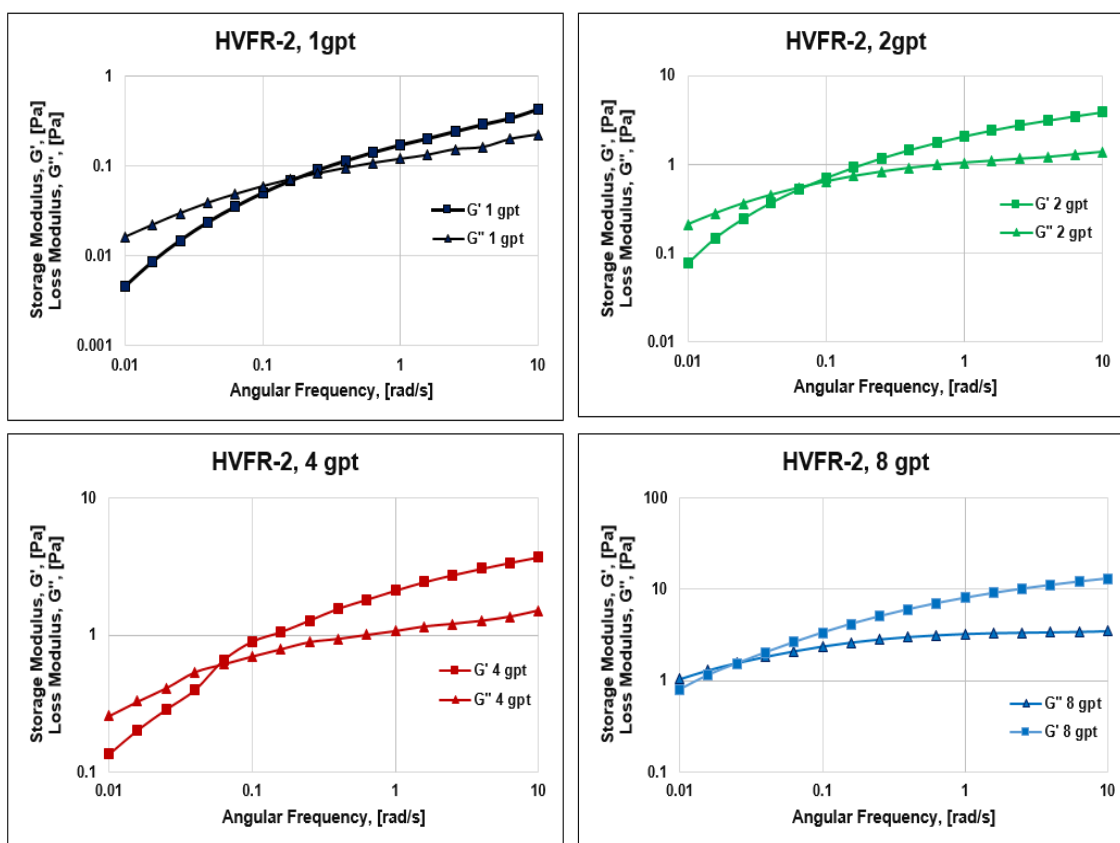


Figure 4. Elastic modulus and storage modulus η' as a function for HVFR-2 at different concentration.

It could be concluded that for all tested fluid samples, HVFRs fluid system have higher elastic properties than linear gel fluid system. Despite increasing the concentration of linear gel to 40 ppt, it still is showing very low elastic properties.

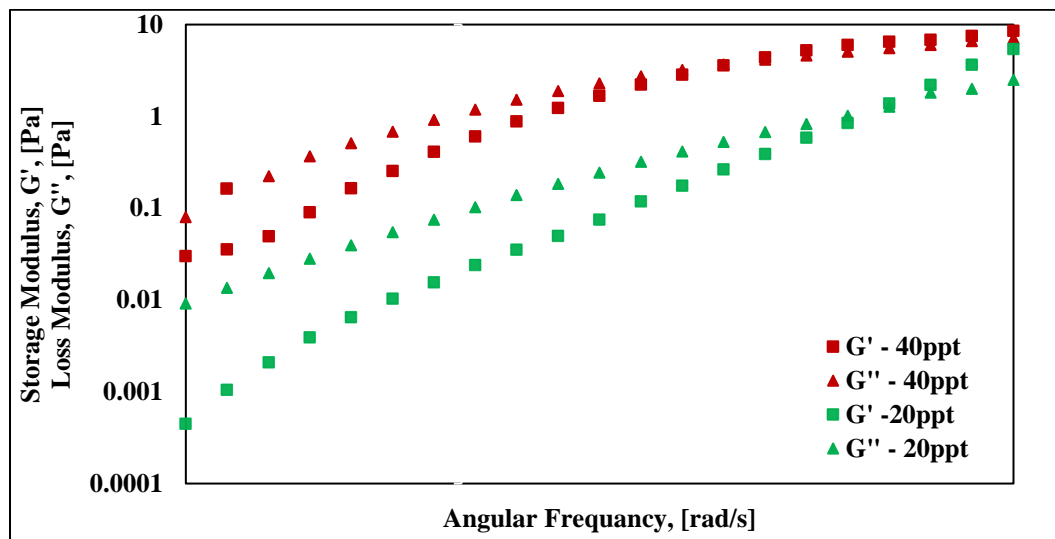


Figure 5. Elastic modulus and storage modulus as a function of angular frequency for linear gel at different concentrations 20ppt and 40ppt.

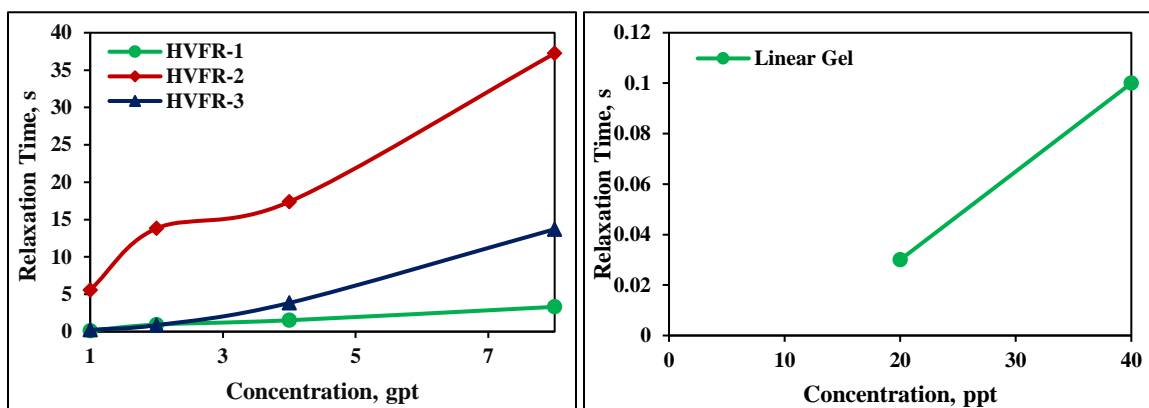


Figure 6. Relaxation time as a function of concentration of HVFR-1, HVFR-2, and HVFR-3 (left) and linear gel (right).

4.2.1. Normal Stress Measurements. Normal stress is another significant elastic property which can be measured by Rheometer as a function of shear rate. Figure 7 shows the normal stress (N1) as a function of shear rate of HVFR-2 at different loading. At low shear rates (from 0.1 to 10 s^{-1}) the normal stress was very low whereas increasing the shear rate above 10 s^{-1} showed an increase in normal stress. Normal stress was increased

substantially as the HVFR concentration increase. For example, at 1000s^{-1} the normal stress was 20 Pa and 285 Pa for 1gpt and 8gpt, respectively. This result is consistent with the elastic range trend measured previously by the relaxation time.

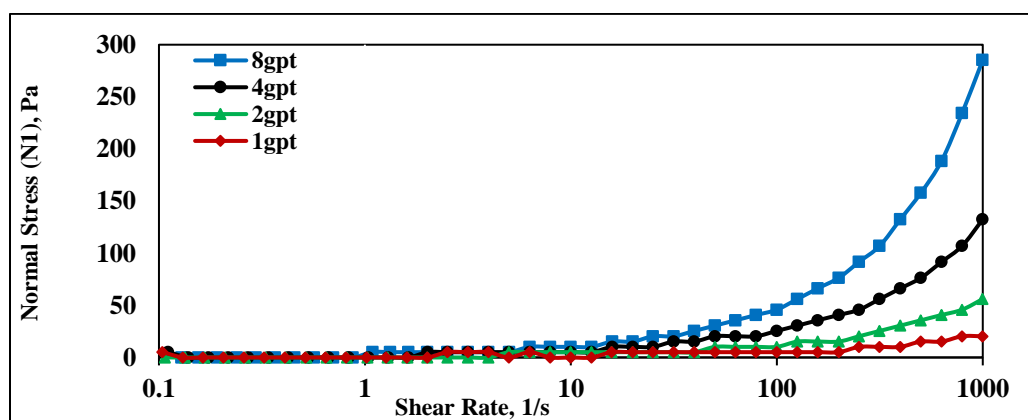


Figure 7. Effect of HVFR 2 concentration as a function in normal stress profile.

In Figure 8, although a high concentration of linear gel (40ppt) has been selected to examine the first normal stress N_1 , at high shear rate 1000s^{-1} , the N_1 was only 50 Pa. This elasticity is however still much less than HVFRs with a concentration of 4 gpt.

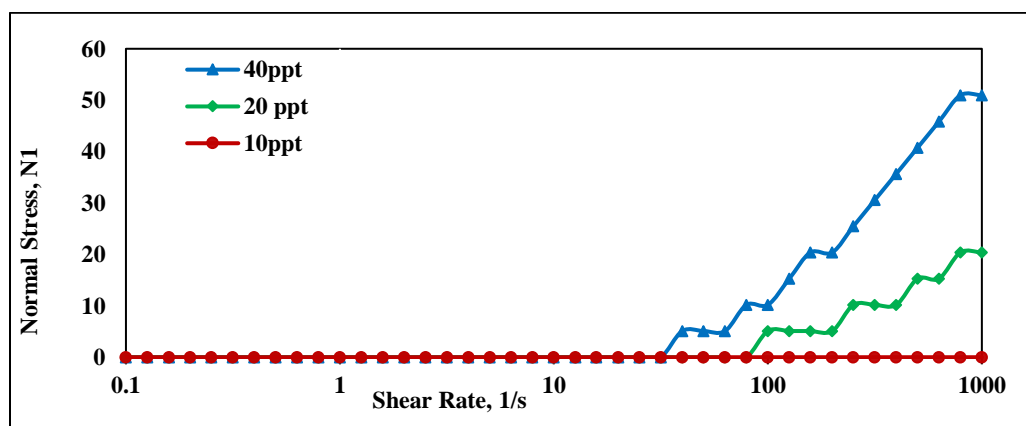


Figure 8. Effect of HVFR 2 concentration as a function in normal stress profile.

4.3. THERMAL STABILITY MEASUREMENT RESULTS

Figure 9 shows the rheological measurements for both HVFR-2 and linear gel at temperature ranges of 25 C°, 50 C°, and 80 C°. Results reveal that polyacrylamide-based HVFs systems have better thermal stability than linear gel at different shear rate ranges. Increased temperature to 50 C° did not show any change in viscosity profile, but when temperature increased to 80 C° little bit changes occurred. However, linear gel loses significantly its viscous properties with increasing shear rate when temperature increased to 80 C°. For example, at shear rate of 1 s⁻¹ the viscosity of linear gel dropped from 1000 cp to 100 cp as the temperature increased from 25 C° to 80 C°.

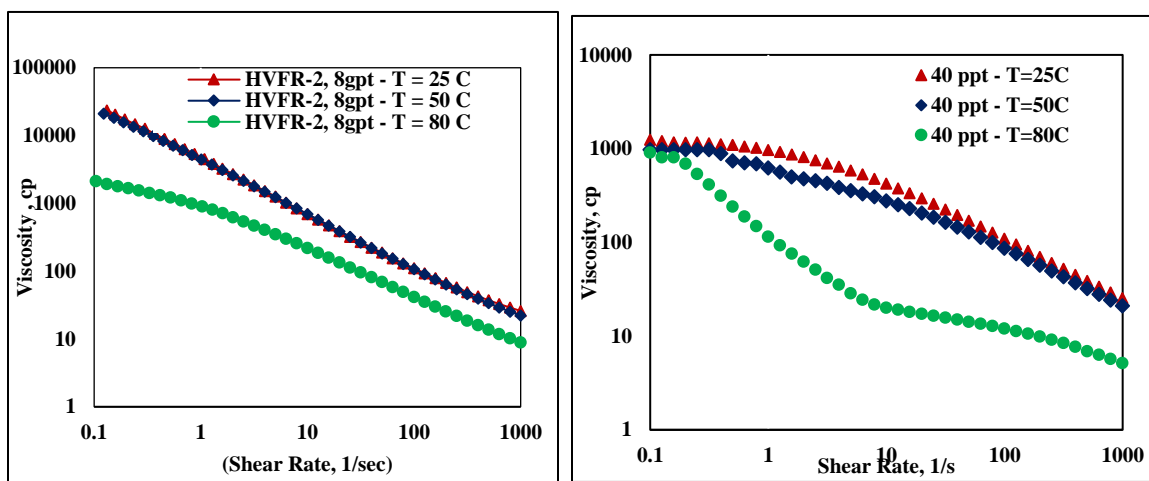


Figure 9. Thermal stability of viscosity as a function of shear rate of HVFR-2 (left) and linear gel (right).

Figure 10 shows the elastic effect (first normal stress N1) loses its properties with increasing temperature for both fracture fluids, but more significant for linear gel. At high shear rate of 1000 S⁻¹, normal stress for HVFR decreased from 340 Pa to 230 Pa and 70 Pa

as temperature increased from 25 C° to 50 C° and 80 C°, respectively. However, at same shear rate, normal stress for linear gel dropped significantly from 50 Pa to 10 Pa and 5 Pa within the same of temperature ranges.

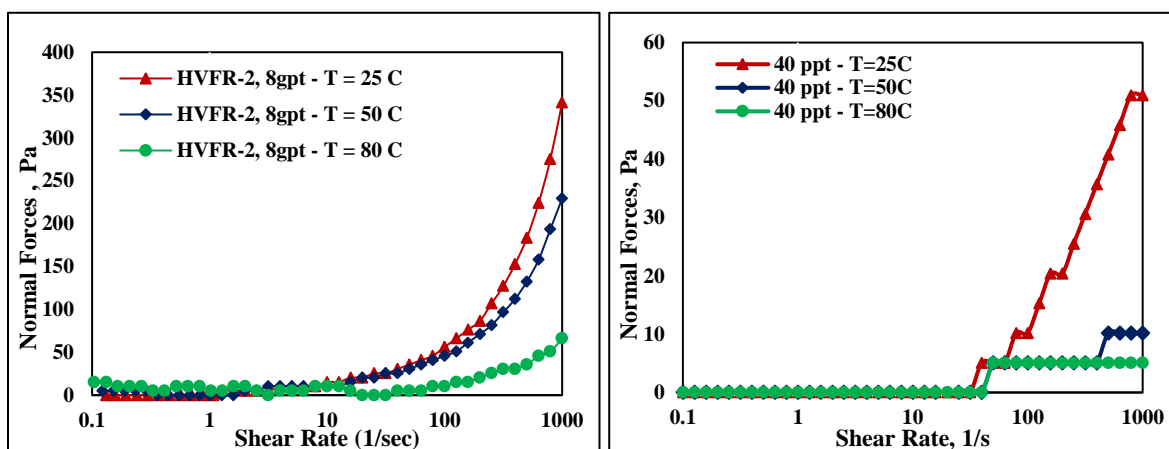


Figure 10. Thermal stability of viscosity as a function of shear rate of HVFR-2 (left) and linear gel (right).

4.4. SETTLING VELOCITY MEASUREMENT RESULTS

Several factors can control the proppant transport in complex fracture system including proppant type, proppant size, fracture geometry, and fracture fluid characteristics including viscosity and elasticity. This section is showing how the rheological and elastic properties of HVFR and linear gel could affect the proppant settling velocity.

4.4.1. Qualitative Multi-Particle Static Settling Velocity. To qualify the settling velocity of multi-particles, two different loadings (2 and 4gpt) of HVFR-2, and a loading of linear gel (20ppt) were hydrated in DI and mixed well with proppant concentration of 2 ppa. The mixture was poured immediately into a 100 ml graduated cylinder. A time lapse

camera was set up to capture the settling rate for certain time. All multi-particle static settling time have been measured in the lab conditions.

Figure 11 shows at a low load of HVFR-2 (2gpt) most of the proppant took 10 minutes to settle with few proppants were still suspended in the fluid. However, as it shown in Figure 12, as the concentration of HVFR increased to 4gpt a longer settling time (60 minute) was observed with more proppant still suspended at fluid. Proppant settling time in linear gel was significantly less than both concentrations of HVFR as it is shown in Figure 13. In linear gel loading of 20ppt, the proppant was settled completely at 15 seconds with very few proppants still suspended in the fluid. The settling rate in linear gel (20ppt) was almost 40 times higher than HVFR-2 (2gpt), this might occur because HVFR-2 has higher viscous and elastic properties than the linear gel fluid.

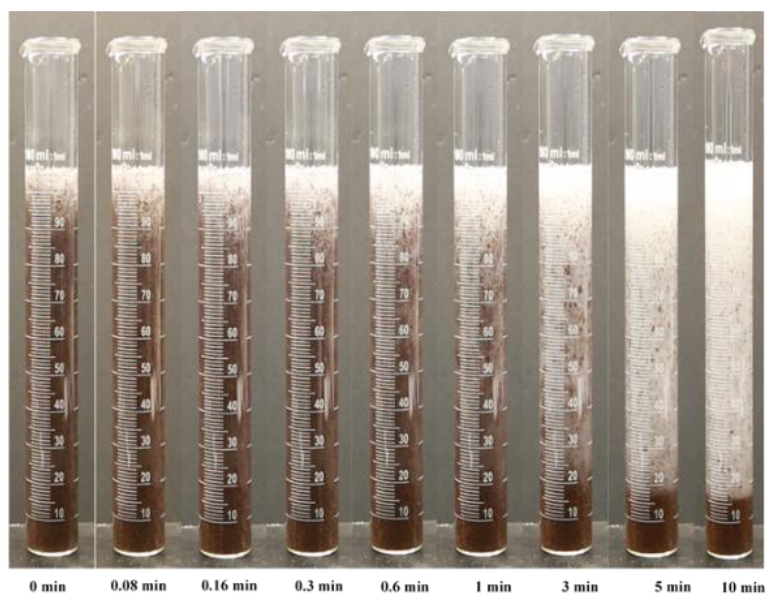


Figure 11. Multi-static measurement for proppant settling time using HVFR-2 (2gpt).

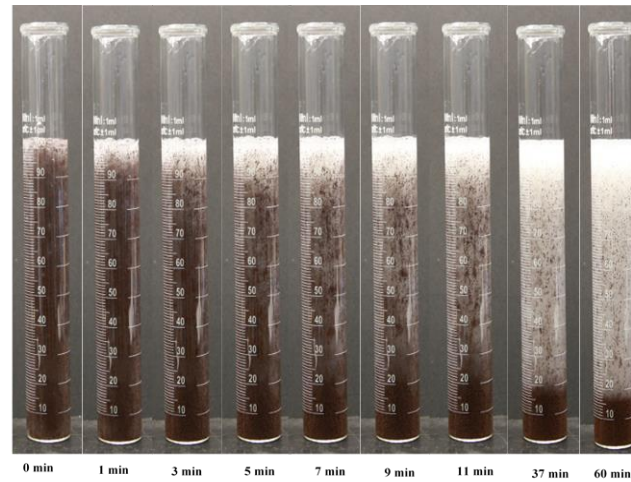


Figure 12. Multi-static measurement for proppant settling time using HVFR-2 (4gpt).

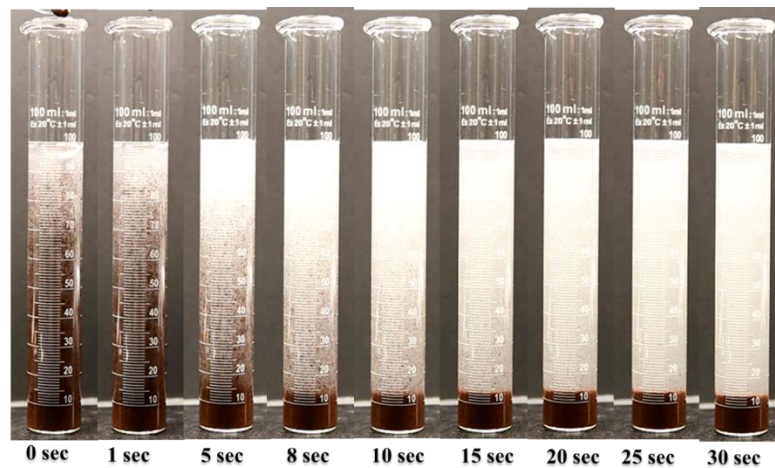


Figure 13. Multi-static measurement for proppant settling time using linear gel, (20 ppt).

4.4.2. Quantitative Single Particle Static Settling Velocity.

4.4.2.1. Proppant size effect on static settling velocity. Single particle static velocity measurements were performed in unconfined conditions using a HVFR-2 loading 2gpt and linear gel loading 20ppt at an ambient temperature. Three different glass beads sizes of 2 mm, 4 mm, and 6 mm were selected to study the effect of proppant sizes on

different fracture fluids. Figure 11 shows the terminal static settling velocity calculations for both fluids. Result clearly indicated that for all proppant sizes, proppant had higher settling velocities when it placed inside the linear gel compared to HVFR. For example, settling velocity of proppant size of 4 mm was 5 cm/sec for HVFR and increased significantly to 20 cm/sec for linear gel. These results indicate that HVFR could have better proppant suspension capability than linear gel. Results also indicated that increasing particle sizes increases the proppant settling velocity.

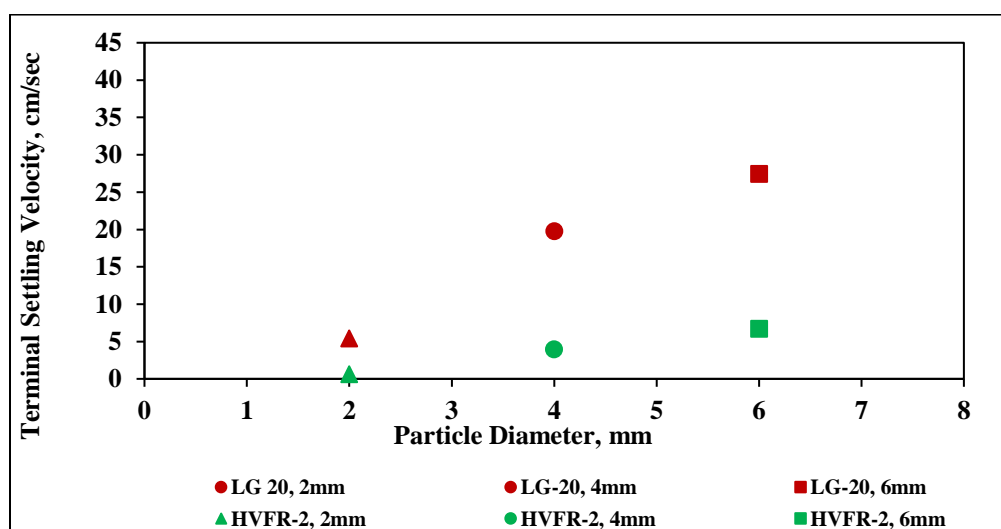


Figure 14. Effect of proppant settling velocity in HVFR-2 gpt vs. linear gel-20 ppt fracture fluids.

4.4.2.2. Effect of elasticity and viscosity properties on settling velocity. Figure 12 presented steady a shear rate-viscosity measurement profile as a function of shear rate for HVFR-2 loading of 2 gpt and linear gel loading of 20 ppt. The power law model (k, n) is fitted only for the shear rate ranges at which proppant shear rate results obtained from Figure 11 (ranges from 6.2 to 98 s^{-1}).

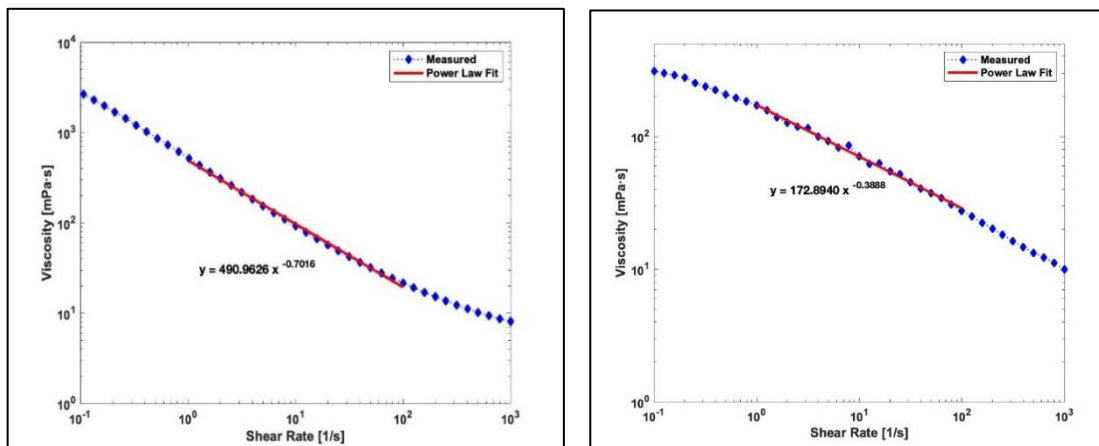


Figure 15. Viscosity as a function of shear rate for HVFR-2 loading 2 gpt (left) and linear gel loading 20 ppt (right).

To illustrate the particle settling behavior profile, the Weissenberg number is measured since it can be used to evaluate elasticity measurements. Table 2 presents the result of calculating the Weissenberg number as a function of experimental settling velocity measurement for different elastic property ($\lambda=14$ and 0.03) and approximately similar viscosity profile shear rate ranges. The results obtained from Weissenberg number was much higher in HVFR compared to linear gel. This implies that elastic properties might have significant effect on settling velocity compared with viscosity properties, but this trend still needs further study because both fracture fluids did not have a very similar viscosity profile.

The Elasticity to Viscosity Ratio ($\lambda e/\nu$) equation was also used to help in determining which properties of the fracture fluids demonstrated the particle settling velocity. Large shear rate ranges were used to cover the possible ranges of proppant transport shear rate that occurred with in hydraulic fracture.

Table 2. Weissenberg Number calculation as a function of relaxation time and particle shear rate.

Test Fluid	Relaxation time (s)	Diameter of Particles (mm)	Settling Velocity (cm/sec)	Weissenberg Number	Particle Shear Rate (1/s)
	14	2	0.63	87.6	6.26
HVFR-2	14	4	3.93	274.8	19.63
	14	6	6.69	312.0	22.29
	0.03	2	5.39	1.6	53.93
LG - 20	0.03	4	17.75	2.7	88.77
	0.03	6	29.43	2.9	98.10

Table 3 presents the Power law model equations for the relationship between viscosity and shear rate as well as the exponential model for the first normal stress for both HVFR-2 and linear gel to calculate elastic/viscous ratio. Figure 13 shows that for HVFR-2 loading 2 gpt, the equation $\lambda_{e/v} = 0.69 \dot{\gamma}^{1.4}$ indicates that elasticity becomes more dominate when the shear rate is larger than $1.26s^{-1}$. For linear gel (20 ppt), elastic effects are almost negligible since the contribution of elasticity become more important when shear rates are larger than $501s^{-1}$ as illustrated by $\lambda_{e/v} = 0.0008 \dot{\gamma}^{1.17}$. The results could also be indicated that elastic properties of HVFR dominate proppant transport within a wide range of shear rates covering large portion of hydraulic fracture where shear rates across fracture decreases as proppant transport deep inside fracture. However, still more

work is needed to confirm these results where fracture fluids with similar viscosity ranges have different elastic properties or vice versa are required for such investigations.

Table 3. Elastic/Viscous ratio $\lambda_{e/v}$ calculations.

The Ratio of Elasticity to Viscosity Calculation			
Fluid name	Viscosity equation from viscosity profile	Elasticity equation from N1 profile	Elastic/Viscous ratio
HVFR-2 gpt	$\eta(\dot{\gamma}) = 0.552\dot{\gamma}^{-0.73}$	$N_1(\dot{\gamma}) = 0.548\dot{\gamma}^{0.665}$	$\lambda_{e/v} = 0.69 \dot{\gamma}^{1.4}$
R-square	0.9996	0.968	
Linear Gel- 20 ppt	$\eta(\dot{\gamma}) = 0.172\dot{\gamma}^{-0.38}$	$N_1(\dot{\gamma}) = 0.096\dot{\gamma}^{0.798}$	$\lambda_{e/v} = 0.0008 \dot{\gamma}^{1.17}$
R-square	0.9955	0.9169	

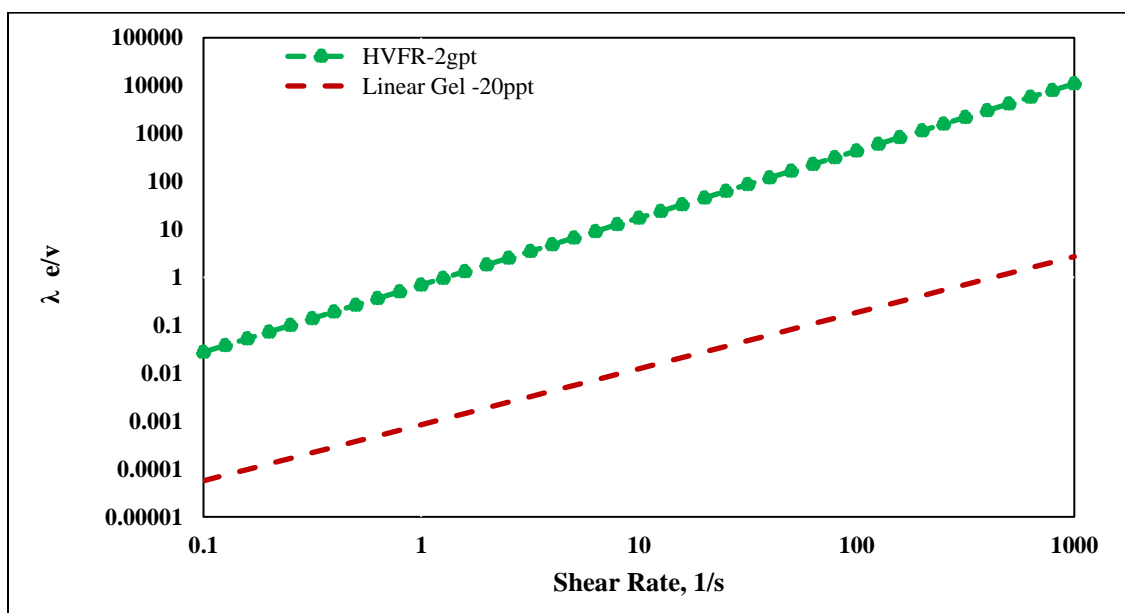


Figure 16. Calculated elastic/viscous ratio as a function of shear rate for HVFR-2, 2 gpt and Linear gel – 20 ppt.

5. COST ANALYSIS

HVFRs are in high demand now in hydraulic fracturing processes instead of conventional linear gel systems due to economical and operational factors. Economically, using HVFRs reduces chemical volume costs from 48 to 33%, and the volume can also be reduced by 30% when switching to the HVFR system (Motiee et al, 2016; Domelen et al, 2017). Moreover, there is potential of using less equipment on location due to HVFRs having high solubility in water so there is no need for a hydration unit or blending in the field. This paper presents that using a low loading of HVFR provides much better result compared to the using a common concentration of linear gel (20 ppt).

Table 4. Stimulation summary of case study (Dahlgren et al, 2018).

	SW	HVFR	18#	18# XL	TOTAL	100	40/70	TOTAL
	MBL	MBL	LIN	MBL	FLUID MBL	MESH	MM#	PROP MM#
			MBL			MM#		
Well 1	243	0	21	41	305.4	4.7	7.6	12.3
Well 2	251	56	0	0	307.3	4.7	7.6	12.3

Dahlgren et al, 2018 presented field case studies of using HVFRs in the STACK play. Interestingly, one of these was a comparison between two wells completed identically in fracturing design. Well 1 was treated with a hybrid guar-based fluid system consisting of 18# linear gel and 18# crosslinked. Well 2 used a HVFR starting with 5 gpt and ending the fracture treatment with 3 gpt of HVFR. All the other parameters were the same in both

stimulation processes in well 1 and well 2 as shown in the Table 4. The field results showed an over 30% improvement in production as well as chemical cost reduction of 32% in well 2 where HVFR was used compared to using guar-based fluids in well 1.

6. CONCLUSIONS

This laboratory study investigated rheological and elastic properties of high viscous friction reducer fracture fluids. Proppant settling velocity was also investigated at different conditions. The outcomes of this work give valuable insights into the properties and performance of high viscous friction reducer fracture fluids compared to linear gel fluids. The following conclusions can be drawn from this work:

- High viscous friction reducer-based fluids with low concentrations of HVFR's have better viscosity and elastic properties than fluids with typical concentrations of linear gel.
- High viscous friction reducers have better thermal stability than linear gel. Viscosity and elastic properties of high viscous friction reducers did not change significantly compared to linear gel at temperature ranges less than 80 °C.
- High viscous friction reducer showed better elastic properties than linear gel for different shear rate ranges. This implies that high viscous friction reducer-based fluids have better proppant carrying capability along fractures than linear gel.

- Proppant static settling velocity was much higher linear gel fluids compared to high viscous friction reducer-based fracture fluids. The proppant settling velocity is approximately 40x less when using high viscous friction reducer.

REFERENCES

- Arnipally, S. K., & Kuru, E. (2018, October 1). Settling Velocity of Particles in Viscoelastic Fluids: A Comparison of the Shear-Viscosity and Elasticity Effects. Society of Petroleum Engineers. <https://doi:10.2118/187255-PA>
- Ba Geri, M., Imqam, A., & Dunn-Norman, S. (2018, October 5). Proppant Transport Behavior in Inclined Versus Vertical Hydraulic Fractures: An Experimental Study. Society of Petroleum Engineers. <https://doi:10.2118/191813-18ERM-MS>
- Ba Geri, M., Imqam, A., & Flori, R. (2019, April). A Critical Review of Using High Viscosity Friction Reducers as Fracturing Fluids for Hydraulic Fracturing Applications. Society of Petroleum Engineers. <https://doi:10.2119/195191-MS>
- Broadbent, J.M., Mena, B., 1974. Slow flow of an elastico-viscous fluid past cylinders and spheres. Chem. Eng. J. 8, 11–19.
- Dahlgren, K., Green, B., Williams, B., Inscore, J., Domelen, M. V., & Fenton, A. (2018, January 23). Case Studies of High Viscosity Friction Reducers HVFR in the STACK Play. Society of Petroleum Engineers. <https://doi:10.2118/189893-MS>
- Drylie, S., Duenckel, R., Barree, R., & Hlidek, B. (2018, September 24). An Investigation of Proppant Transport in Friction Reducer Fluid Systems Utilizing a Large Slot Flow Apparatus. Society of Petroleum Engineers. <https://doi:10.2118/191720-MS>
- Hu, Y. T., Chung, H., & Maxey, J. E. (2015, February 3). What is More Important for Proppant Transport, Viscosity or Elasticity? Society of Petroleum Engineers. <https://doi:10.2118/173339-MS>
- Hu, Y. T., Fisher, D., Kurian, P., & Calaway, R. (2018, January 23). Proppant Transport by a High Viscosity Friction Reducer. Society of Petroleum Engineers. <https://doi:10.2118/189841-MS>

- Johnson, M., Winkler, A., Aften, C., Sullivan, P., Hill, W. A., & VanGilder, C. (2018, October 5). Successful Implementation of High Viscosity Friction Reducer in Marcellus Shale Stimulation. Society of Petroleum Engineers. <https://doi:10.2118/191774-18ERM-MS>
- Khan, A.R., Richardson, J.F., 1987. The resistance to motion of a solid sphere in a fluid. Chem. Eng. Sci. 62, 135–150
- Lali, A. M., Khare, A. S., Joshi, J. B. et al. 1989. Behaviour of Solid Particles in Viscous Non-Newtonian Solutions: Settling Velocity, Wall Effects and Bed Expansion in Solid-Liquid Fluidized Beds. Powder Tech. 57 (1): 39–50. [https://doi.org/10.1016/0032-5910\(89\)80102-0](https://doi.org/10.1016/0032-5910(89)80102-0).
- Loveless, D., Holtsclaw, J., Saini, R., Harris, P. C., & Fleming, J. (2011, January 1). Fracturing Fluid Comprised of Components Sourced Solely from the Food Industry Provides Superior Proppant Transport. Society of Petroleum Engineers. <https://doi:10.2118/147206-MS>
- Malhotra, S. & Sharma, M.M. Settling of Spherical Particles in Unbounded and Confined Surfactant-Based Shear Thinning Viscoelastic Fluids: An Experimental Study. Chemical Engineering Science. 84, 646-655 (2012).
- Montgomery, C. (2013, May 20). Fracturing Fluid Components. International Society for Rock Mechanics and Rock Engineering.
- Motiee, M., Johnson, M., Ward, B., Gradl, C., McKimmy, M., & Meeheib, J. (2016, February 1). High Concentration Polyacrylamide-Based Friction Reducer Used as a Direct Substitute for Guar-Based Borate Crosslinked Fluid in Fracturing Operations. Society of Petroleum Engineers. <https://doi:10.2118/179154-MS>
- Renaud, M., Mauret, E., Chhabra, R.P., 2004. Power-law fluid flow over a sphere: average shear rate and drag coefficient. Can. J. Chem. Eng. 82,1066–1070.
- Shah, S.N., Fadili, Y.E., Chhabra, R.P., 2007. New model for single spherical particle settling velocity in power law (visco-inelastic) fluids. Int. J. Multiphase Flow 33, 51–66.
- Schein, G. (2005, January 1). The Application and Technology of Slickwater Fracturing. Society of Petroleum Engineers.
- Shen, L., Vigderman, L., Heller, D., & Fu, D. (2018, August 9). Can Friction Reducers Transport Sand During Fracturing Treatment? Unconventional Resources Technology Conference. <https://doi:10.15530/URTEC-2018-2873723>

- Van Domelen, M., Cutrer, W., Collins, S., & Ruegamer, M. (2017, March 27). Applications of Viscosity-Building Friction Reducers as Fracturing Fluids. Society of Petroleum Engineers. <https://doi:10.2118/185084-MS>
- Tripathi, A., Chhabra, R.P., Sundararajan, T., 1994. Power-law fluid over spheroidal particles. *Ind. Eng. Chem. Res.* 33, 403–410.
- Uhlherr, P.H.T., Le, T.N., Tiu, C., 1976. Characterization of inelastic power-law fluids using falling sphere data. *Can. J. Chem. Eng.* 54, 497–502

III. STATIC PROPPANT SETTLING VELOCITY CHARACTERISTICS IN HIGH-VISCOSITY FRICTION REDUCERS FLUIDS FOR UNCONFINED AND CONFINED FRACTURES

Mohammed Ba Geri¹, Ralph Flori¹, Abdulmohsin Imqam¹, Andrey Bogdan², and Lingjuan Shen²

1: Department of Petroleum Engineering, Missouri University of Science and Technology, Rolla, MO 65409

2: BJ Services, Tomball, TX

ABSTRACT

Measuring proppant settling velocity in high viscosity friction reducers (HVFRs) plays a critical key for evaluating proppant transport in hydraulic fracture treatment. Settling of particles is governed by several factors such as fluid rheology (viscosity and elasticity), proppant size, retardation confining walls effect, and fracture orientation. The objective of this experimental study was to determine how these factors would influence particle settling velocity in hydraulic fracturing applications.

The experiments were conducted in unconfined and confined fluid conditions. Fracture cell was designed in certain ways to capture the impact of fracture orientation by 45°, 60°, and 90° on settling velocity.

Results showed HVFR provided better proppant transport capability than regular FRs used in slickwater. Proppant settling velocity using HVFR was decreased by 80%. Results obtained from confined fluid experiments showed that proppant settling velocity decreased due to the confining walls exert retardation impact. The wall retardation was also

reduced as the fracture width increased. Changing fracture orientation from vertical position (90 degree) to 45 degree led to high reduction in proppant settling velocity.

1. INTRODUCTION

The free settling velocity of solid particles in different fluid media is generally encountered in a wide variety of industrial processes. Understanding particles behavior and particles settling plays a vital role in optimizing design and operation in various industrial applications including proppant transport in hydraulic fracturing, gas flow through pipe lines, and cutting transport during drilling operations as discussed by Arnipally and Kuru, 2018. Increasing the efficiency of proppant transport distribution in hydraulic fracture treatment is required and relies on the knowledge of settling velocity of the particles. Settling of particles is governed by several factors such as fluid rheology (elasticity and viscosity), proppant size, retardation confining walls effect, and fracture orientation. Since quantifying the relationship between drag coefficient and Reynolds' number of particles is the most significant to know, it is required to get the values of the particles settling velocity. Settling velocity at higher Reynolds numbers has been studied extensively and expressed for the calculation of drag force (Clift et al., 1978; Khan and Richardson, 1987; Zapryanov and Tabakova, 1999; Michaelides, 2002, 2003).

Recently, the oil industry started to use HVFRs as a direct replacement for linear and crosslinked gels due to several operational and economic reasons (Motiee et al., 2016; Ba Geri et al., 2019), such as reducing pipe friction during the fracturing process, placing more proppant, creating more complex fracture networks due to a less viscous system,

possible higher fracture conductivity, and potentially lower costs due to fewer chemicals and less equipment on location (Motiee et al., 2016; Van Domenlen et al., 2017; Dahlgren, et al., 2018; Ba Geri et al. 2019b).

Predicting particles settling velocity and proppant transport in different types of hydraulic fracturing fluids was attained by (Clark and Zhu, 1996; Gadde et al. 2004) studied how settling velocity can be affected by changing proppant size, fracture width, velocity of fluid, and rheology properties of fluids. The study concluded that Stoke's law is not accurate for predicting proppant settling rate. Motiee et al. (2016) studied high concentration friction reducers (HCFR) as a direct substitute for guar-based fluid. Different concentrations of HCFR (2, 4, 6, and 8 gpt) were compared with 25 ppt linear gel to study proppant settling velocity. HCFR showed better proppant settling velocity relative to guar-based fluids. Tong et al. (2017) conducted experimental and simulation studies about proppant transport in fracture intersections using slickwater. They concluded that increasing shear rate causes reduction on equilibrium bed height, and increased proppant dune length.

Shen et al. (2018) investigated rheological characterization of HVFRs and measured the settling velocity of multi-particle proppant. They concluded that both the viscosity and elasticity of HVFRs can affect the proppant carrying capacity during hydraulic fracturing treatments. Hu et al. (2018) addressed some concerns related to proppant transport capability using HVFRs and linear gel. They observed that normal forces for linear gels are much lower than HVFRs with increased shear rate. Dahlgren et al., (2018) identified three case studies in which the operator in STACK play replaced traditional fracturing fluid with HVFR. The study noticed that the viscosity profile was

negatively affected by breaker. Johnson et al. (2018) presented a successful implementation of high brine friction reducers (HBFRs) in high TDS water exceeding 60,000TDS. They observed that the viscosity of HBFRs decreased with increased brine concentration ranges. Drylie et al. (2018) conducted viscosity measurements at a high shear rate of 511 s^{-1} and a low shear rate 0.01 s^{-1} for 1 gpt and 6 gpt of HVFR and 24 ppt of guar. The study noticed that 1gpt of HVFR did not change the viscosity profile significantly; in contrast, at a low shear rate HVFRs had much higher viscosity than guar. Ba Geri et al. (2018) investigated experimentally the effect of fracture inclination on proppant transport. The study concluded that inclination of fractures can significantly impact on proppant transport due to the friction or contact force, which comes from the fracture wall. Although this work studied the proppant transport using HVFR, there was not much work comparing this settling velocity of HVFRs with traditional slickwater fluids.

Additionally, even though a lot of work has been performed to understand the proppant settling velocity in HVFR, the effect of confined and unconfined fractures on static proppant settling velocity measurements has not been thoroughly investigated. This work will conduct laboratory work intensively to fill the knowledge gap. This study investigated five factors that could affect proppant settling velocity performance: viscosity profile, elasticity (Normal forces and relaxation time), proppant size, wall effect, and fracture orientation.

2. PROPPANT STATIC SETTLING VELOCITY

This study provides insights on the wall effect factor on measuring proppant static settling velocity. It also evaluates the elastic and viscous properties of HVFRs fluid through calculating the elasticity to viscosity ratio.

2.1. WALL EFFECT (F_w)

Proppant settling velocity plays vital factor during proppant transport in complex fracturing system due to the very narrow widths of natural fractures. Therefore, the ratio between the proppant diameters and the fracture width is pointed out in this study. For Newtonian fluids, (Faxen, 1922) addressed the wall effect on settling velocity on creeping flow regime. The study concluded that wall factor depends on the ratio between particle diameters to cell width. A retardation effect of walls on particle settling velocity reduced the settling velocity. This retardation effect can be quantified as wall factor (F_w). The wall factor defines as the ratio between the particles settling velocity in confined walls to settling velocity in unconfined fluids as shown in the Eq. 1 (Malhotra and Sharma, 2013)

$$F_w = \frac{\text{Settling velocity in confining walls}}{\text{Settling velocity in unconfining fluid}} \quad (1)$$

If $F_w > 1$, settling velocity is affected by confining walls;

if $F_w \leq 1$, wall effect is negligible.

2.2. PARTICLE SHEAR RATE ($\dot{\gamma}$)

Calculating apparent particle shear rate leads to avoid overestimation or underestimation of the right value of particle shear rate, therefore, determine the particle

shear rate range within the Power law model (K, n) is essential step to describe the shear thinning effect of the HVFRs fluids Ba Geri et al., (2019b). Eq. 2 can be used to estimate the particle shear rate:

$$\dot{\gamma} = 2 * V_s d_p \quad (2)$$

where $\dot{\gamma}$ is the particle shear rate; V_s is the terminal settling velocity; d_p is the particle diameter.

2.3. ELASTICITY TO VISCOSITY RATIO ($\lambda_{e/v}$)

Viscoelastic fluids consist of two main properties (viscosity and elasticity). To evaluate which property gives the greatest contribution during proppant transport. Equation 4 was used to measure the elasticity to viscosity ratio ($\lambda_{e/v}$) (Shen et al., 2018):

$$\lambda_{e/v} = \frac{0.5\tau N_1(\dot{\gamma})}{\eta(\dot{\gamma})} \quad (3)$$

where, $\lambda_{e/v}$ is the elasticity to viscosity ratio $N_1(\dot{\gamma})$ is the first normal stress, τ is relaxation time, and $\eta(\dot{\gamma})$ is the shear viscosity.

The numerator consists of the elasticity portion (relaxation time τ and first normal stress $N_1(\dot{\gamma})$) and the denominator is a function of only the viscosity profile ($\eta(\dot{\gamma})$). The elastic/viscous ratio demonstrated by elasticity once their value more than one while if the elastic/viscous ratio less than one that indicates is the viscosity play main role during proppant transport.

2.4. FORCES INFLUENCED PARTICLES SETTLING VELOCITY

The most common correlation was derived by Stokes which can be used to calculate settling velocity V_s if the Reynolds number and drag coefficient C_D are known, which are shown in Eq. 6 – 8 (Arnipally and Kuru, 2018):

$Re_p < 1$ (creeping flow regime)

$$Re_p = \frac{D_p V_s \rho_f}{\mu_f} \quad (4)$$

$$C_D = \frac{24}{Re_p} \quad (5)$$

$$V_s = \frac{(\rho_s - \rho_f) g D_s^2}{18 \mu_f} \quad (6)$$

Three main forces dominate the vertical motion of solid particles in a fluid: gravitational force; F_G , buoyancy force F_B ; and drag force; F_D (Arnipally, 2018).

$$F_g = \rho_p v_p g \quad (7)$$

$$v_p = \pi d_p^3 / 6 \quad (8)$$

$$F_b = \rho v_p g \quad (9)$$

$$F_D = \frac{C_D A \rho_f V^2}{2} \quad (10)$$

where ρ_p is the particle density, v_p is the volume of the particle, ρ_f is the fluid density, d_p is the particle diameter, g is the acceleration due to gravity (9.81 ms^{-2}). C_D is the drag coefficient, A is the projected area, and V is the settling velocity.

3. EXPERIMENT DESCRIPTION

3.1. MATERIALS

3.1.1. Hydraulic Fracturing Fluids. The fracturing fluid tested was regular FR (without adding any chemical additives) and HVFR-3.

3.1.2. Preparing Fracturing Fluids. According to standard industry practice of using HVFR-3, four different concentrations (1, 2, 4, 8 gpt) of HVFRs were prepared by mixing with deionized (DI) water Shen et al., (2018).

3.1.3. Proppant Sizes. Sand proppant size 20/40, 30/50, and 40/70 mesh obtained from U.S. Silica and spherical glass beads sizes (2mm, 4mm, and 6mm) were used to measure proppant terminal settling velocity.

3.1.4. Rheometer. A high accuracy advanced MCR 302 Anton-Paar rheometer with a parallel-plate system was used to measure viscosity-shear profile, normal forces, and the dynamic oscillatory-shear measurements at lab temperature conditions.

3.2. EXPERIMENT SETUP

3.2.1. Unconfined Fracture Wall Experiments. Figure 1 shows the setup of an unconfined settling velocity measurement. The experiment was performed in a 1000 ml transparent glass graduated cylinder with a diameter at least 25 times of the proppant diameter to ensure that proppant settling velocity was not influenced by the walls of the glass container Malhotra and Sharma, (2013). In addition, a foot ruler was placed alongside the glass container to measure the fluid level inside the model.

3.2.2. Confined Fracture Wall Experiments. Figure 2 shows the schematic of the experimental fracture cells setup. The fracture cell model dimensions are 50 cm height and 7 cm length and kept the same for all the experiments. Fracture cells were constructed of two Plexiglas plates in parallel. The spacing between the two parallel Plexiglasses of the cell is made by gasket rubber to mimic the fracture width. Two different fracture widths were studied: 3 mm, and 9 mm. At this point, the cell was filled by either regular FR or HVFR fluid and positioned vertically. High-resolution video camera up to 2000 fps used to record the proppant settling process. Captured videos were tracked and analyzed using a video analysis software. The fracture slot apparatus was illuminated with 4000 Lumens 2X2 ft – LED Vapor tight fixture to add extra light. Proppant sizes of 20/40, 30/50, and 40/70 mesh were used to conduct experiments.

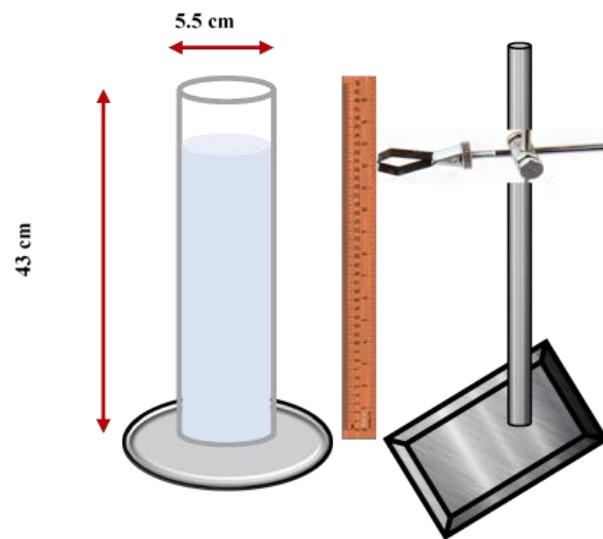


Figure 1. Schematic of fracture setup for unconfined fluids.

Numerous of natural fractures might be inclined from the main fracture by different angles during fracturing. Understanding proppant settling behavior in inclined fracture is essential for proppant transport in fracture treatment. Three different angles 45° , 60° and 90° have been investigated to mimic inclined fracture. The configuration of this experiment is to model the particle-wall friction occurred due to the interaction between particles and inclined walls effect. Confined fracture wall setup was positioned as illustrated in Figure 3 to observe the fracture inclination effect. Spherical proppants were used with diameter ranges of 2 mm, 4 mm, and 6 mm. The motion of proppant rolling down in the inclined cells acting under four forces gravitational force, F_G , buoyancy force F_B , drag force, F_D , and F_r friction force.

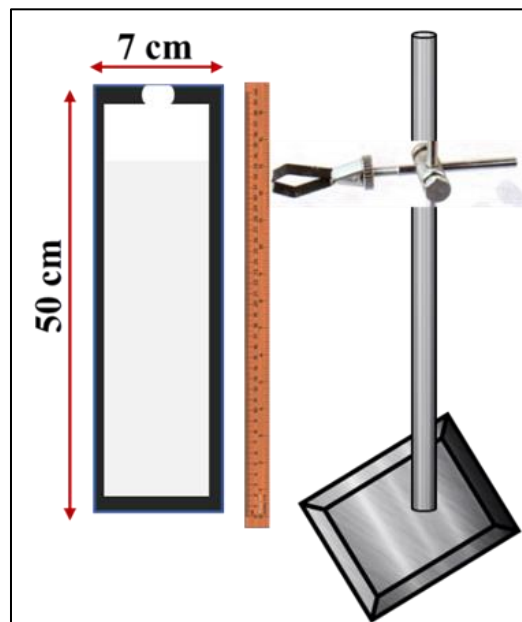


Figure 2. Schematic of fracture setup for confined fluids.

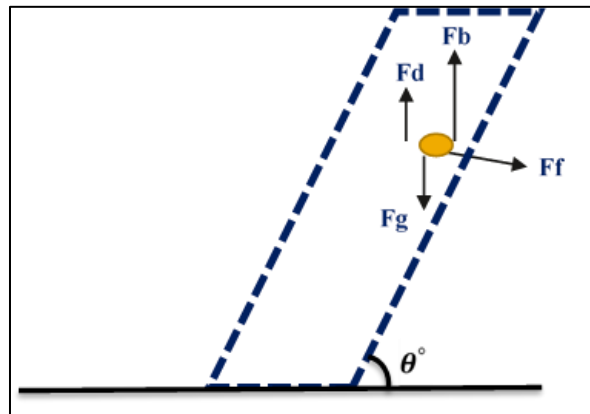


Figure 3. Schematic of the experimental fracture cell for measuring inclination angle effect.

3.3. EXPERIMENT PROCEDURES

3.3.1. Viscosity Rheological Characterization of the HVFRs.

3.3.1.1. Viscosity profile measurement. Steady shear-viscosity rheological test was performed using an advanced rheometer with a parallel-plate system (PP50/TG using a 0.30 mm gap). To investigate the viscous behavior, the test was implemented by varying shear rate from 0.1-1000 s^{-1} with measurements at 21 point/decade.

3.3.1.2. Elasticity profile measurement. The dynamic oscillatory-shear were conducted to measure the elasticity profiles including first normal stress N1, relaxation time, and elastic modulus G' . The oscillatory test was implemented over a range of frequencies from 0.01-100 Hz. All rheological property measurements were conducted at 25 °C.

3.3.1.3. Static settling velocity measurement. Once the fracturing fluid samples were prepared at the desired concentration, these samples were placed in unconfined and confined fluids to measure the proppant settling velocity. To achieve more accurate results,

air bubbles were removed from the test fluid by leaving the fluid to rest overnight, as bubbles affect both rheology and settling velocity measurements. Next, the proppant was dropped into the fluid column and the camera started capturing the proppant movement.

An image analysis tool called “Tracker” (<http://www.cabrillo.edu/~dbrown/tracker/>) was applied to get accurate measurements of vertical position of the proppant at different time steps. The slope relationship between proppant vertical positions to time steps is called terminal settling velocity. For more accurate results, settling velocity of each particle was repeated several times Ba Geri et al., 2018.

3.3.2. Static Settling Velocity Calculations Based on Power Law Parameters

(K, n). Static settling velocity of spherical particles in viscoelastic power law fluids can be calculated using the developed model of Shah et al., (2007). Two constants (A, B) were employed as a function of power law parameters n, k. The procedure to calculate the settling velocity of a spherical particle in viscoelastic Power law fluid is as follows:

Step-1:

$$A = 6.9148 n^2 - 24.838n + 22.642 \quad (11)$$

$$B = -0.5067 n^2 + 1.323n - 0.1744 \quad (12)$$

Step-2:

$$(C_D^{2-n} Re^2)^{\frac{1}{2}} = \left(\frac{13.08^{2-n} d_p^{n+2} \rho_f^n (\rho_p - \rho_f)^{2-n}}{2^{2(n-1)} K^2} \right)^{\frac{1}{2}} \quad (13)$$

Step-3:

$$Re = \left[\frac{(C_D^{2-n} Re^2)^{\frac{1}{2}}}{A} \right]^{\frac{1}{B}} \quad (14)$$

Step-4:

$$V_{\infty INEL} = \left[\frac{2^{n-1} K Re}{d_p^n \rho_f} \right]^{\frac{1}{2-n}} \quad (15)$$

$$Velocity\ Ratio = \frac{V_{\infty EL}}{V_{\infty INEL}} \quad (16)$$

$V_{\infty EL}$: Experimental settling velocity of a particle in unconfined fluid

$V_{\infty INEL}$: Calculated on the basis of apparent viscosity data based on the power-law parameters (k, n)

4. RESULTS AND DISCUSSION

4.1. VISCOSITY MEASUREMENT RESULTS

Figure 4 shows viscosity measurement profile as a function of loading concentration. All the results exhibit that the HVFRs fluids follow a shear thinning behavior that as shear rate increases the viscosity decreases. At a loading of 8gpt, results for HVFR showed that HVFRs had high viscosity (7766 cp) at a lower shear rate of 0.1 s^{-1} which is around 46 times of the viscosity when the concentration decreased to 1gpt.

Table 1 shows the viscosity profile of four different concentrations (1, 2, 4, 8 gpt) of HVFR-3. All the measurements result of HVFRs exhibited that HVFR-3 fluid follows shear thinning behavior.

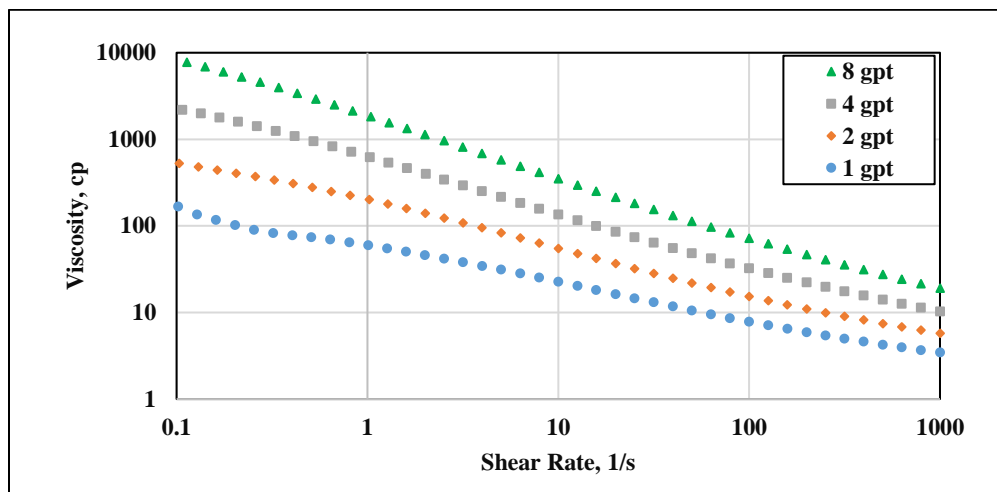


Figure 4. Effect of HVFR-3 concentration as a function in viscosity shear profile.

Table 1. Power law model equations and parameters (n, k) for HVFR-3.

HVFR Concentration, gpt (gallons per thousands of gallons)				
Fluid Name	1	2	4	8
HVFR-3	$\mu = 61.52\gamma^{-0.43}$	$\mu = 206\gamma^{-0.570}$	$\mu = 607.08\gamma^{-0.63}$	$\mu = 1815.35\gamma^{-0.69}$
R-square	0.9984	0.9987	0.9992	0.9994

4.2. ELASTICITY MEASUREMENT RESULTS

The Relaxation time τ can be used to quantify the elasticity of the polymer fluids. Since the HVFRs have high molecular weight, the understanding of the elasticity is very important. To evaluate viscoelastic characterizations of HVFR-3, small amplitude oscillatory shear was carried out in fluid solution's linear viscoelastic regime using an advanced rheometer with a parallel-plate system. Storage modulus (G') which represents elastic response, and loss modulus (G''), represents viscous response were both measured

at wide range of angular frequencies from 0.01-100 Hz. Relaxation time referred as the inverse of the cross over point ($t = 1/\omega$) where the G' equal to G'' . Figure 5 shows G' and G'' measurements as a function of angular frequency. The results showed that low loading at 1 gpt and 2 gpt had very low relaxation time. As the concentration of HVFR increased, the relaxation time became more significant. For example, at loading of 4 gpt the relaxation time was 4s and increased to 8 s when loading increased to 8 gpt. Normal stress is another significant elastic property of HVFRs which can be measured as a function of shear rate.

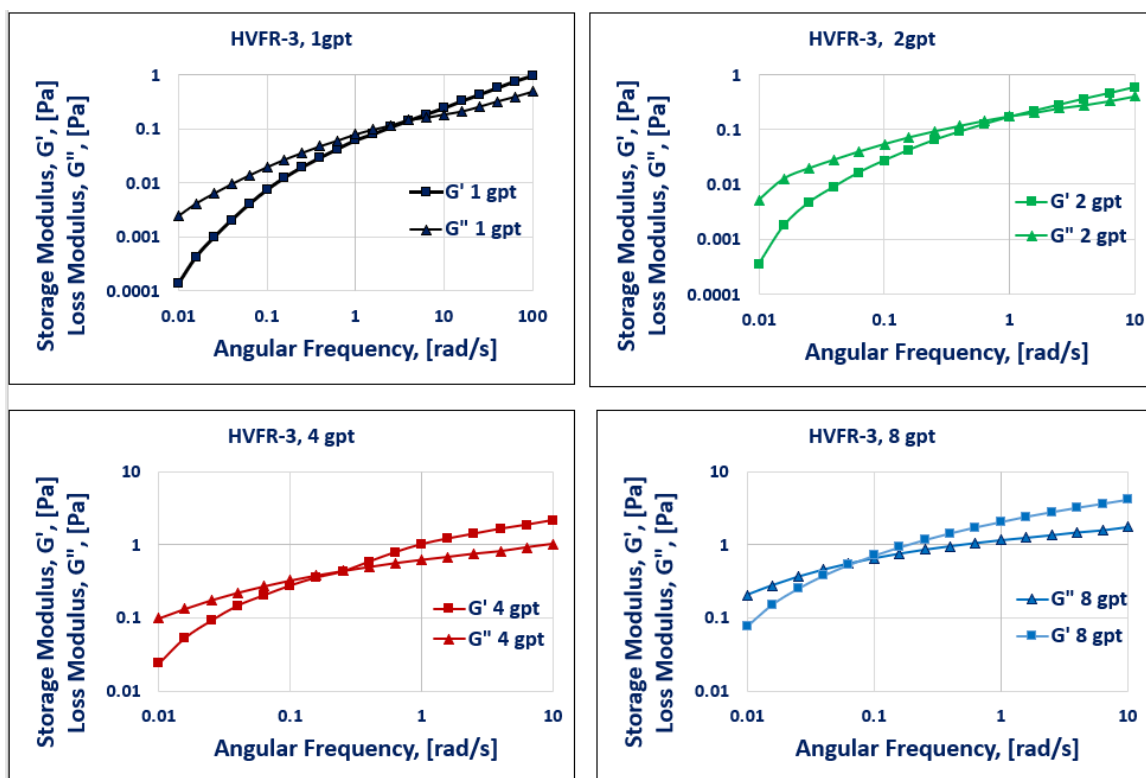


Figure 5. Elastic modulus G' and storage modulus G'' as a function of HVFR-3 concentrations.

The normal stress is zero in Newtonian fluids due to the isotropic of the fluid. However, in polymeric fluids such as friction reducers which can develop anisotropy in the

orientation between flow-gradient direction (τ_{yy}) and the flow (τ_{xx}) due to their microstructures, N_1 usually is not zero:

$$N_1 = \tau_{xx} - \tau_{yy} \quad (17)$$

$$N_1 = \tau_{yy} - \tau_{zz} \quad (18)$$

Figure 6 presents elastic property (normal force N_1) as a function of shear rate. At low shear rate the normal stress was very low and started to increase as the shear rate and loading of HFVRs increased. At low shear rates (from 0.1 to 10 s^{-1}) the normal stress was very low whereas increasing the shear rate above 10 s^{-1} showed an increase in normal stress. Normal stress was increased substantially as the HFVR concentration increase. For example, at 1000 s^{-1} the normal stress was approximately 20 Pa and 130 Pa for 2 gpt and 8gpt, respectively. This result is consistent with the elastic range trend measured previously by the relaxation time.

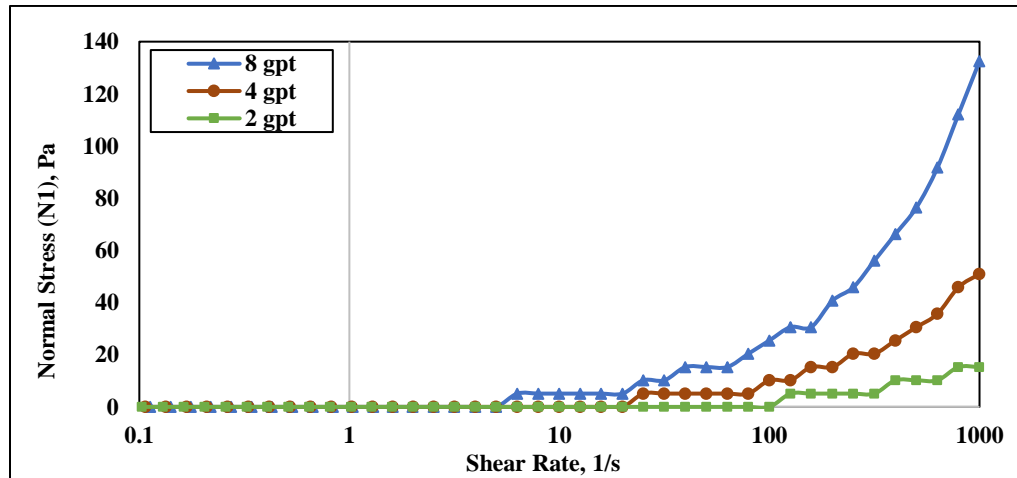


Figure 6. Effect of HFVR 3 concentration as a function in Normal stress profile.

4.3. SETTLING VELOCITY MEASUREMENT RESULTS

Several factors can control the proppant transport in complex fracture system including proppant type, proppant size, fracture geometry, and fracture fluids characteristics e.g. viscosity and elasticity (Loveless et al., 2011; Montgomery, 2013). In this section, single particle static velocity measurements were performed in confining and unconfining using HVFR-3 loading 2gpt in ambient temperature setup. The importance of measuring proppant static settling velocity is to mimic the conditions of fracture treatment after stop pumping which represents low shear rate.

4.4. PROPPANT SETTLING VELOCITY PERFORMANCE IN UNCONFINED FRACTURE WALL

Three different glass beads of diameter sizes 2 mm, 4 mm, 6 mm were selected to study the effect of settling velocity in HVFR and slickwater. Figure 7 shows terminal settling velocity as a function of particle diameter and fluid types. At same particle size of 2 mm, the settling velocity in HVFR was 3.5 cm/sec while in slickwater settling velocity increased by factor 5.6 to reach 19.7 cm/sec. All the tested particle sizes showed HVFR has better settling performance compared to slickwater. This reduction in settling velocity using HVFR-3 could help to transport the proppant farther into the fractures.

4.5. PROPPANT SETTLING VELOCITY PERFORMANCE IN CONFINED FRACTURE WALL

The fracture orientations were examined because in inclination fractures fraction force plays main factor to reduce the proppant settling velocity (Kou et al., 2018, and Ba

Geri et al., 2018). HVFR-3 with loading 2gpt and slickwater were both used in this investigation.

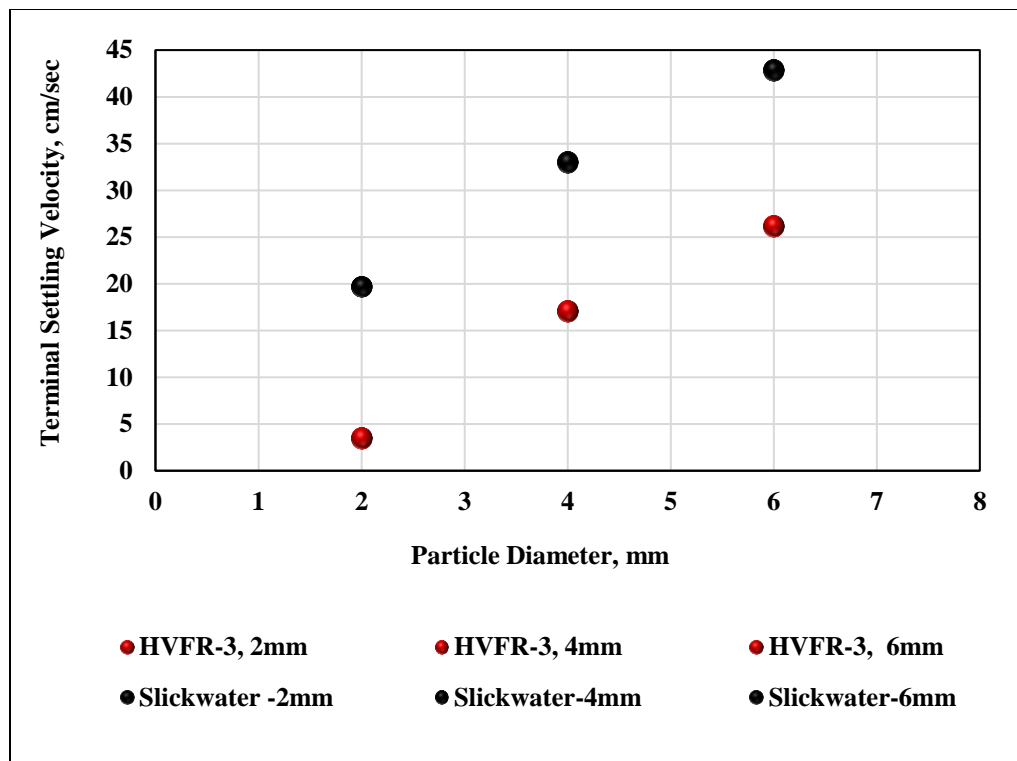


Figure 7. Effect of proppant settling velocity in HVFR-3 gpt vs. slickwater fracture fluids.

Three different fracture orientations (fracture angle 90° , fracture angle 60° , and fracture angle 45°) and three different proppant glass beads sizes (2 mm, 4 mm, 6 mm) were used. Figure 8 shows settling velocity as a function of proppant sizes and fracture fluid types at different fracture orientations. The results showed that settling velocity measurements decreased by increasing fracture inclination from 90° to 45° . At same particle size 6 mm of using HVFR, the settling velocity in vertical fracture was 26 cm/sec while settling velocity was 9.6 cm/sec in 45° inclined fracture. All the results for different particle sizes and different fracture fluids were showing the same effect of fracture

inclination. Results also confirmed our previous observation where HVFR had better settling velocity performance than slickwater.

Figure 9 shows further analysis to understand the effect of HVFR on proppant settling velocity in comparing with slickwater at different fracture orientations. Proppant size of 2 mm results were used to make this comparison. At same condition of fracture orientation with 45 degree, the reduction on settling velocity was over 90% by changing fracture fluids from slickwater to HVFR-3. The reduction on settling velocity not only in inclined fractures, but also in vertical fracture (angle 90 degree) which reached around 80% once changing fracturing fluids from slickwater to HVFR-3. This substantial reduction in settling velocity the HVFR could be better alternative for conventional slick water.

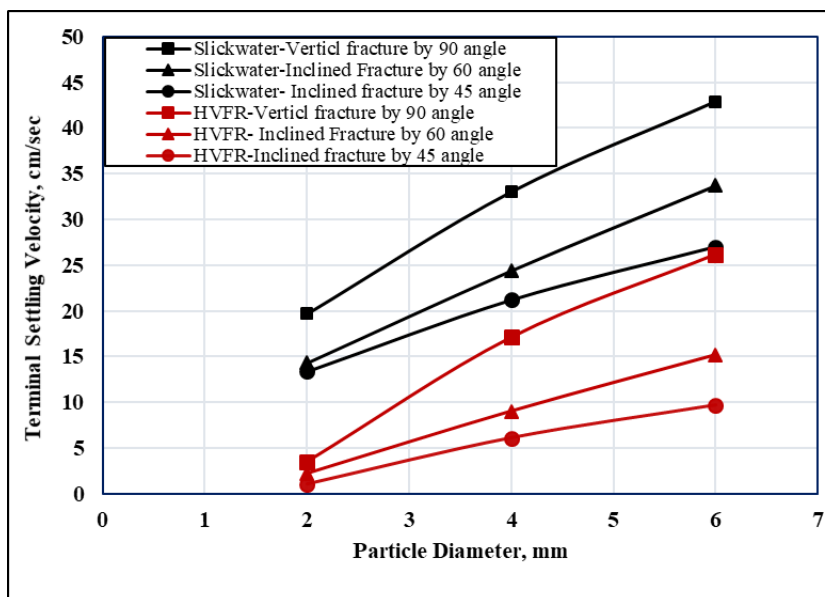


Figure 8. Settling velocity of HVFR vs. Slickwater in vertical fractures by 90 angle vs. inclined fractures angles 60 and 45 degree in confined fractures of 9 mm fracture width.

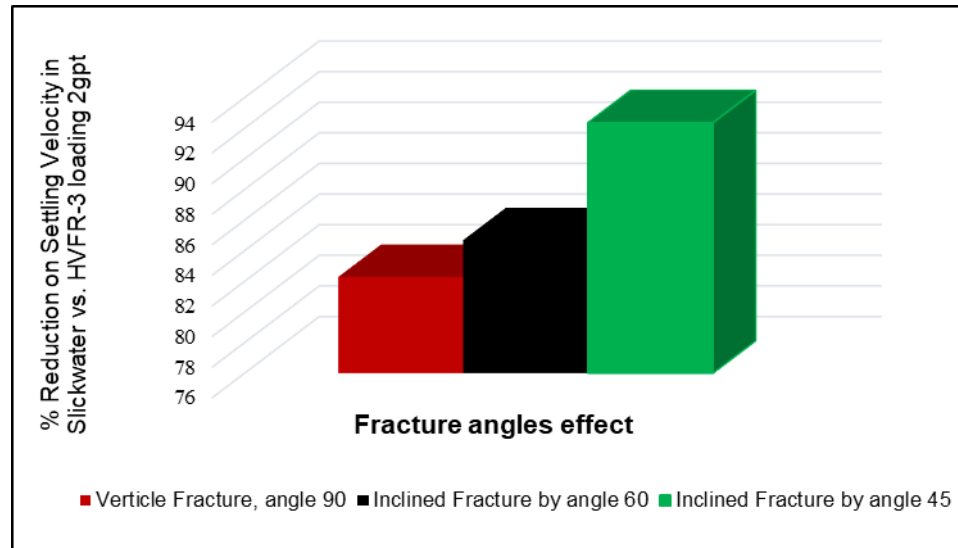


Figure 9. Settling velocity reduction in slickwater versus HVFR-3 loading 2 in different fracture orientation.

4.6. WALL EFFECT ON STATIC SETTLING VELOCITY

Referring to the settling velocity results illustrated in Figures 7 and 8 for unconfined fluid and confined fluids, the wall effect for HVFR was obtained. Settling for these particles were occurred in the creeping flow regime. Figure 10 shows F_w as a function of r (ratio between particle diameter and wall spacing) for the two different fracture widths of 9 mm and 3 mm. It can be seen that wall factors decrease with increase in value of r . This occurred because wall retardation effects increase as particle diameter becomes comparable to wall spacing. In addition to the wall retardation to reduce the proppant settling velocity, fluid elasticity plays main effect to decrease settling velocity of proppant.

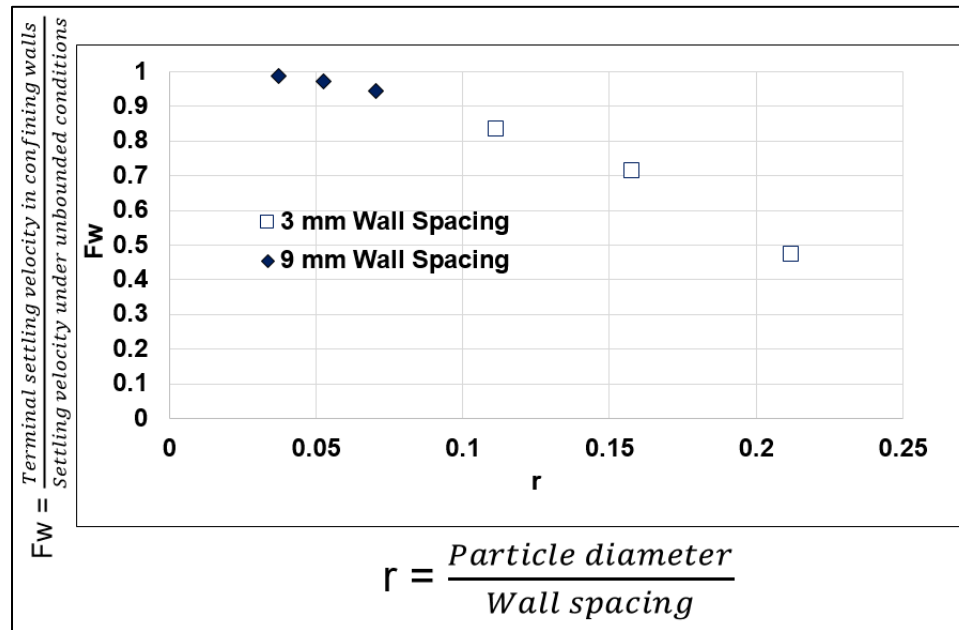


Figure 10. Wall factors as a function of particle diameter to wall spacing in the HVFR-3 loading 2 gpt.

4.7. EFFECT OF VISCOSITY AND ELASTICITY OF HFVR ON PROPPANT SETTLING VELOCITY

Figure 11 shows steady shear rate-viscosity measurements profile as a function of shear rate for HVFR-3. HVFRs follow shear thinning model behavior. The power law model (k, n) was fitted in the measured data of experimentally in range of particle shear rate from 3.3 to 86 s^{-1} . The particle shear rate range was selected based on shear particle calculation using Eq. 2, and it summarized in Table 2 for each proppant particle sizes.

Figure 12 shows the velocity ratio calculation using HVFR-3 loading 2 gpt as a function of proppant diameter. Equation 16 was used to calculate the velocity ratio between the measured settling velocity in the lab divided by the calculated velocity based on power law model parameters (n, k). Results showed that velocity ratio for the proppant

sizes were less than 1. This could imply that viscosity properties of HVFR3 with loading of 2 gpt had greater effect on proppant settling velocity than elasticity did.

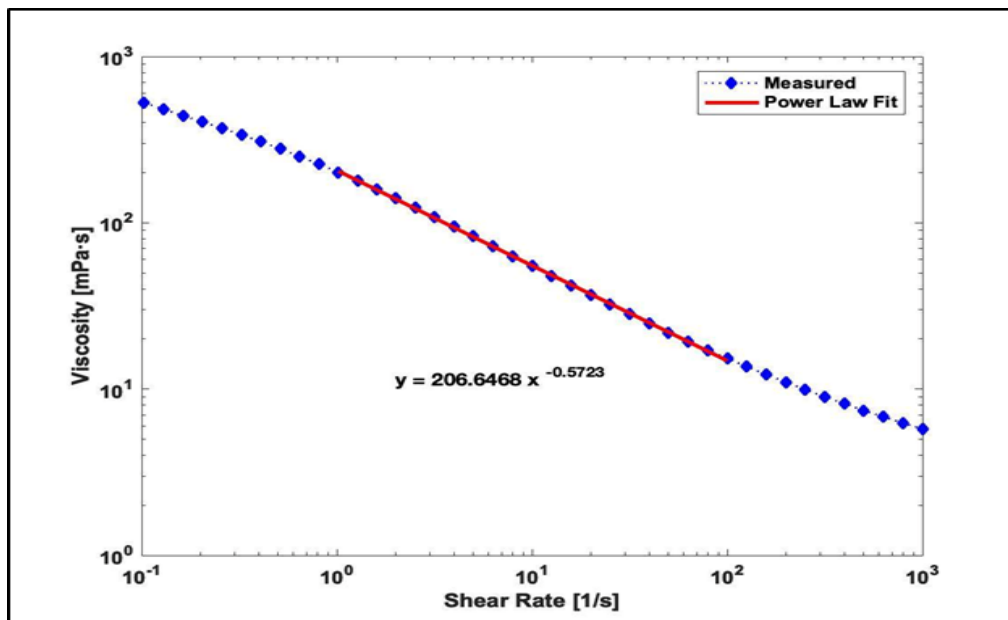


Figure 11. Viscosity as a function of shear rate for HVFR-3 loading 2gpt.

Table 2. Particles shear rate calculations for HVFR.

Particle size	Particle Size (cm)	Particle Shear Rate (1/sec)	K (Pa.sn)	n
40/70 mesh	0.033	3.3	0.206	0.57
30/50 mesh	0.473	8.7		
20/40 mesh	0.635	18.7		
2 mm	0.20	37		
4 mm	0.40	85		
6 mm	0.60	86.7		

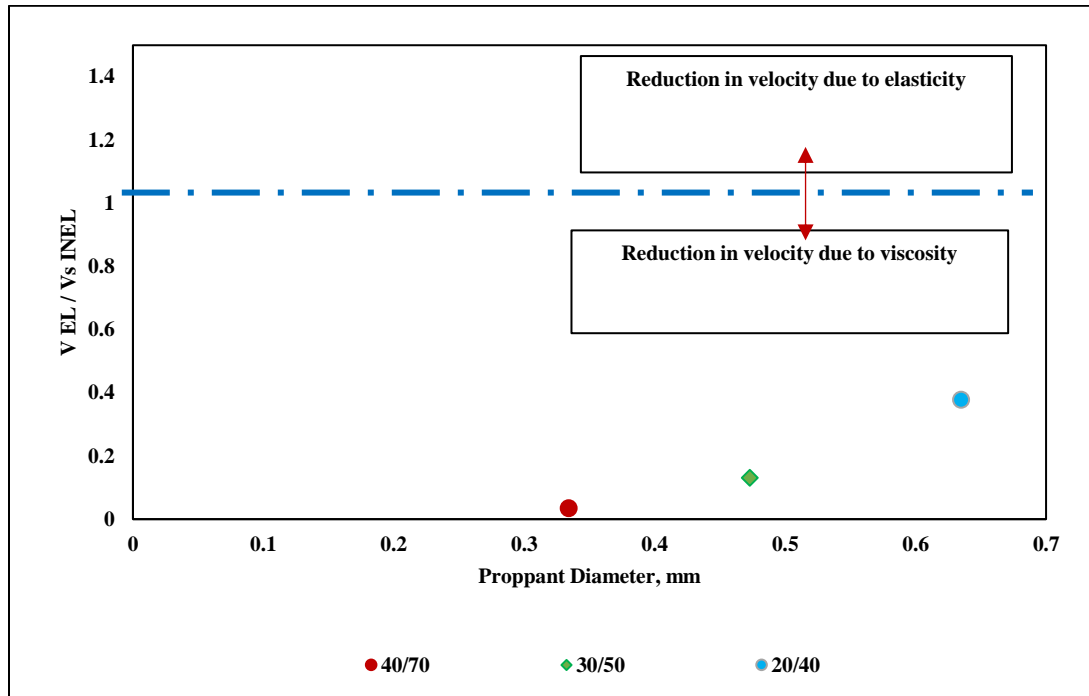


Figure 12. Velocity ratio as a function of proppant diameter in HVFR-3 loading 2 gpt.

4.8. EFFECT OF ELASTICITY TO VISCOSITY RATIO ($\lambda_{e/v}$)

Equation 3 used to determine which properties of the fracture fluids demonstrated the particle settling velocity at wide ranges of shear rates. The estimation of shear rate range is varying during hydraulic fracturing treatments; where typically fracturing treatment conducting within range 300 s^{-1} to 900 s^{-1} . Friction loss caused reduction on shear rate to become in the range of 10 s^{-1} to 100 s^{-1} and continue decreasing until the shear rate goes to zero at fracture tip. Table 3 presents the power law model equations of the relationship between viscosity and shear rate as well as exponential model for first normal stress for both HVFR-3 to calculate elastic/viscous ratio.

Figure 13 shows that for HVFR-3 loading 2 gpt, $\lambda_{e/v} = 0.004 * \dot{\gamma}^{0.55}$ indicates that elasticity effect almost negligible since the contribution of elasticity become more

important when shear rate larger than $1000s^{-1}$. The results could imply that viscous properties of HVFR-3 loading 2 gpt dominate proppant transport. The results could imply that viscous properties of HVFR-3 loading 2 gpt dominate proppant transport within a wide range of shear rate from injection point until delivering proppant to fracture tip, whereas plays somehow effect at high shear rate $> 1000 s^{-1}$.

5. COST ANALYSIS

This laboratory study investigated several factors that affect the Proppant settling in high viscous friction reducer fracture fluids. Proppant settling velocity was investigated as function of fluid rheology (viscosity and elasticity), proppant size, retardation confining walls, and fracture orientation.

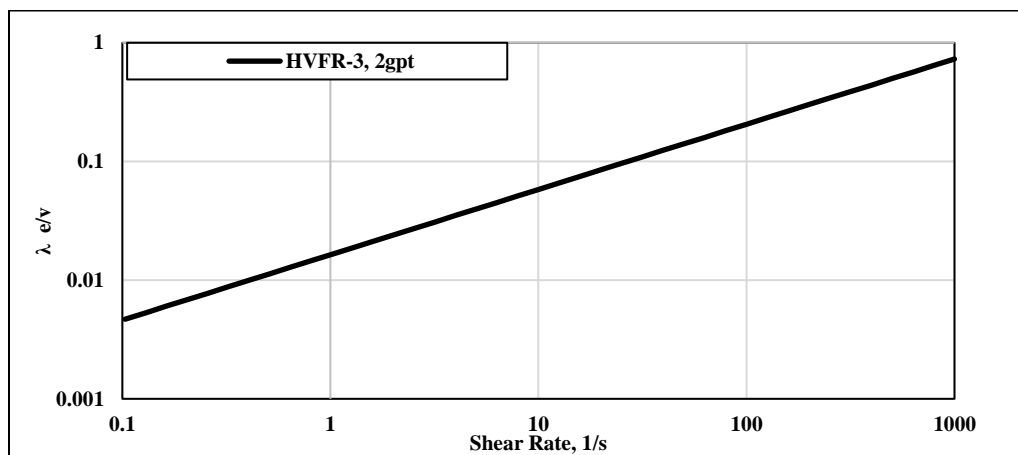


Figure 13. Calculated elastic/viscous ratio as a function of shear rate for HVFR-3 loading 2 gpt.

Table 3. Elastic/Viscous ratio $\lambda_{e/v}$ calculations.

The Ratio of Elasticity to Viscosity Calculation			
Fluid name	Viscosity equation from viscosity profile	Elasticity equation from N1 profile	Elastic/Viscous ratio
HVFR-3-2gpt	$\eta(\dot{\gamma}) = 0.195\dot{\gamma}^{-0.54}$	$N_1(\dot{\gamma}) = 0.018\dot{\gamma}^{0.005}$	$\lambda_{e/v} = 0.0039 \dot{\gamma}^{0.55}$
R-square	0.9988	0.8674	

The outcomes of this work have provided interesting perceptions into the understanding of high viscous friction reducer fracture fluids compared to slickwater fracture fluids. The following conclusions can be drawn from this work:

- High viscosity friction reducers provided better proppant transport capability than using slickwater fracturing fluids. Proppant settling velocity could be reduced by above 80% when slickwater was replaced by HVFR.
- Viscosity properties dominated proppant settling velocity while elasticity effect was almost negligible for HVFR at low loading concentration of 2 gpt.
- Wall retardation effect increase as particle diameter becomes comparable to wall spacing and it can also depend on HVFR elasticity.
- Changing fracture orientation from vertical position (90 degree) to incline by 45 degree caused high reduction in proppant settling velocity. This reduction could be caused by wall friction forces when proppant settle into the bottom of the fracture.

REFERENCES

- Arnipally, S. K., and E. Kuru. 2018. Settling Velocity of Particles in Viscoelastic Fluids: A Comparison of the Shear-Viscosity and Elasticity Effects. In *Proceedings of the SPE Annual Technical Conference and Exhibition, 9-11 October, San Antonio, Texas, USA*. <https://doi:10.2118/187255-PA>
- Ba Geri, M., A. Imqam, and S. Dunn-Norman. 2018. Proppant Transport Behavior in Inclined Versus Vertical Hydraulic Fractures: An Experimental Study. In *Proceedings of the SPE/AAPG Eastern Regional Meeting, 7-11 October, Pittsburgh, Pennsylvania, USA*. <https://doi:10.2118/191813-18ERM-MS>
- Ba Geri, M., A. Imqam, A. Bogdan, A.L. Shen. 2019b. Investigate the rheological behavior of high viscosity friction reducer fracture fluid and its impact on proppant static settling velocity. In *Proceedings of the SPE Oklahoma City Oil & Gas Symposium, Oklahoma, 7 – 11 April 2019*. <https://doi:10.2118/195227-MS>
- Ba Geri, M., A. Imqam, and R. Flori. 2019a. A critical review of using high viscosity friction reducers as fracturing fluids for hydraulic fracturing applications. In *Proceedings of the SPE Oklahoma City Oil & Gas Symposium, Oklahoma, 7 – 11 April 2019*. <https://doi:10.2118/195191-MS>
- Clark, P. E., and Q. Zhu. 1996. Convective Transport of Propping Agents During Hydraulic Fracturing. In *Proceedings of the SPE Eastern Regional Meeting, 23-25 October, Columbus, Ohio*. <https://doi:10.2118/37358-MS>
- Dahlgren, K., B., Green, B., Williams, J., Inscore, V. Domelen, V., and A., Fenton. 2018. Case Studies of High Viscosity Friction Reducers HVFR in the STACK Play. In *Proceedings of the SPE Hydraulic Fracturing Technology Conference and Exhibition, 23-25 January, The Woodlands, Texas, USA*. <https://doi:10.2118/189893-MS>
- Drylie, S., R., Duenckel, R., Barree, and B. Hlidek. 2018. An Investigation of Proppant Transport in Friction Reducer Fluid Systems Utilizing a Large Slot Flow Apparatus. In *Proceedings of the SPE Annual Technical Conference and Exhibition, 24-26 September, Dallas, Texas, USA*. <https://doi:10.2118/191720-MS>
- Faxen, H., 1922. Der Widerstand gegen die Bewegung einer starren Kugel in einer zähen Flüssigkeit, die zwischen zwei parallelen ebenen Wänden eingeschlossen ist. *Ann. Phys.* 68, 89–119.

- Gadde, P. B., Y., Liu, J., Norman, R., Bonnecaze, and M. M. Sharma. 2004. Modeling Proppant Settling in Water-Fracs. In *Proceedings of the SPE Annual Technical Conference and Exhibition, 26-29 September, Houston, Texas*. <https://doi:10.2118/89875-MS>
- Hu, Y. T., D., Fisher, P., Kurian, and R. Calaway. 2018. Proppant Transport by a High Viscosity Friction Reducer. In *Proceedings of the SPE Hydraulic Fracturing Technology Conference and Exhibition, 23-25 January, The Woodlands, Texas, USA*. <https://doi:10.2118/189841-MS>.
- Johnson, M., A., Winkler, C., Aften, P., Sullivan, W. A., Hill, and C. VanGilder. 2018. Successful Implementation of High Viscosity Friction Reducer in Marcellus Shale Stimulation. In *Proceedings of the SPE/AAPG Eastern Regional Meeting, 7-11 October, Pittsburgh, Pennsylvania, USA*. <https://doi:10.2118/191774-18ERM-MS>
- Khan, A.R., J.F., Richardson, 1987. "The resistance to motion of a solid sphere in a fluid. *Chem*". *Eng. Sci.* 62, 135–150.
- Kou, R., G. J., Moridis, and T. A. Blasingame. 2018. Analysis and Modeling of Proppant Transport in Inclined Hydraulic Fractures. In *Proceedings of the SPE Hydraulic Fracturing Technology Conference and Exhibition, 23-25 January, The Woodlands, Texas, USA*. <https://doi:10.2118/189856-MS>.
- Lali, A. M., A. S., Khare, Joshi, J. B. et al. 1989. Behaviour of Solid Particles in Viscous Non-Newtonian Solutions: Settling Velocity, Wall Effects and Bed Expansion in Solid-Liquid Fluidized Beds. *Powder Tech.* 57 (1): 39–50. [https://doi.org/10.1016/0032-5910\(89\)80102-0](https://doi.org/10.1016/0032-5910(89)80102-0).
- Loveless, D., J., Holtsclaw, R., Saini, P. C., Harris, and J. Fleming. 2011. Fracturing Fluid Comprised of Components Sourced Solely from the Food Industry Provides Superior Proppant Transport. In *Proceedings of the SPE Annual Technical Conference and Exhibition, 30 October-2 November, Denver, Colorado, USA*. <https://doi:10.2118/147206-MS>
- Malhotra, S., and M. M. Sharma. 2013 "Settling of Spherical Particles in Unbounded and Confined Surfactant-based Shear Thinning Viscoelastic fluids: An Experimental Study", *Chemical Engineering Science*, vol. 84, 09/2013.
- Michaelides, E.E. 2002. Analytical expressions for the motion of particles. In: DeKee, D., Chhabra, R.P. (Eds.), *Transport Processes in Bubbles Drops and Particles, 2nd ed. Taylor & Francis, New York (Chapter 2)*.
- Michaelides, E.E.. 2003. "Hydrodynamic force and heat/mass transfer from particles, bubbles and drops – the Freeman Scholar Lecture". *J. Fluid Eng. (AMSE)* 125, 209–238.

- Montgomery, C. 2013. Fracturing Fluid Components. International Society for Rock Mechanics and Rock Engineering.
- Motiee, M., Johnson, M., Ward, B., Gradl, C., McKimmy, M., and J. Meeheib. 2016. High Concentration Polyacrylamide-Based Friction Reducer Used as a Direct Substitute for Guar-Based Borate Crosslinked Fluid in Fracturing Operations. In *Proceedings of the SPE Hydraulic Fracturing Technology Conference*, 9-11 February, The Woodlands, Texas, USA. <https://doi:10.2118/179154-MS>
- Shah, S.N., Fadili, Y.E., Chhabra, R.P., 2007. New model for single spherical particle settling velocity in power law (visco-inelastic) fluids. *Int. J. Multiphase Flow* 33, 51–66.
- Shen, L., L., Vigderman, D., Heller, and D. Fu. 2018. Can Friction Reducers Transport Sand During Fracturing Treatment? In *Proceedings of the SPE/AAPG/SEG Unconventional Resources Technology Conference*, 23-25 July, Houston, Texas, USA. <https://doi:10.15530/URTEC-2018-2873723>
- Tong, S., R., Singh, & K. K. Mohanty. 2017. Proppant Transport in Fractures with Foam-Based Fracturing Fluids. In *Proceedings of the SPE Annual Technical Conference and Exhibition*, 9-11 October, San Antonio, Texas, USA. <https://doi:10.2118/187376-MS>
- Van Domelen, M., W., Cutrer, S., Collins, and M.Ruegamer. 2017. Applications of Viscosity-Building Friction Reducers as Fracturing Fluids. In *Proceedings of the SPE Oklahoma City Oil and Gas Symposium*, 27–31 March, Oklahoma City, Oklahoma, USA. <https://doi:10.2118/185084-MS>
- Zapryanov, Z., and S.,Tabakova. 1999. Dynamics of Bubbles, Drops and Rigid Particles. *Kluwer Academic Publishers, Dordrecht, The Netherlands*.

IV. INVESTIGATE PROPPANT TRANSPORT WITH VARYING PERFORATION DENSITY AND ITS IMPACT ON PROPPANT DUNE DEVELOPMENT INSIDE HYDRAULIC FRACTURES

Mohammed Ba Geri¹, Abdulmohsin Imqam¹, and Mohammed Suhail²

1: Department of Petroleum Engineering, Missouri University of Science and Technology, Rolla, MO 65409

2: King Saud University, Riyadh, Saudi Arabia

ABSTRACT

Proppant transport adequately during hydraulic fracturing treatment assumes same perforation contribution through multi-perforation system. Proppant transport performance into the different ordination fracture system using multi-entry perforation technique is still not fully understood. This experimental study was aimed to deeply investigate five factors that affect proppant transport performance: number of perforations, perforation opening size, shear rate, fracture orientation, and proppant size distribution. The impact of these factors on proppant transport performance from different perspective was studied. Fracture slot model was designed and built to observe easily the effects of perforation density and fracture orientation.

The results of this experimental work show that limited-entry perforation technique has significant impact on proppant transport within fractures where single top perforation had better proppant placement than multi-perforation system. Fracture area was approximately propped with 66% and 48% using top perforation and multi-perforation system, respectively. Slurry with high shear rate has a negative effect on the proppant

equilibrium dune level (EDL) and fracture propped area (FPA). Fracturing treatment using high shear rate causes high pressure drop in the fracture that leads to decreasing EDL by 17% and fracture propped area by 23% comparing to using low shear rate. Using large proppant size (20/40) leads to form high EDL and FPA compared to 100 mesh size. Proppant transport dominated by four mechanisms and the vertexes near wellbore plays main mechanism to carry proppant farther inside the fracture.

1. INTRODUCTION

Pressurized low viscosity fracture fluids (e.g., slickwater) have been used in hydraulic fracturing treatments for a long time because low viscous fluids have the ability to create desirable fracture geometries and long fracture lengths in ultra-tight permeability reservoirs. Many experimental studies have been conducted in vertical fracture slots to highlight the factors that affect the proppant transport process (Kern et al. 1959; Medlin et al. 1985; Patankar et al. 2002; Wang et al. 2003; Woodworth and Miskimins 2007). Multi-stage fracturing techniques are essential to providing effective pathways for hydrocarbon fluids to flow from unconventional reservoirs to the wellbore. Each stage is comprised of many clusters, and each cluster consists of several reservoir entry points called perforations. Analysis of well logging data in horizontal wells in unconventional reservoirs indicated that there was no contribution from 20 to 40% of perforation clusters on well production Miller et al. (2011); Crump and Conway, (1988); Economides and Nolte, (2000). They observed that not all perforation is produced in shale basins for instance 21%,

32%, and 39% in the Eagle Ford shale, the Woodford shale, and the Haynesville shale, respectively.

Therefore, meeting performance expectations requires enhancing the effective completion quality and reducing completion cost by selecting optimum designs for completion parameters like clusters and number of perforations. Although the previous work concluded that the production rate in multi-system perforation is less than limited-perforation systems, the reasons behind this are still not understood. This study will highlight the effect of perforation density and perforation number on proppant transport performance in terms of proppant equilibrium dune level and fracture propped area.

Predicting particle settling velocity and proppant transport in different types of hydraulic fracturing fluids, including Newtonian and non-Newtonian fluids, was attained by (Clark and Zhu, 1996). Gadde et al. (2004) studied how settling velocity can be affected by changing proppant size, fracture width, velocity of fluid, and rheological properties of fluids. The study concluded that using Stoke's law is not an accurate way of predicting proppant settling rate. Liu and Sharma (2005) used different rheological characterizations of fracturing fluids to study the effect of particle diameter on fracture width and settling velocity. They concluded that for large particle diameters, the horizontal velocity of proppant is less than the fluid velocity due to a large wall effect. Alotaibi et al. (2015) extensively investigated the development of dune level and proppant transport mechanisms at different stages of fracturing treatment using slickwater. They observed that proppant was sorted from smallest to largest until reaching EDL. Mohanty et al. (2016) conducted experimental and simulation studies about proppant transport in fracture intersections using slickwater.

They concluded that increasing shear rate causes reduction in equilibrium bed height, while proppant dune length increases by increasing the shear rate. Kadhim et al. (2017), conducted experimental study using slot fracture model to investigate the heterogeneous fracture width, wall roughness, and leak-off on proppant settling mechanisms. They found that fracture wall roughness plays significant role on proppant transport where noticed that settling velocity decreased and leads to decreased equilibrium dune level. They also observed that fracture width has more influence on settling velocity than horizontal proppant velocity. Despite of the amount of previous work, the effect of perforation density on EDL and FPA has not been investigated thoroughly. This paper will provide a full understanding of proppant transport from different angles including, pressure loss across fractures, injection shear rate and number of perforations that contributed to proppant transport treatment.

In addition, due to the understanding that a created fracture orients perpendicular to the minimum horizontal principal stress, most existing studies assumed that proppant transport occurred in a vertical geometry model. Wright et al. (1995) presented field studies illustrating that over the production time of the Chevron Lost Hills, the inclination changed from 82° to 45° degrees between fracture treatments. Dinh et al. (2009) studied field examples showing that fracture orientation is vertical near the wellbore, but deviated inclination as the moved away from the wellbore. Kou et al. (2018) developed a simulation model to evaluate proppant transport in inclined fractures.

Their results observed that proppant performance is better placement in inclined fractures. Ba Geri et al. (2018) experimentally investigated the effect of fracture inclination on proppant transport. The study concluded that inclination of fractures can have a

significant impact on proppant transport due to the friction or contact force, that comes from the fracture wall. This friction affects the settling velocity of the proppant and the proppant distribution efficiency inside the fracture. Increasing the fracture inclination angle increases the fracture propped area. This current study is extended work to our previous publication Ba Geri et al. (2018) in terms of studying perforation density and opening size perforation impact on EDL and FPA.

Based on the author's knowledge, most of the previous lab work did not seriously consider the impact of perforation density and fracture orientation on proppant transport. Thus, this work will conduct intensive laboratory work to fill that knowledge gap. This study has deeply investigated five factors that affect proppant transport performance: number of perforations, perforation opening size, slurry shear rate, fracture orientation, and proppant size distribution. The impacts of these factors on proppant transport performance from different perspectives was investigated based on the following: 1) Behavior of proppant transport in fracture half-length (X_f) at first fracture pore volume (FPV). 2) Dune bed level development and fracture propped area at first FPV and EDL. 3) Pressure drops along fracture slot during proppant transport inside fracture. This study also identifies and define the mechanisms of proppant transport inside fractures.

2. EXPERIMENT DESCRIPTION

2.1. EXPERIMENT MATERIALS

The experiments were conducted using white sand proppant supplied by US Silica company and slickwater (without any chemicals additives). Three different sand sizes

(20/40, 40/70, and 100 mesh) were used to investigate proppant size distribution effect. US silica proppant properties are shown in Table 1. All the experiments were conducted using a proppant concentration of 0.5 lb/gal.

Table 1. API/ISO properties of the tested US silica white sand proppants.

Proppant Type	Roundness	Sphericity	Particle Density (g/cc)	Mean Particle Diameter (mesh)
White sand	0.7	0.8	2.65	100 40/70 20/40

2.2. FRACTURE MODEL SETUP

Figure 1 shows the proppant transport model apparatus that was built to mimic proppant slurry transport in hydraulic fracturing treatments. A lab fracture model is 61 cm in length and 61 cm in height with fracture width of 0.635 cm. The orientation of the model can be adjusted from vertical to inclined positions. Four injection points (representing four perforations of 0.635 cm diameter) were made perpendicular to the fracture slot. Along the height of fracture slot, four perforations were installed at the inlet and outlet of the fracture slot. During the proppant slurry injection, all the four inlet perforations were used and only one perforation at the outlet (the bottom one) was opened. The other components of the apparatus are the mixer, mixing tank, cameras, pressure sensors, flowmeters and safety valve. The fracture slot apparatus was illuminated with 4000 Lumens 61 cm x 61 cm – LED vapor tight fixture to add extra light to capture clearly the proppant transport inside fracture.

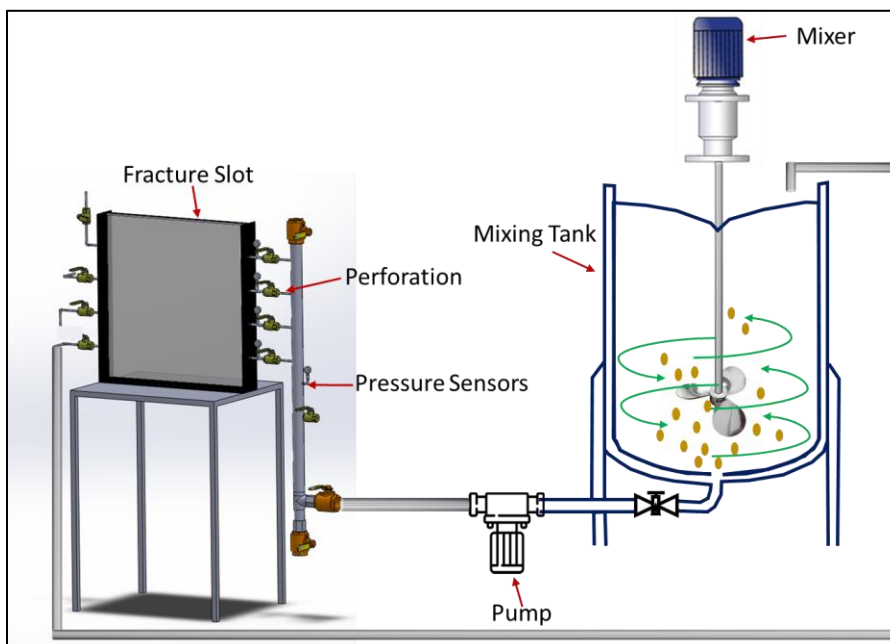


Figure 1. Schematic Schematic of the experimental proppant transport evaluation system.

2.3. EXPERIMENT PROCEDURE

To mimic a low viscosity slickwater stimulation treatment in a reservoir, water initially filled the fracture slot as shown in Figure 1. Three different US Silica White sand sizes (20/40, 40/70, and 100 mesh) were used to study the fracture propped area due to proppant size distribution in transport treatment. Eleven experiments were designed and conducted to investigate proppant transport behavior using different perforation density and oriented fractures. The number of experiments that conducted with their descriptions are summarized in Table 2.

Table 2. List of experiments and parameters.

List of Experiments and Parameters						
Case #	Perforation Opening Size (%)	Proppant (mesh)	Shear Rate (s⁻¹)	Proppant Loading (ppg)	Number of Perforation	Fracture Orientations
1	100	100	60	0.5	Top single	Vertical
2	100	100	60	0.5	Bottom Single	Vertical
3	100	100	60	0.5	Multi-Perforation	Vertical
4	100	100	35	0.5	Top single	Vertical
5	100	100	35	0.5	Bottom Single	Vertical
6	100	100	35	0.5	Multi-Perforation	Vertical
7	60	100	60	0.5	Multi-Perforation	Vertical
8	40	100	60	0.5	Multi-Perforation	Vertical
9	100	100	60	0.5	Multi-Perforation	Inclined
10	100	40/70	60	0.5	Multi-Perforation	Vertical
11	100	20/40	60	0.5	Multi-Perforation	Vertical

To perform these experiments, the experimental procedure used is as follows:

1. The fracture slot was filled with only fracture fluid. In our case, slickwater to mimic the pad stage on the hydraulic fracturing treatment.
2. The mixer was turned on and proppant was added. The proppant concentration was 0.5 ppg in order to make the slurry.
3. The slurry was pumped into the fracture slot at different shear rate ($60s^{-1}$, $35s^{-1}$, and $8s^{-1}$). The injection process was continued until no change could be observed in the dimensions of the proppant dune bed inside the fracture.
4. High-resolution cameras were used to capture and record the proppant transport during the experiments.
5. The captured videos were tracked and analyzed using a video analysis MATLAB code.

6. All the above procedures were repeated for all the experiment cases mentioned in Table 2.

2.4. EXPERIMENT ANALYSIS APPROACHES

The experiment results were analyzed using the following calculation parameters:

2.4.1. Equilibrium Dune Level (EDL). Equilibrium dune level (EDL) is the ratio of sand dune height to fracture model height multiplied by 100%. It is measured by using the program Plot Digitizer where the fracture slot height is divided to the highest point of proppant bed inside the fracture. The ratio between proppant dune to fracture height can be obtained by applying the following equation (Alotaibi and Miskimins, 2018):

$$\text{Equilibrium Dune Level (EDL), \%} = \frac{\text{Equilibrium dune height}}{\text{Fracture slot height}} \times 100 \quad (1)$$

2.4.2. Proppant Dune Level Development (PDL). Proppant dune level development, (PDL) is defined as the ratio between proppant dune levels before reaching EDL to the EDL Kadhim, et al. (2017):

$$\text{Proppant Dune Level Development, (PDL), \%} = \frac{\text{Dune Level (DL)}}{\text{Equilibrium dune height (EDL)}} \times 100 \quad (2)$$

2.4.3. Equilibrium Dune Length (EDL). Proppant dune length, (EDL) is defined as the ratio between the average dune lengths to the fracture model length multiplied by 100% as shown by the following equation:

$$\text{Fracture propped area (FPA), \%} = \frac{\text{area of proppant distributed in the fracture}}{\text{Total fracture area}} \quad (3)$$

2.4.4. Pressure Losses Calculations. Since the pressure loss across the fractures is a function of flow rate of the fluid, pressure losses effect calculations were investigated to study the effect of pressure loss across fracture on fracture propped area. Typically, the

following equation (Clark and Zhu, 1996) is used to calculate the pressure drop across the fracture slot:

$$\Delta P = \frac{12l\mu Qs}{hw^3} \quad (4)$$

where ΔP is the pressure losses across the slot in psi, Q_s is the slurry flowrate in cm^3/s , μ is the slurry viscosity in poise, h , l , w are the slot dimensions high and length in cm, respectively.

3. RESULTS AND ANALYSIS

3.1. NUMBER OF PERFORATION EFFECT

To study the perforation impact on proppant transport, a 100% perforation opening size, high shear rate 60 (1/s), fracture orientation (vertical fracture), proppant size 100 mesh were used. Figure 2 illustrates that changing the number of perforations at first FPV had similar results in terms of height of proppant and distance the proppant travels inside the fracture. For instance, at the first FPV all change the perforation position from the top perforation system to bottom perforation system had the same delivered amount of proppant where the fluid carried proppant farther than 56 cm of the fracture length (X_f). As well as using multi-perforation system at first FPV had the same X_f of proppant as the single point system. At the beginning of injection treatment, the fracture propped area looks similar. Later of this treatment, the fracture propped area changes because the contribution of perforations were changed.

Figure 3 presents the EDL of different perforation numbers. A multi-perforation system setup used consists of four perforations, single-perforation system (top perforation

and bottom perforation). The results show that EDL varied tediously in all cases. For example, the EDL of the top perforation (single point) was around 71%, whereas the EDL of the multi-perforation system was about 67%. Therefore, the changes in EDL are very small between the two different perforation systems.

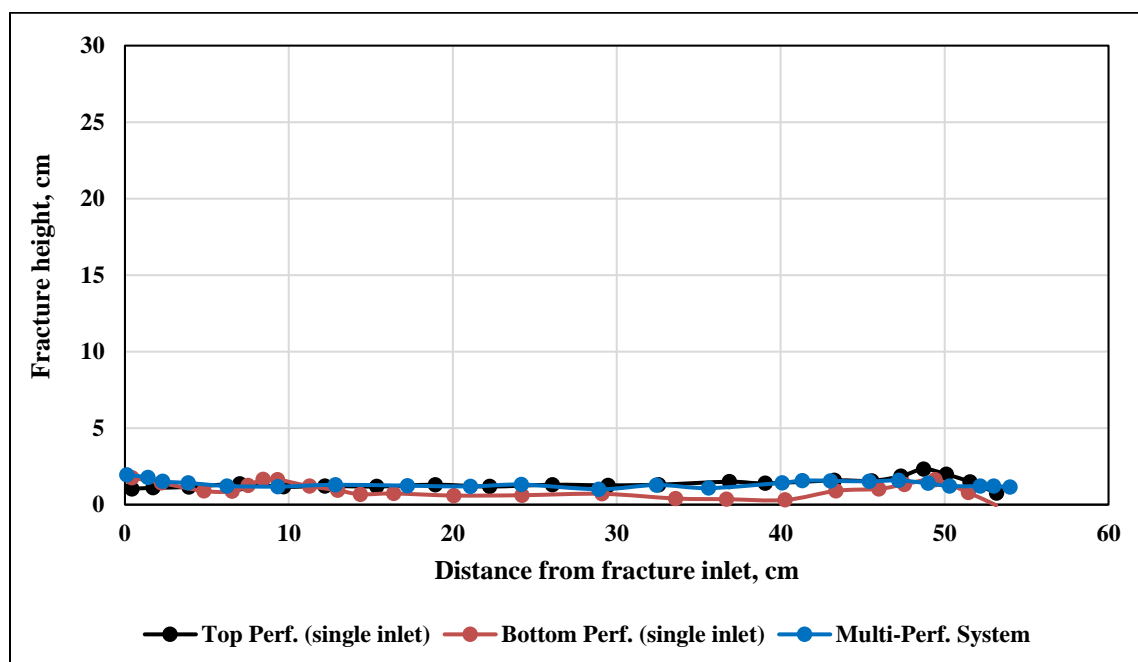


Figure 2. Effect of number of perforations at first FPV.

Interestingly, Figures 4 and 5 display how different numbers of perforations can influence the fracture propped area. Contribution of proppant transport during top perforation (single point) leads to have better results compared to a multi-perforation system. Approximately, 66% and 48 % of fractures were propped using top perforation and multi-perforation, respectively. Based on this findings, limited-perforation system would have probably better propped fracture area compared to multi-perforation system.

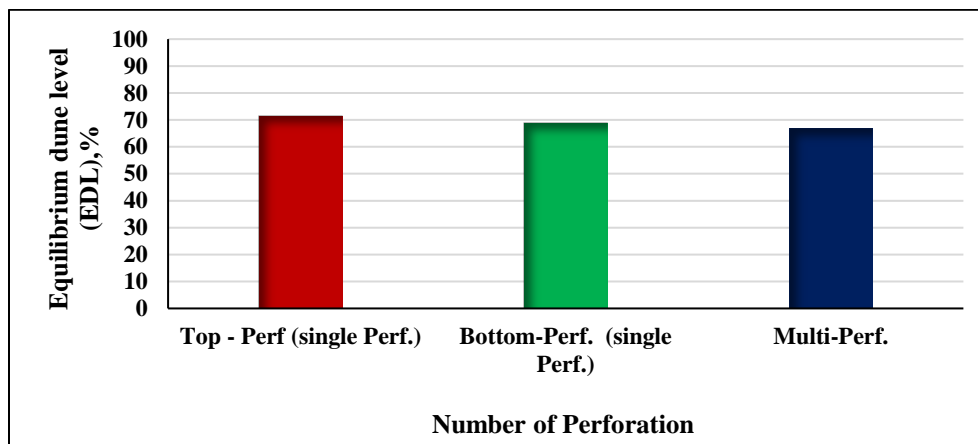


Figure 3. Effect of number of perforations on EDL.

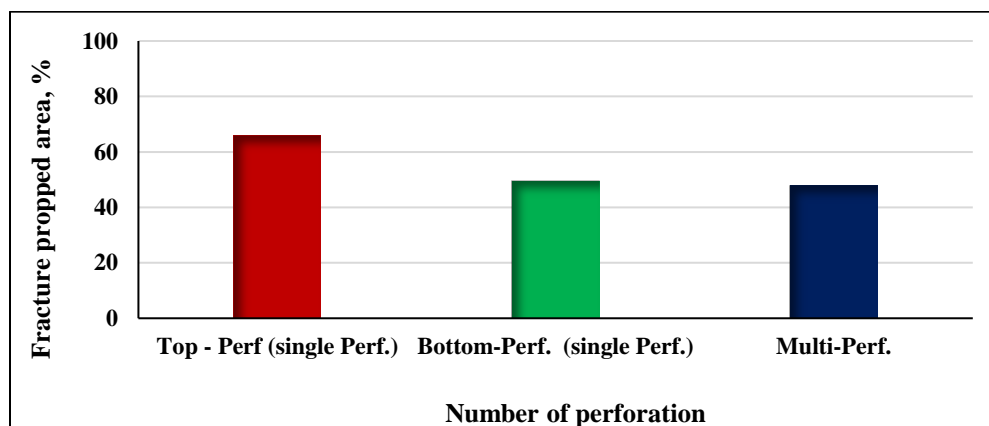


Figure 4. Effect of number of perforations on fracture propped area.



Figure 5. Real picture of experiment results shown number of perforation effect on proppant transport, Top-perf (left), Bottom-perf (middle) and Multi-perf. (right).

3.2. PERFORATION OPENING SIZE EFFECT

To study the perforation opening size impact on proppant transport, 100%, 60%, 40% perforation opening size, high shear rate 60 (1/s), fracture orientation (vertical fracture), proppant size 100 mesh, and multi-perforation system were used. Figure 6 shows that at the first FPV, proppant is transported farther by decreasing the perforation opening size from 100% to 40% because fluid velocity increases with decreasing perforation diameter. To illustrate this, at the first FPV, the X_f of proppant inside the fracture was 56 cm, 52 cm, and 48 cm from the fracture inlet of 40%, 60%, and 100% perforation opening size, respectively.

Gruesbeck and Collins (1982) noticed that changing the perforation diameter from 3/8 to 1/2 inch did not affect proppant transport performance. However, our study results do not completely agree with their conclusion. In 60% perforation opening size case, the EDL reached to over 80% EDL which represented almost 17% of the EDL higher than both perforation opening size cases 100% and 40% EDL as shown in Figure 7.

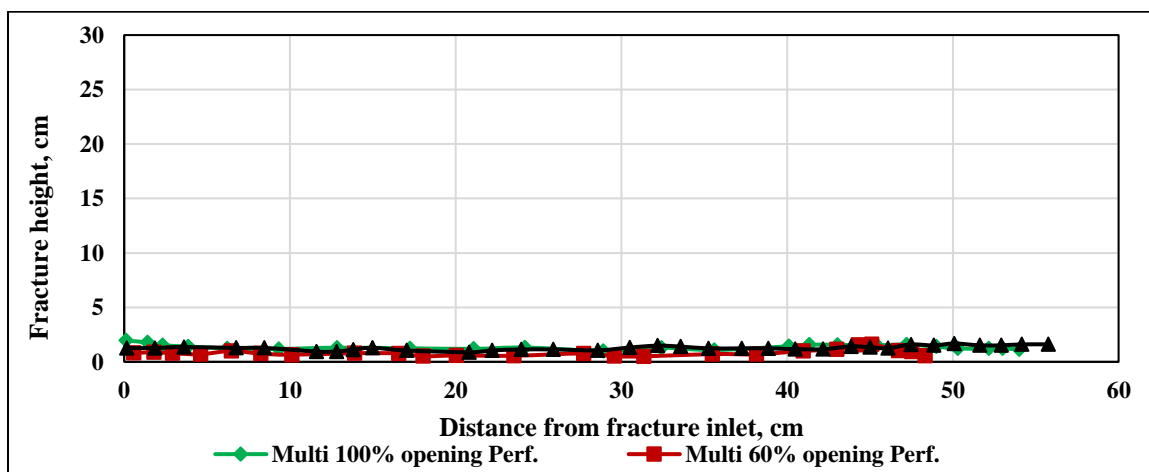


Figure 6. Effect of perforation opening size at first FPV.

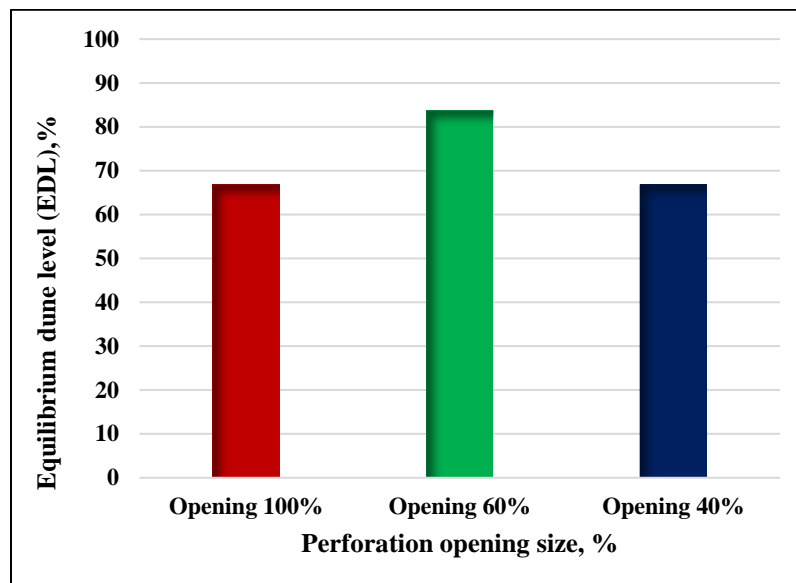


Figure 7. Effect of perforation opening size on EDL.

Figures 8 and 9 show a similar trend for fracture propped area where decreasing perforation opening size to 60% leads to a 21% increase in fracture propped area compared to the 100% opening. When the opening size was decreased to 40%, only a 3% impact on fracture propped area was observed compared to 100% fully opened perforations.



Figure 8. Real picture of experiment results shown perforation opening size effect on proppant transport, perf opening 100% (left), perf opening 60% (middle) and perf opening 40% (right).

3.3. SHEAR RATE EFFECT

To study the shear rate impact on proppant transport, 100% perforation opening size, multi-perforation system, fracture orientation (vertical fracture), and proppant size 100 mesh were all kept constant for this investigation. Figure 9 based on results attained from the first FPV, proppant reached farther into fracture tip at high shear rate of 60 s^{-1} with a height around 2 cm of the total fracture height in the sand bed. At a low shear rate of 35 s^{-1} proppant did not transport deep and proppant height was larger with approximately 4 cm proppant height. Overall, it could be said that, at the beginning of fracture treatment, higher shear rates can form a smaller proppant bed and a longer distribution close to the fracture tip, while at low shear rates there is less proppant distribution and larger sand beds.

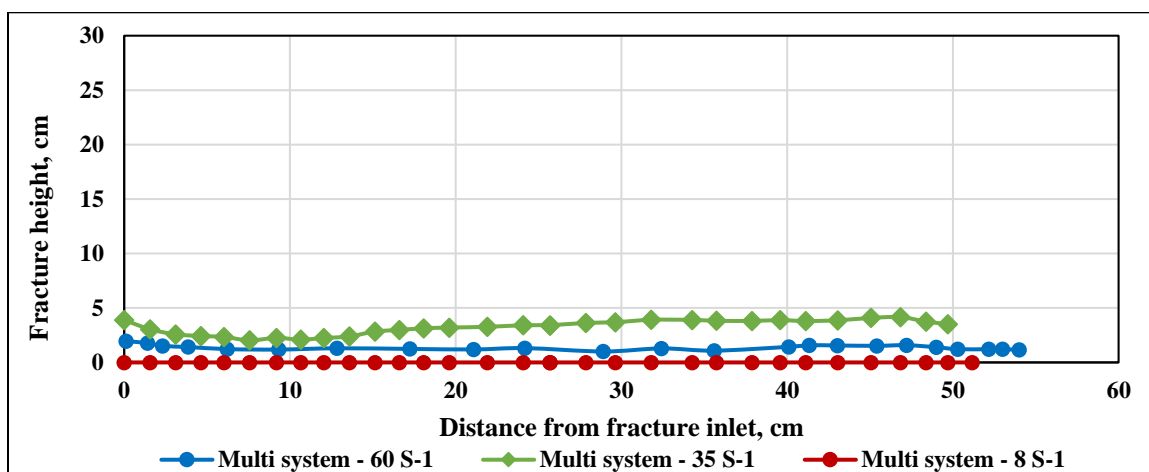


Figure 9. Effect of fracture shear rate at first FPV.

Figure 10 & 11 show EDL inside the fracture at high (60 s^{-1}) and low shear rate (35 s^{-1}). At low shear rate proppant bank formed near wellbore whereas. However, due to

vertexes around wellbore, proppant bank moved farther because swirls play major mechanism during proppant transport so proppant bank near well wellbore is less. In contrast, decreasing shear rate leads to high proppant dune level and much proppant accumulate near wellbore. Erosional effects play a major role at high shear rates which majority affect EDL. This consistency in results with ALotibi et al. (2015) confirming that better proppant performance can be obtained by applying a lower shear rate.

Figure 12 shows the EDL as a function of shear rate. At low shear rates, increasing the settling velocity increases EDL by 78%, while the increasing shear rate to $60s^{-1}$ caused increased erosional forces and decreases EDL by 65%. Generally, these results implied that equilibrium dune level is inversely proportional with shear rate.

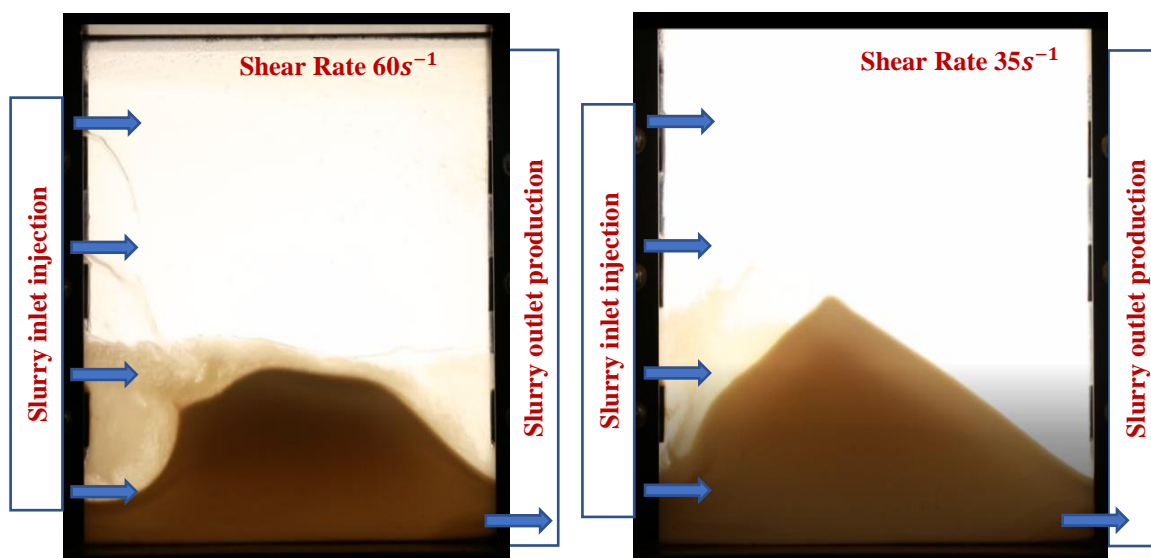


Figure 10. Real picture of experiment results shown shear rate effect on proppant transport, high shear rate (left) and low shear rate (right).

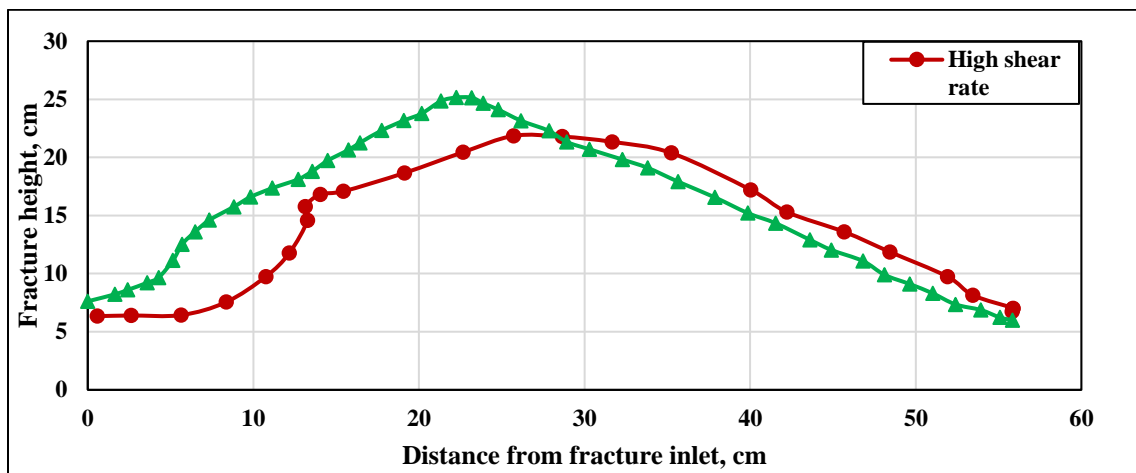


Figure 11. Effect of high ($60s^{-1}$) and low ($35s^{-1}$) shear rates on EDL.

Additionally, Figure 13 showed that varying shear rate from $60 s^{-1}$ to $35 s^{-1}$ causes a 23% reduction in fracture propped area. Decreasing fracture propped area can negatively affect fracture conductivity and reduce productivity of the well. These results agree with previous work done by Melhotra, (2016) and Li et al. (2016) whose results found that increasing injection rate leads to a decrease in the dune height level.

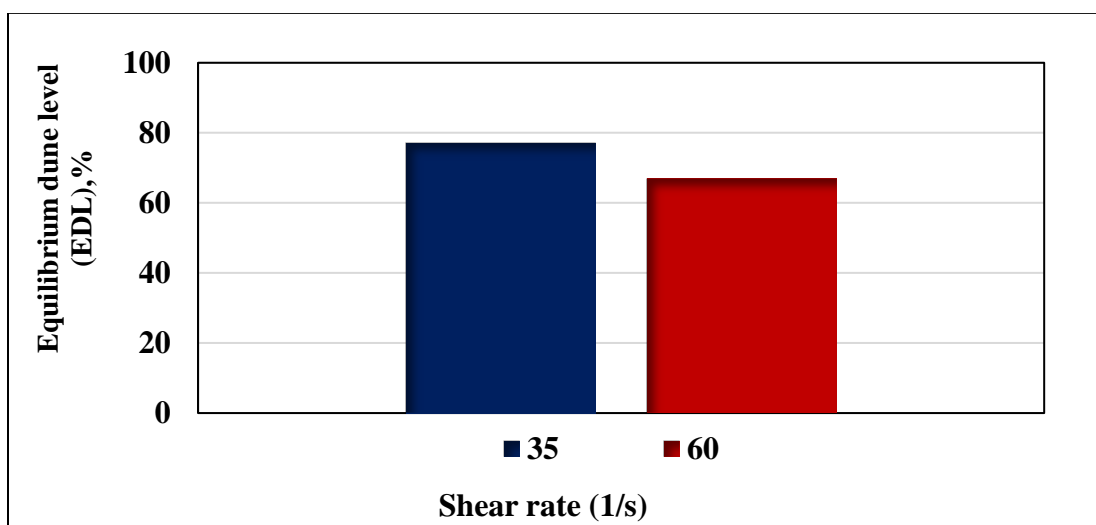


Figure 12. Effect of shear rate on EDL.

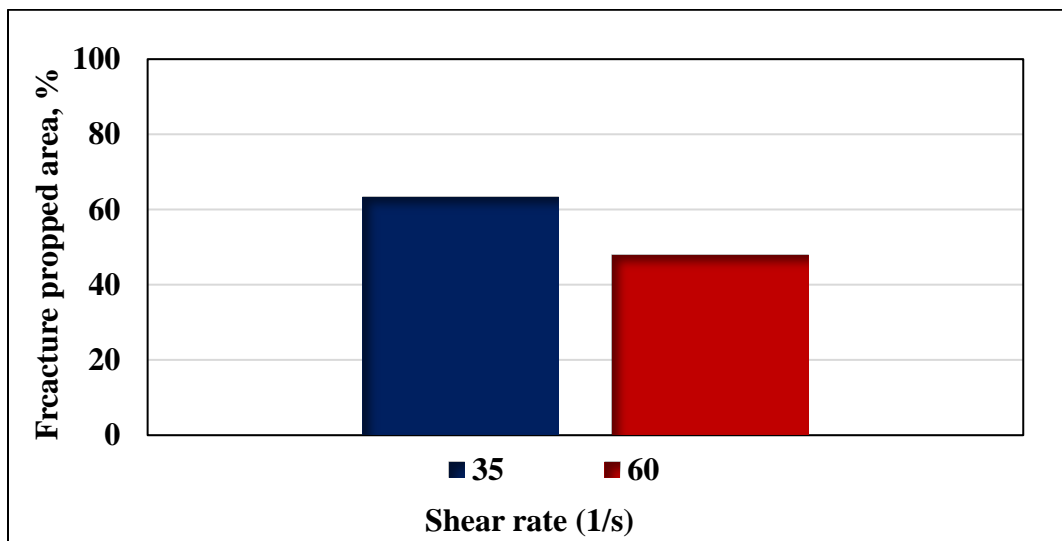


Figure 13. Effect of shear rate on on fracture propped area.

3.4. FRACTURE ORIENTATION EFFECT

To study the fracture orientation impact on proppant transport, 100% perforation opening size, multi-perforation system, high shear rate of 60 (1/s), and proppant size 100 mesh were all kept constant variables. Figure 14 shows proppant transport behavior at the first FPV of the fracturing treatment. Results show that proppant amount had delivered deeper to fracture tip in inclined fracture compared to vertical fracture. At the fracture tip, proppant dune height in inclined fracture was three times (3 cm) the proppant dune height (1 cm) in vertical fracture. The placement of proppant transport during vertical fractures remaining stable on proppant bed. The reason behind this is that in vertical fractures, three forces (gravity, buoyancy, drag) control particle settling, whereas in inclined fractures, in addition to the original three forces, frictional forces dominate the particles movements and reduce proppant settling velocity.

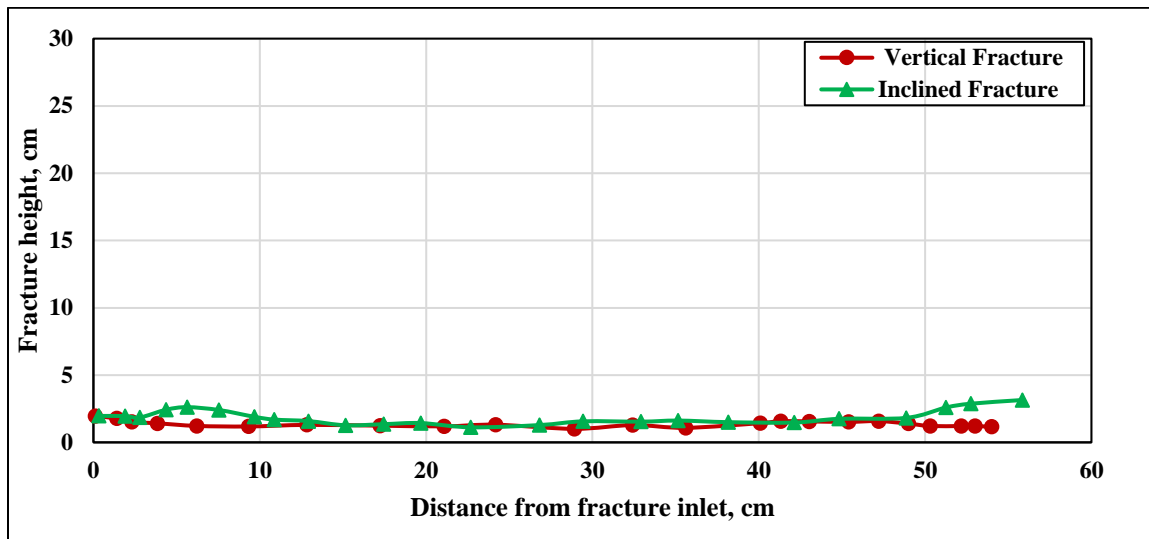


Figure 14. Effect of fracture orientation (vertical vs. inclined) at first FPV.

Figure 15 shows the fracture orientation effect on equilibrium dune level. In inclined fractures, EDL is larger than in vertical fractures because reduction in settling velocity is a function of friction forces Ba Geri et al. (2018). As a result, 13% of EDL enhancement occurred in inclined fractures compared to vertical fractures.

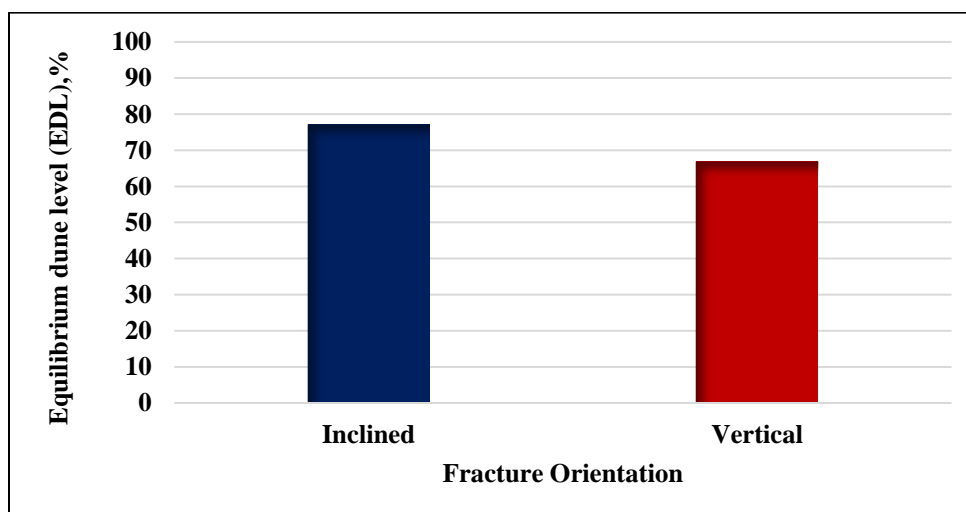


Figure 15. Effect of fracture orientation (vertical vs. inclined) on EDL.

Figures 16 and 17 show the fracture orientation effects on fracture propped area. The fracture propped area was around 52% and 48% in the inclined fracture and vertical fracture, respectively. This result indicated that fracture propped area has the same trend as EDL, which is around 8% improvement on fracture propped area noticed in inclined fracture compared to vertical fracture. This result might imply that inclined fracture could have better fracture conductivity compared to vertical fracture. These observations matched our previous experimental results Ba Geri et al. (2018) and simulation work results Kou et al. (2018) where both confirmed that proppant transport efficiency is much better in inclined fractures than in vertical fractures.

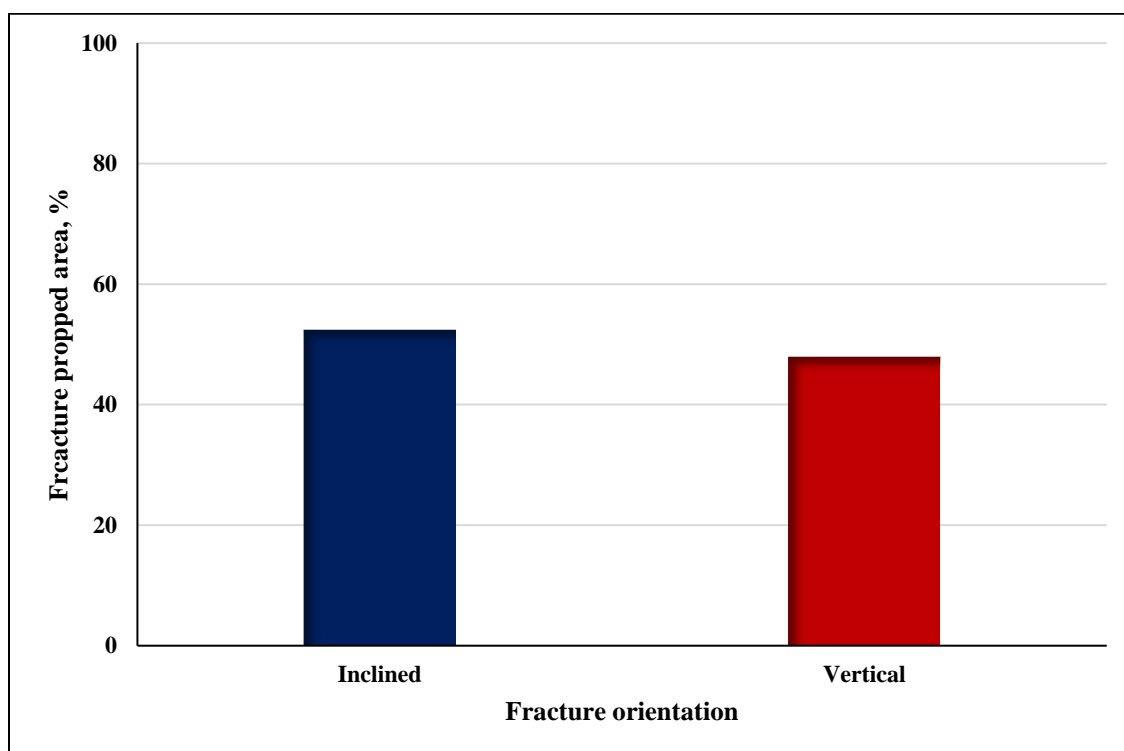


Figure 16. Effect of fracture orientation (vertical vs. inclined) on fracture propped area.

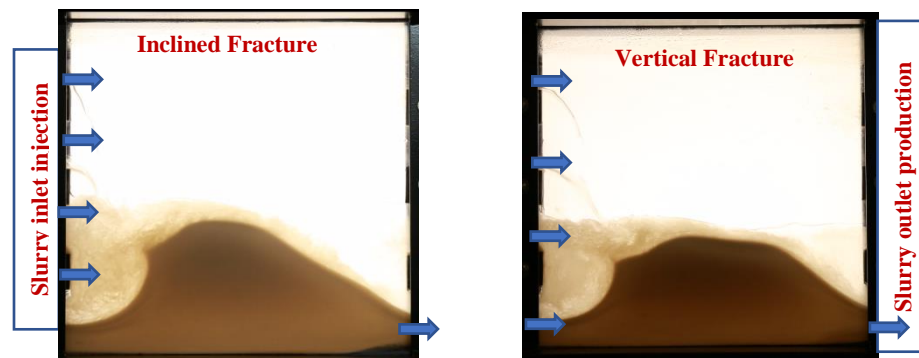


Figure 17. Real picture of experiment results shown perforation opening size effect on proppant transport, inclined fracture (left), and vertical fracture (right).

3.5. PROPPANT SIZE DISTRIBUTION EFFECT

To study the proppant size impact on proppant transport, 100% perforation opening size, multi-perforation system, high shear rate 60 (1/s), and fracture orientation (vertical fracture) were all kept constant during experiment. Figure 18 shows proppant height in the fracture as a function of proppant traveled distance from fracture inlet at 1st FPV. Due to the size effect, it is clearly observed that using large proppant size 20/40 settled near the wellbore whereas small proppant sizes (100 mesh and 40/70 mesh) settled uniformly across the whole fracture section. The results observed from using proppant size 20/40 mesh showed that proppant height near wellbore was 6 cm while the proppant height decrease farther from wellbore inlet to about 2 cm in fracture center and fracture tip. In contrast, using small size of proppant like 100 mesh formed same level of proppant height along the fracture slot without any significant change near wellbore.

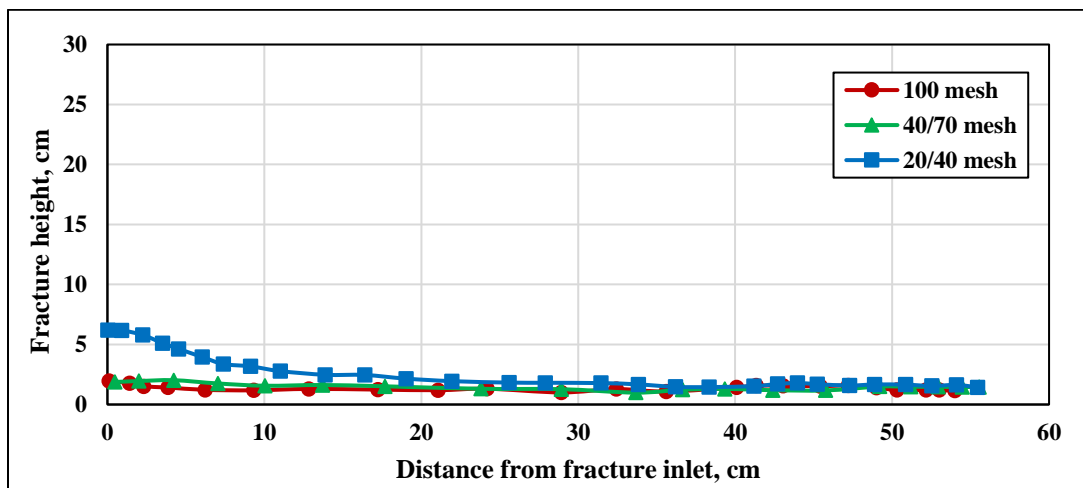


Figure 18. Effect of proppant size at first FPV.

Figure 19 shows that there is a linear relationship between equilibrium dune level and proppant size distribution. The EDL is increased rapidly from 67% to 90% when size of proppant increased from 100 mesh to 20/40 mesh at higher shear rate $60s^{-1}$ respectively. The results agree with Tong et al. (2016) including that equilibrium dune level increased with increasing proppant size at higher shear rates.

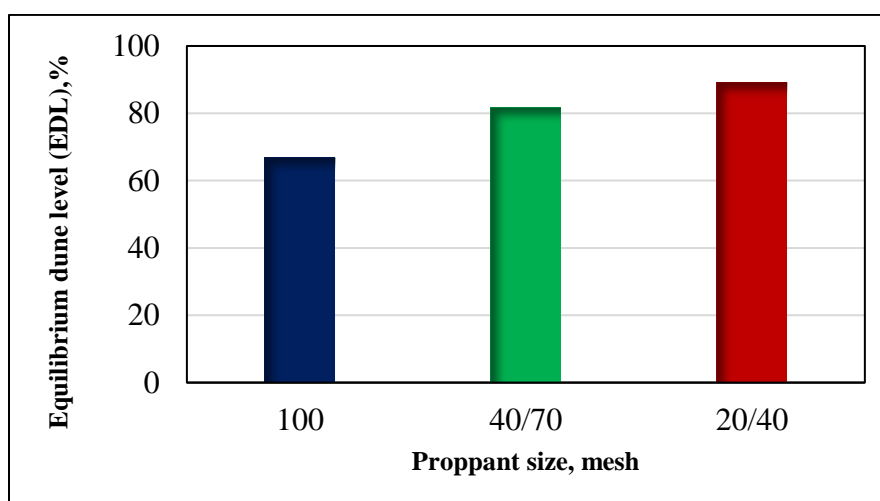


Figure 19. Effect of proppant size on EDL.

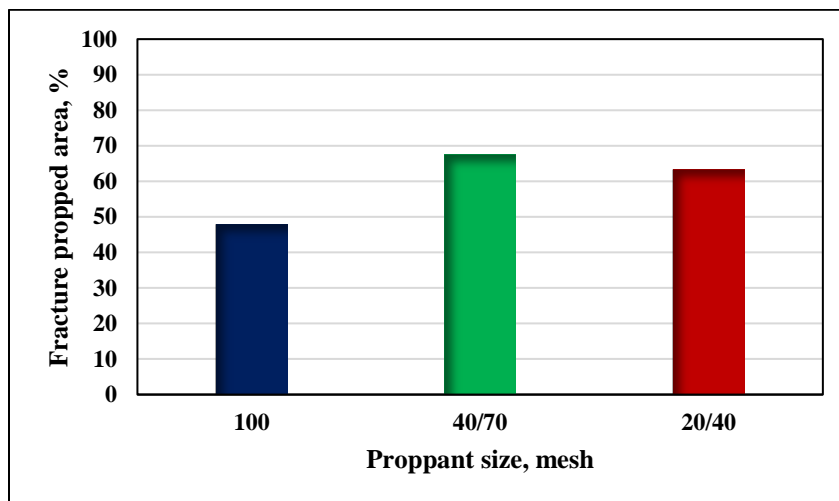


Figure 20. Effect of proppant size on on fracture propped area.

Figures 20 and 21 present the effect of proppant size on fracture propped area. The graph shows that increasing proppant size cause a reduction in proppant settling velocity and proppant bank formed around wellbore as shown when 20/40 proppant size used. On contrast, using a small size of proppant such as 100 mesh leads to less proppant FPA. Interestingly, 40/70 proppant size provided the best results where FPA almost close of 20/40 FPA.

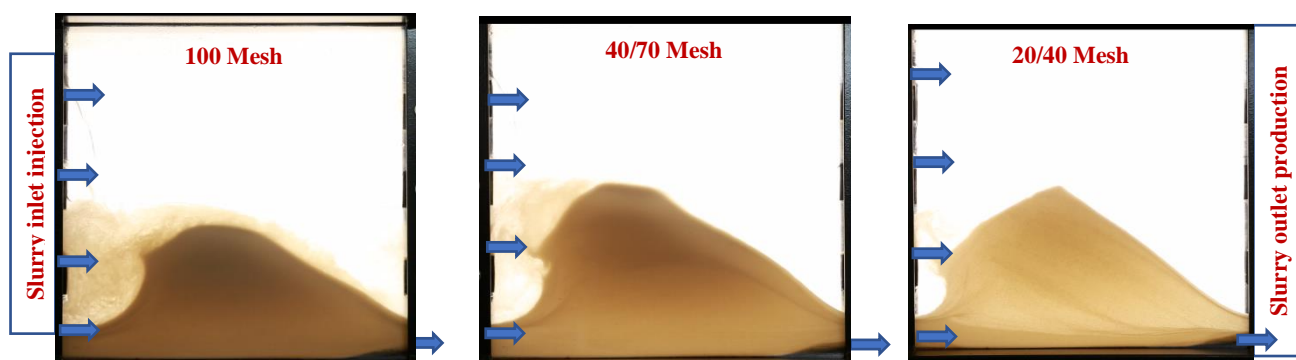


Figure 21. Real picture of experiment results shown proppant size effect on proppant transport, 100 mesh (left), 40/70 mesh (middle) and 20/40 mesh (right).

4. DISCUSSION

4.1. EFFECT OF PRESSURE LOSS ALONG THE FRACTURE SLOT ON PROPPANT TRANSPORT PERFORMANCE.

Figures 22 a, and b show pressure difference across fracture calculated from equation 5 and propped fracture area as a function of slurry shear rate. Results show a linear relationship between pressure loss across fracture and propped fracture area with shear rate. Fracture treatments using high shear rate because high pressure drops in the fracture which decreasing fracture propped area by 23% compared to using low shear rates.

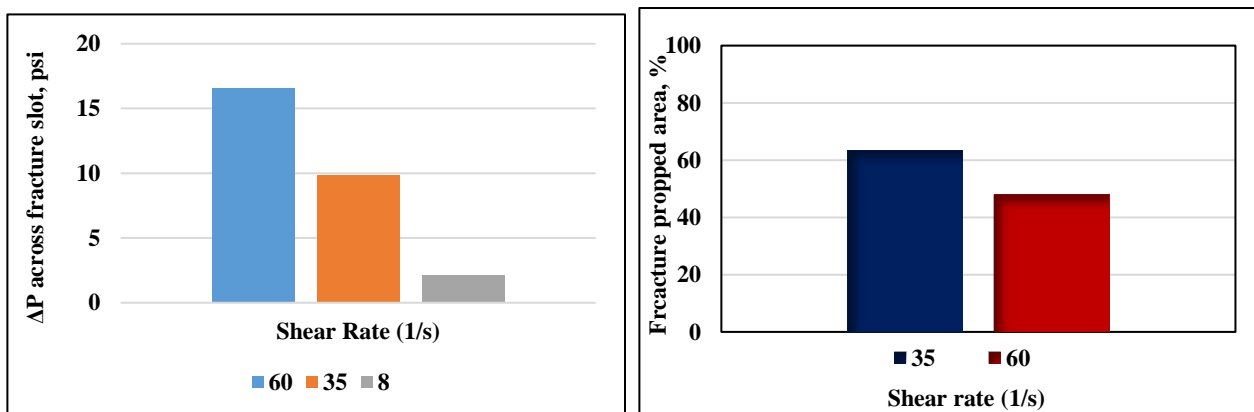


Figure 22. a. and b pressure loss along fracture slot on shear rate (left) and shear rate effecton Fracture propped area (right).

Applying equation (5) to calculate pressure drop across fracture slot is shown in Table 3. Linear relationship between pressure losses and EDL and X_f at 1st fracture pore volume (FPV) was noticed. At the beginning of injection treatment, high shear rate $60s^{-1}$ delivered the proppant fracture to fracture tip 54 cm with EDL 1.58 cm. In contrast, we noticed that by decreasing the shear rate to $35s^{-1}$ the EDL was 4.1 cm while the proppant to 50cm of fracture length. As result of increasing shear rate, changing on EDL and

proppant X_f occurred because the pressure loss across the fracture increased from 9.8 psi to 16.2 psi.

Table 3. Shows pressure losses effect at 1st FPV on EDL and X_f .

At 1st FPV				
	Shear rate (s^{-1})	ΔP across slot (psi)	EDL (cm)	X_f (cm)
High	60	16.2	1.58	54
low	35	9.8	4.1	50

4.2. MECHANISMS OF PROPPANT TRANSPORT

The mechanisms of developing proppant transport within the fracture slot are summarized in Table 5. Proppant dune level development (PDL) was used to determine the dominate mechanism of each stage of these four stages by applying Equation.

4.2.1. Stage 1: Hindered and Free Settling. This stage occurs when EDL started forming height and continues until the of PDL is 15% and the buildup angle is between 0° to 9.3° . Due to increasing of sand dune height at the beginning of this stage, proppant particles do not roll inside the fracture. Thus, large size 20/40 mesh of proppants were moving as clusters or groups and spread along the fracture referring as “hindered settling”. While changing proppant size to the fine particles 100 mesh settled freely farther in fracture.

4.2.2. Stage 2: Saltation. In this stage, PDL reaches 15 to 42% while the buildup angle ranges from 9.3° to 19.3° . Saltation is the only mechanism observed in this stage due to lift force of the proppant. The physical dynamics of the is lifting force plays a major role in moving the particles by causing the proppant to jump and leave the sand bed surface.


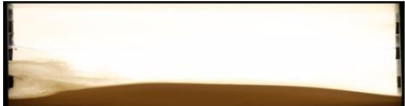


Because of the speed difference between the flow above and below the particles, the pressure difference acts as a lifting force. Therefore, the particle jumps and leaves as a result of the force caused by the pressure difference exceeding the force of gravity. Around 18% of PDL is developed in this stage, leading to reduction in the cross-section flow area.

4.2.3. Stage 3: Suspension, Rolling, and Swirl at Inlet. This stage occurs when PDL is between 42% to 71% and the buildup angle is from 19.3° to 26° . Three different mechanisms dominate proppant performance and transport within the fracture: suspension, rolling, and swirl at the inlet. Erosional forces increased causing rolling of the proppant on the sand bed due to the particle drag force being higher than the gravitational force. The major development above 30% of EDL happened in this stage leading to the presence of swirl and vortices at the inlet due to high flow turbulence. Therefore, proppant transport efficiency is dominated mainly by these vortices.

4.2.4. Stage 4: Saltation, Rolling, and Swirl at Inlet. This stage occurs when PDL is between 71% and 100% and the buildup angle is between 26° to 42° . The combination of three mechanisms controls the proppant transport performance: saltation, rolling, and swirl at the inlet. The vortices which assist in forming the proppant pile shape. The vortex diameter can sometimes be $1/5$ the fracture half-length.

The dynamic oscillatory-shear measurements were conducted to measure the elasticity profile characterizations and first normal stress N_1 . The oscillatory test was implemented over a range of frequencies from 0.01-100Hz. All rheological properties measurements were conducted at lab and high temperature ranges.

Table 4. Four proppant transport mechanisms to reach the PDL.

Stage Number	Mechanism	PDL, Fraction	Buildup angle, degree	Picture of proppant transport into fracture
1	Hindered & Free settling	0.0 – 0.15	0.0 – 9.33	
2	Saltation	0.15 – 0.42	9.33 – 19.32	
3	Suspension, Rolling, Swirl @ inlet	0.42 – 0.71	19.32 – 26	
4	Rolling, Saltation & Swirl	0.71 – 1.0	26 – 42	

4.2.5. Thermal Stability Measurement. The influence of temperature during fracturing operations has not been fully understood in shale oil reservoirs. This paper investigated the effect of thermal stability of rheology characterizations of HVFRs, which tends to alter parameters such as time dependency, fluid elasticity, viscosity and first normal stress. To better mimic the real fracturing process, the experiments were performed under elevated temperatures by using an advanced rheometer. Viscosity-shear profile measurements for three different temperatures of 77°F, 122°F, 176 °F have been conducted for both HVFRs and linear gel fracture fluids.

4.2.6. Static Settling Velocity Measurement. At this point, the graduated cylinder is filled with HVFR and the cell is positioned vertically. To measure proppant settling

velocity in unconfined fluids, high-resolution video camera is used to record the settling process. In this setup, proppant diameter ranged from 0.453 mm to 6 mm. A single proppant was dropped in the HVFR and allowed to settle. A high-resolution video camera has been used to capture the process of free proppant settling. An image analysis tool called “Tracker” (<http://www.cabrillo.edu/~dbrown/tracker/>) was applied to get accurate measurements of vertical position of the proppant at different time steps (Ba Geri et al 2018). The slope of relationship between proppant vertical positions to steps time step is called terminal settling velocity. For more accurate results, settling velocity of each particle were repeated three times.

5. CONCLUSIONS

This laboratory study investigated several factors that affect proppant transport efficacy. It has provided new and interesting perceptions into the understanding of proppant placement and distribution across the fracture. The following conclusions can be drawn from this work:

- Limited-entry technique has a large impact on proppant transport within fractures. A single top perforation had a 27% improvement in the fracture propped area compared to a multi-perforation system.
- High shear rates have negative effects on the EDL and fracture propped area. Increasing the shear rate caused a decrease in both the EDL by 17 % and on fracture propped area by 23%.

- Decreasing the perforation opening size can help proppant to travel closer to the fracture tip at the beginning of the treatment. A 60% perforation opening size provided better results in terms of the EDL and fracture propped area.
- Pressure loss in the fracture slot leads to a decrease in the EDL and fracture propped area. Pressure losses were found to get significantly affected by changing shear rate from $60s^{-1}$ to $35s^{-1}$.
- Four proppant transport mechanisms were noticed that could potential dominate proppant transport behavior during fracturing treatments. Vortices play a major role when the dune height increases and accumulated near wellbore.

REFERENCES

- Alotaibi, M. A., & Miskimins, J. L. (2018, May 1). Slickwater Proppant Transport in Hydraulic Fractures: New Experimental Findings and Scalable Correlation. Society of Petroleum Engineers. <https://doi:10.2118/174828-PA>
- Ba Geri, M., Imqam, A., & Dunn-Norman, S. (2018, October 5). Proppant Transport Behavior in Inclined Versus Vertical Hydraulic Fractures: An Experimental Study. Society of Petroleum Engineers. <https://doi:10.2118/191813-18ERM-MS>
- Daneshy, A. A. (1973, April 1). A Study of Inclined Hydraulic Fractures. Society of Petroleum Engineers. <https://doi:10.2118/4062-PA>
- Dinh, A. V., & Tiab, D. (2010, December 1). Transient-Pressure Analysis of a Well with an Inclined Hydraulic Fracture Using Type Curve Matching. Society of Petroleum Engineers. <https://doi:10.2118/120540-PA>
- Gruesbeck, C., & Collins, R. E. (1982, December 1). Particle Transport through Perforations. Society of Petroleum Engineers. <https://doi:10.2118/7006-PA>
- Kadhim, D., Imqam, A., & Dunn-Norman, S. (2017, July 24). Ceramic Proppant Transport and Placement in Heterogeneous Fracture Systems. Unconventional Resources Technology Conference. <https://doi:10.15530/URTEC-2017-2697613>

- Kern, L. R., Perkins, T. K., & Wyant, R. E. (1959, July 1). The Mechanics of Sand Movement in Fracturing. Society of Petroleum Engineers. <https://doi:10.2118/1108-G>
- Kou, R., Moridis, G. J., & Blasingame, T. A. (2018, January 23). Analysis and Modeling of Proppant Transport in Inclined Hydraulic Fractures. Society of Petroleum Engineers. <https://doi:10.2118/189856-MS>
- Liu He, Zhang Guangming, Zhang Jin, et al. (2010, May). Friction calculation and surface pressure prediction in oil well hydraulic fracturing. *Chinese Journal of Rock Mechanics and Engineering*. Vol. 29, Supp. 1.
- McMechan, D. E., & Shah, S. N. (1991, August 1). Static Proppant-Settling Characteristics of Non-Newtonian Fracturing Fluids in a Large-Scale Test Model. Society of Petroleum Engineers. <https://doi:10.2118/19735-PA>
- Medlin, W. L., Sexton, J. H., & Zumwalt, G. L. (1985, January 1). Sand Transport Experiments in Thin Fluids. Society of Petroleum Engineers. <https://doi:10.2118/14469-MS>
- Miller, C. K., Waters, G. A., & Rylander, E. I. (2011, January 1). Evaluation of Production Log Data from Horizontal Wells Drilled in Organic Shales. Society of Petroleum Engineers. <https://doi:10.2118/144326-MS>
- Patankar, N.A., Joseph, D.D., Wang, J., Barree, R.D., Conway, M. and Asadi, M. 2002. Power Law Correlations for Sediment Transport in Pressure Driven Channel Flow. *International Journal of Multiphase Flow*, Vol. 28, Pg. 1269 – 1292.
- Sahai, R., Miskimins, J. L., & Olson, K. E. (2014, February 4). Laboratory Results of Proppant Transport in Complex Fracture Systems. Society of Petroleum Engineers. <https://doi:10.2118/168579-MS>.
- Tong, S., & Mohanty, K. K. (2016). Proppant transport study in fractures with intersections. *Fuel*, 181, 463-477.
- Wang, J., Joseph, D.D., Patankar, N.A., Conway, M., and Barree, R.D. 2003. Bi-Power Law Correlations for Sediment Transport in Pressure Driven Channel Flows. *International Journal of Multiphase Flow*, Vol. 29, Pg. 475 - 494.
- Warpinski, N. R. (2010, November 1). Stress Amplification and Arch Dimensions in Proppant Beds Deposited by Waterfracs. Society of Petroleum Engineers. <https://doi:10.2118/119350-PA>

Willingham, J. D., Tan, H. C., & Norman, L. R. (1993, January 1). Perforation Friction Pressure of Fracturing Fluid Slurries. Society of Petroleum Engineers. <https://doi:10.2118/25891-MS>

Woodworth, T. R., & Miskimins, J. L. (2007, January 1). Extrapolation of Laboratory Proppant Placement Behavior to the Field in Slickwater Fracturing Applications. Society of Petroleum Engineers. <https://doi:10.2118/106089-MS>

Wright, C. A., & Conant, R. A. (1995, January 1). Hydraulic Fracture Reorientation in Primary and Secondary Recovery from Low-Permeability Reservoirs. Society of Petroleum Engineers. <https://doi:10.2118/30484-MS>

V. VISCOELASTIC CHARACTERIZATION EFFECT OF HIGH-VISCOSITY FRICTION REDUCERS AND PROPPANT TRANSPORT PERFORMANCE IN HIGH-TDS ENVIRONMENT

Mohammed Ba Geri¹, Abdulaziz Ellafi², Ralph Flori¹, Jerry Noles³, and Sangjoon Kim³

1: Department of Petroleum Engineering, Missouri University of Science and Technology, Rolla, MO 65409

2: Department of Petroleum Engineering, University of North Dakota, Grand Forks, ND 58202

3: CoilChem LLC, Washington, Oklahoma

ABSTRACT

The viscoelastic property of high-viscosity friction reducers (HVFRs) was developed as an alternative fracturing fluid system because of advantages such as the ability to transport particles, higher fracture conductivity, and the potential of a lower cost due to fewer chemicals and equipment required on location. However, concerns remain about using HVFRs to transport proppant in DI water and harsh brine solutions (e.g. 2wt% KCl and 10 lbs. brine). The primary objective of this study is to investigate the viscoelastic property in order to understand the true proppant transporting capacity of fracturing fluids in a high-TDS environment.

To address the evaluation performance of HVFRs, numerous papers associated with the viscoelastic property of hydraulic fracturing fluids were investigated and summarized. This paper also provides a full comparison study of viscosity and elastic modulus between HVFRs and among fracturing fluids such as xanthan, polyacrylamide-based emulsion polymer, and guar. Moreover, viscosity profiles and elastic modulus were

conducted at different temperatures. Better proppant transportation effect though higher viscosity through Stoke's law and the effect on proppant transportation from the elastic modulus comparison were also investigated. Finally, the results of the HVFR Conductivity test and the successful field test were explained.

The results of the experimental work show that the viscoelastic property of HVFRs provides behavior that is able to transport proppant. The viscosity profile decreased slightly as the temperature increased from 75 to 150°F when the DI water was used. While using 10 lbs. brine, the viscosity was reduced by 33%. The longer polymer chains of HVFR indicated a better elastic modulus in DI water. The elastic modulus also indicated that the highest values were found at frequency 4.5 Hz from each amplitude, and lower values were found as the amplitude was increased. Although high molecular weight HVFRs were utilized on the conductivity test, the results observed that the regained permeability was up to 110%. Finally, the promising results from the case study showed that HVFRs could be economically and efficiently used for the purpose of proppant transportation and pressure reduction in high TDS fluids.

1. INTRODUCTION

The ultimate aim of hydraulic fracturing treatments in horizontal wells is to increase the flow and conductivity of unconventional oil/gas reservoirs by creating a long fracture from 100 to 1,000 ft and a conductive fracture width in the order of a tenth of an inch. The success of the process strongly relies on selecting appropriate slurry fluids and proppants since these factors govern the proppant transport to place and fill the conductive pathways

connecting with the proppant particles. Furthermore, the effective behavior of the proppant distribution is essential to understand increasing the well productivity and economics especially in the case of tight formations (Ba Geri et al., 2018; Shrivastava and Sharma, 2018). Therefore, fracture fluids and proppants characterization are crucial parameters that require detailed study in order to achieve a predictable and reliable performance as well as avoiding the early proppant settling near the wellbore (Acharya, 1988; Shah, 1993).

Common fracturing fluids that have been used in industry are Newtonian fluids, such as slickwater, and non-Newtonian viscous fluids with varying degrees of elasticity, including complex polymer solutions, crosslinked, foams, emulsions, and surfactant gels. Early in the shale boom, high viscosity fluid conventional crosslinked gel was used as the Frac fluid system in the formation, such as the Bakken Formation, to add viscosity and create fracture width. However, the post-treatment production test indicates that the fluid does not achieve the desired hydraulic fracturing design objectives because of its low capability to carry proppant in the fractures. Also, field results reported high damage causes with the high-cost operation as well as environmental concerns (Ba Geri et al., 2019a). Although 95% of fracture treatment jobs switched the pumping fluids to hybrid and slickwater, since their low cost and reaching proppant loading improved long term production in most U.S shale plays, the water-based fracturing stimulation requires an enormous consumption of clean water to perform the treatments and tends to increase environmental issues because of the large amount of flow back water, which contains chemicals and toxic components that impact underground water resources (Li and Zhang, 2019). As a result, slickwater fracturing fluid becomes undesirable, and high viscosity friction reducers (HVFRs) in fracturing fluids have recently been adopted for use in shale

plays since they are low cost and provide an effective proppant transport mechanism (Harris et al. 2009; Hu et al. 2015; Gomaa et al., 2015; Srinivasan et al., 2018; Ellafi, A. et al., 2019; Ba Geri et al., 2018; Ba Geri et al., 2019 b&c).

In 1988, Acharya studied the settling rates of proppants and the rheological parameters of two types of cross-linked gels (titanate and borate cross-linked) using theoretical transport equations and experimental works. This paper concluded that the proppant's characteristics and rheological parameters for fracturing fluids are crucial considerations for modeling the proppant transport in hydraulic fracturing design. Moreover, Shah (1993) investigated the rheological characterization of the various concentrations of slurry fluid (hydroxypropyl guar (HPG)) in the range of 30,40, and 60 lbm HPG/1,000 gal to obtain the flow behavior as a result of differential pressure vs. flow rate into the experimental vertical-fracture-flow model. This work used proppant sizes of 20/40-mesh sand with three concentration values that varied from 0 to 12 lbm/gal at three temperature conditions (80, 110, and 140°F). The data that was gathered presented correlations of apparent viscosity as a function of fluid concentration, fracture shear rate, experiment temperature, and proppant concentration. Also, the correlation can be used to model 2D or 3D fracture-design simulators in order to estimate fracture geometry and extension.

In 2000, Samuel et al. studied the application of viscoelastic surfactant in tight formations to minimize fracture height growth and increase effective fracture length. The paper presented case studies for low permeability gas wells in Rock Springs, Wyoming, and El Reno, Oklahoma. Field results based on the pressure transient analysis and tracer indicated that the viscoelastic surfactant fracturing fluid was more beneficial as fracture

fluid treatments in both unconventional and conventional formations compared to traditional and new generations of cross-linked gels.

Furthermore, Asadi et al. (2002) discussed the method for obtaining fracturing fluids with zero shear viscosity and how this factor is important to evaluate, model, and predict the proppant transport in hydraulic fractures. Viscoelastic parameters of the fracturing fluids were measured as a function of oscillatory frequency to determine zero shear viscosity by involving Maxwell's model at various relaxation times. The authors reported examples and a detailed explanation on the methodology of the fluid viscosity, elasticity, and relaxation time measurements to obtain the zero-shear fluid viscosity. In 2005, Harris et al. conducted an experimental work on fracturing fluids, such as metal and borate crosslinked fluids, linear gel fluids, and surfactant gel fluids, to show how these fluid types are different in terms of proppant transport by considering the size and concentration of proppants using a modified Fann Model 50-type viscometer. The experiment outcomes divided fracturing fluids into three major fluid classes with different capabilities to transport proppant by considering fracture transport velocity, a permanent network structure, and a transient network structure.

After that, Harris et al. (2008) compared three measurement techniques: steady shear measurements, dynamic oscillatory shear measurements, and slurry viscosity. The approaches were applied to the same fracturing fluids in a previous study for verification of transport prediction. Moreover, Walters et al. (2009) introduced a new clean biopolymer-based fracturing fluid that has high conductivity, stable viscosity, low pipe friction, excellent proppant transport, and the capability to be used with produced water. They discussed field trials of 14 frac stages over four wells. Based on their evaluation, this

fracturing treatment fluid can provide excellent proppant transport with high fracture conductivity in tight formations. In 2015, Gomaa et al. studied the minimum rheological properties required for effective transport behavior of the proppants by using combinations of rotational and oscillatory measurements. They observed that fracturing additives may or may not enhance the carrying of the proppants, based on the internal fluid structure.

Furthermore, Hu et al. (2015) examined the settling behavior of the carboxymethyl hydroxypropyl guar (CMHPG) crosslinked with borate by correlating with the rheological properties of the fluids. The authors concluded that the main mechanisms during proppant transport to enhance particle suspension or transportation are shear thickening and elastic lifting. The research outcome provided guidance to develop the chemistry of fracturing treatment fluids. Huang et al. (2018) conducted experimental research to study the effect of injection parameters on the proppant transport behavior by using different polymer concentrations in rough vertical hydraulic fractures. The results showed that effective vertical proppant flow occurred when a high polymer slurry concentration was used.

In 2018, Aften studied five HVFRs to investigate the viscosities and apply eight factors, for example, temperature, hydration approach, polymer concentration, brine composition, additive interaction, and pumping and tubular transport using response surface methodology. This study established a reliable approach for gauging performance and examining the field operations of HVFR systems in a high-TDS environment. Finally, Ba Geri, M. et al. (2019 a, b, c, & d) conducted several studies on HVFR fluids to investigate the rheological behavior and its effect on the static proppant settling velocity. The research outcomes showed interesting insights into the understanding of high viscous friction reducer fracture fluids compared to linear gel and slickwater fracture fluids. To

evaluate the performance of HVFRs on proppant transport, a comprehensive literature review was developed, including laboratory work, simulation investigation, and field case studies that were summarized and analyzed to understand the viscoelasticity properties of HVFRs.

This research aims to investigate the viscoelastic property that can help to understand the true proppant transport capacity of fracturing fluids. To evaluate HVFRs performance, a full comparison study between HVFRs and three different fracturing fluids such as xanthan, polyacrylamide-based emulsion polymer, and guar was provided. These fracturing fluids were examined on different water quality, DI water, 2 wt% KCl, and 10 lbs. brine (saturated NaCl Solution (TDS: 347,000 ppm)). In addition, viscosity profiles and elastic modulus were conducted at different temperatures; also, proppant settling rates were tested. Finally, successful field implementations using the new HVFR system were fully explained.

1.1. PRODUCED WATER IN USA BASINS

Using produced water instead of fresh water is gaining traction to minimize freshwater usage, reduce environmental impacts, and increase hydrocarbon recovery from unconventional formations. However, generally polymer friction reducers perform more poorly in high salinity waters. High salinity produced waters are more common in the Marcellus, the Permian, and the Bakken basins with TDS (total dissolved solids) levels measured at 43,000 ppm, 350,000 ppm, and over 225,000 ppm, respectively (Be Geri, M. et al., 2019a; Whitfield, S., 2017).

A high salinity environment and hardness are the main barriers to using produced water as a fracturing fluid-based system, due to their negative effect on the fracture fluid elastic profile as well as the hydration process required to build up enough viscosity to carry or transport proppant. The lifetime and the magnitude of the viscoelastic property of fracturing fluids depends on several factors, such as the source of water (e.g., levels of TDS and hardness), polymer dosage, fluid pH, and test temperature (Li, L. et al., 2014). Thus, switching based-fracturing fluids from fresh water to a high-TDS water system was not an easy task for the operators and service oil companies.

This research used a new high viscosity friction reducer (HVFR) as an alternative fracturing fluid for downhole conditions with temperature ranges between 150 to 250°F. The HVFR system proved compatible with high-TDS environments that exceed 340,000 ppm. Four different fracturing fluids (HVFR, xanthan, polyacrylamide emulsion polymer, and guar) were tested. The HVFR displayed have better viscoelastic performance than the other tested fluids for transporting the proppant.

2. EXPERIMENT DESCRIPTION

2.1. EXPERIMENT MATERIALS

2.1.1. Fracturing Fluids. Four different samples of friction reducers were prepared: HVFR, xanthan, polyacrylamide-based emulsion polymer, and guar. HVFR, xanthan, and guar were slurries containing 3 lbs. per gal. The polyacrylamide emulsion polymer was used by itself. In this test, each product sample was added in DI water, 2 wt% KCl, and 10 lbs. brine (saturated NaCl Solution (TDS: 347,000 ppm)), following the ratio

of 2 gal per 10 bbl. The HVFR is anionic polymer, and the molecular weight is 18 to 26 million (g/mole). Table 1 shows the molecular weight of the tested friction reducers.

2.1.2. Frac Sand and Dosage. To measure the settling rate, Ottawa Frac Sand 20/40 (particle density: 22.12 lbs./gal) employed was. The dosage of frac sand in each HVFR fracturing fluid was 0.5 lbs. per gallon.

Table 1. The molecular weight of friction reducers.

Friction Reducers	Molecular Weight (g/mole)
HVFR	18,000,000-26,000,000
Xanthan	1,000,000-7,000,000
Emulsion	6,000,000-11,000,000
Guar	50,000 – 8,000,000

2.2. MEASUREMENTS OF RHEOLOGICAL PROPERTY

Based on the hydraulic fracturing industry practice, the shear rates while pumping the fluid slurry into the fractures are within the range 10 s^{-1} to 170 s^{-1} as well as 511 s^{-1} to determine fluid apparent viscosity. In lab studies, the common shear rate was either 40 s^{-1} or 100 s^{-1} (Hu et al., 2015; Gomaa et al., 2015; Ba Geri, M. et al., 2019d).

2.2.1. Friction Reducers Preparation for Rheological Property. Four friction reducers were prepared: HVFR, xanthan, polyacrylamide emulsion polymer, and guar. HVFR, xanthan, and guar were dry powder and were mingled with modified base oil to be compared with the viscosity profile of emulsion polymer. The HVFR, xanthan, and guar slurries contained 3 lbs. of dry solid per gal. The polyacrylamide emulsion polymer was

used by itself in this test. Each product sample was added in DI water, 2 wt% KCl, and 10 lbs. brine (saturated NaCl solution (TDS: 347,000 ppm)) as the ratio of 2 gal per 10 bbl.

2.2.2. Fracturing Fluid Viscosity Measurement. This study investigated the viscosity of fracturing fluids at shear rates 40 s^{-1} , 100 s^{-1} , and 170 s^{-1} . Before measuring the viscosity of each fracturing fluid, the fluid was vigorously stirred in the beaker for 30 min. The viscosity reading was set to two temperatures, ambient: 75 °F and 150 °F.

2.2.3. Elasticity Characterization (Elastic Modulus, G'). Several methods can be used to measure the elastic properties of viscoelastic fluid, such as the viscoelastic characterization of the fracturing fluids, N1, relaxation time, the dynamic oscillatory frequency test, and the amplitude sweep test. This study investigated the viscoelasticity behavior of the tested fluid by testing dynamic oscillatory frequency through M5600 (Grace Instrument).

2.2.4. Friction Reducers Preparation for Elasticity Property. HVFR, xanthan, polyacrylamide emulsion polymer, and guar were prepared to compare the elastic modulus of each fracturing fluid. Dry HVFR, xanthan, and guar were suspended in modified base oil. The slurry contained 3 lbs. of active ingredient per gal. In addition, polyacrylamide emulsion polymer was tested by itself. The dosage rate of each slurry was 2 gal per 10 bbl. of DI water and 10 lbs. brine solution. The hydraulic fracturing fluid was stirred for 30 min. prior to measuring the elastic modulus.

2.2.5. Elastic Modulus Measurement. The elastic modulus was measured by oscillatory motion. M5600 (Grace Instrument) was used for this test and set up with frequencies in increments from 0.5 to 4.5 Hz by 0.5 Hz, and amplitudes at 50, 200, and 400%. The elastic modulus value was calculated by averaging four times measurement.

2.3. THE SETTLING RATE MEASUREMENT OF FRAC SAND IN HVFR FRACTURING FLUID

2.3.1. HVFR Fracturing Fluid Preparation. Four HVFR fracturing fluids were prepared to research the frac sand settlement rate in a viscous solution. The HVFR dosage was 0.5, 0.75, 1.0, and 1.25 gal per 1,000 gal of fresh water. The HVFR fracturing fluid was stirred for 30 min., and then was poured into a 1,000 ml round glass cylinder.

2.3.2. Test Method on Frac Sand Settlement Rate. Following the ratio of 0.5 lbs. of frac sand per 1,000 gal of fracturing fluid, frac sand was placed in a 1,000 ml cylinder. The cylinder stopper was completely sealed to prevent fluid loss. The cylinder was vigorously shaken to disperse frac sand evenly in the cylinder for 20 sec. As soon as the cylinder was placed on the table, the time was started, and then stopped once all of the frac sand had settled to the bottom of the cylinder. The measurement was repeated three times on each fracturing fluid and the values were averaged.

3. RESULTS AND ANALYSIS

3.1. THE VISCOSITY PROFILES OF VARIOUS FRICTION REDUCERS IN DI WATER, 2 WT% KCL, AND 10 LBS. BRINE (SATURATED NACL SOLUTION (TDS: 347,000 PPM))

Of all fluid sources, HVFR represented the highest viscosity, as shown in Figures. 1, 2, and 3, while xanthan, polyacrylamide emulsion, and guar showed mixed results depending on water conditions. The viscosity variation in different water conditions might be affected by molecular weight and chemical structure. Table. 1. shows the different molecular weights of HVFR, xanthan, emulsion polymer, and guar. HVFR has a relatively high molecular weights, while xanthan, emulsion polymer, and guar have low molecular

weight. At about 50% higher the molecular weight of HVFR helped it become heat resistant and viscous in all types of fluids. Thus, the HVFR fracturing fluid system can suspend and transport proppant deeper into the fractures. Proppant suspension and transportation can be explained by Stoke's law, which is covered by a later section, in this paper proppant settling rate result.

From Figure 1, using DI water at a low shear rate of 40 s^{-1} and increasing the temperature from 75 to 150 °F caused the viscosity profile of HVFR to slightly decrease from 148.68 cp to 141.47 cp, respectively. The same trend was noticed at a high shear rate of 170 s^{-1} . In contrast, Figure 3. shows that changing the water quality from DI water to 10 lbs. Brine (Saturated NaCl Solution) at the low shear rate 40 s^{-1} caused the viscosity of HVFR to drop sharply by 33% from 27.24 cp to 18.26 cp while increasing the temperature from 75 to 150 °F.

The effect of fracture fluid on the viscosity profile can be illustrated by Figure 3. At room temperature 75 °F and high-TDS water, both HVFR and guar indicated quite close viscosity readings, and both polyacrylamide emulsion and xanthan fluids exhibited similar viscosity profiles; however, synthetic polymers, HVFR and polyamide emulsion polymer, represented better viscosity reading. This means that the synthetic chemical structure is more heat resistant than guar and xanthan structures created by nature. The results revealed similar thermal properties of HVFR and emulsion polymer from the viscosity readings in the 2wt% KCl solution as well. HVFR and emulsion showed less viscosity reduction than guar and xanthan, comparing the viscosity values at 75 °F and 150 °F.

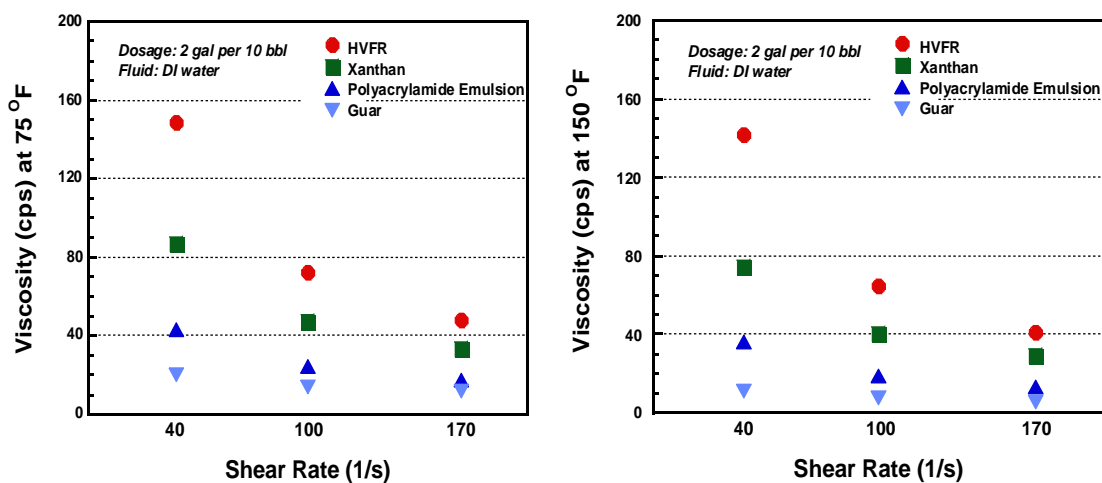


Figure 1. The viscosity profile of various friction reducers in DI water.

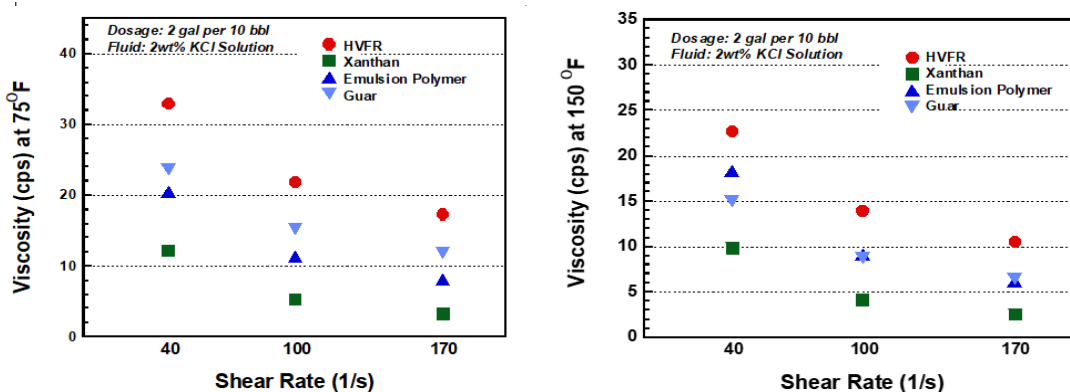


Figure 2. The viscosity profile of various friction reducers in 2wt% KCl solution.

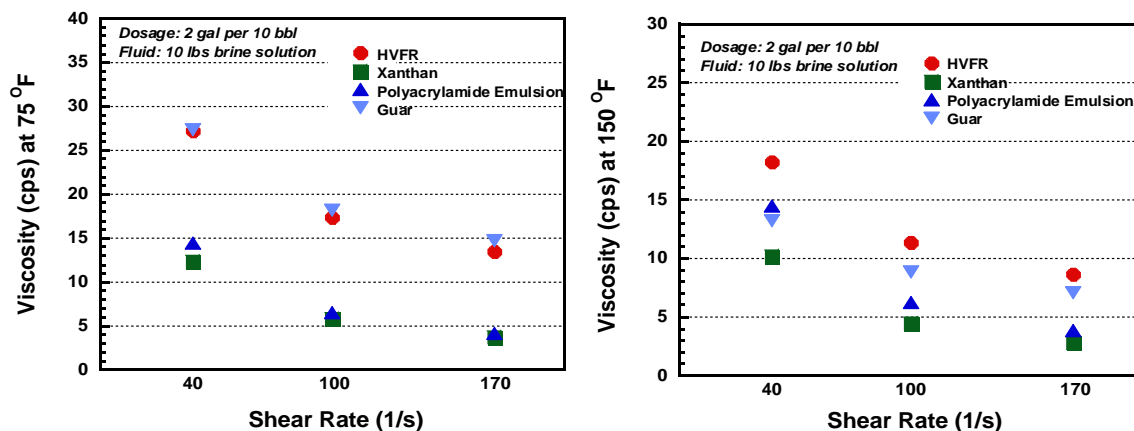


Figure 3. The viscosity profile of various friction reducers in 10 lbs. brine.

3.2. THE n' AND K' VALUES OF VARIOUS FRICTION REDUCERS IN DI WATER, 2 WT% KCL, AND 10 LBS. BRINE (SATURATED NACL SOLUTION (TDS: 347,000 PPM))

Table. 2 represents the values of n' and K' , which are called flow behavior index and flow consistency index, respectively. Flow behavior index determines rheological properties, Newtonian or non-Newtonian, while flow consistency index measures the yield stress of fluid. As published in other papers, all of the friction reducers in this test have indicated a non-Newtonian fluid, shear thinning as n' value is less than 1. In Di water, HVFR showed the most shear thinning characteristics through the lowest n' , while guar was less affected by the shear rate than others. In 2 wt% KCl and 10 lbs. brine solutions, the n' values of HVFR and k guar are relatively higher, comparing to xanthan and emulsion polymer. It means the viscosity of HVFR and guar is less affected by the shear rate increments. Although considering the true viscosity value, the higher n' value may be interpreted as better suspension effect on proppant transportation because the viscosity reduction percentage from low shear rate to high shear rate should be smaller than other cases with lower n' value. The viscosity reading at various shear rates and the n' value should be helpful to evaluate the capability of fracturing fluid to transport proppant.

3.3. THE ELASTIC MODULUS COMPARISON OF VARIOUS FRICTION REDUCERS IN DI WATER AND 10 LBS. BRINE SOLUTION (TDS: 347,000 PPM)

Figure 4 shows the effect of frequency and amplitude on the elastic modulus. The elastic modulus was increased as the frequency was increased, while the amplitude increment lowered the elastic modulus.

Table 2. The n' and K' values with viscosities reading of friction reducers in various fluids.

Fluids	Friction Reducers	Temp. (°F)	n'	K'	Visc@ 40(1/s) cP	Visc@ 100(1/s) cP	Visc@ 170(1/s) cP
DI Water	HVFR	76	0.22	4.71	148.68	72.52	47.86
		150	0.15	5.79	141.47	64.93	41.36
	Xanthan	80.2	0.33	1.78	86.93	47.26	33.2
		151	0.37	1.31	72.42	40.67	29.12
	Emulsion Polymer	81	0.37	0.77	43.36	24.43	17.53
		151	0.31	0.81	35.87	19.03	13.19
Guar	80	0.60	0.16	20.53	14.26	11.55	
	151	0.54	0.11	11.48	7.52	5.89	
2 wt% KCl	HVFR	74.4	0.55	0.31	32.99	21.9	17.28
		151	0.47	0.29	22.76	14.01	10.58
	Xanthan	76	0.10	0.61	12.2	5.36	3.33
		152	0.06	0.58	9.83	4.17	2.54
	Emulsion Polymer	74	0.36	0.38	20.41	11.35	8.07
		151	0.24	0.52	18.35	9.18	6.15
Guar	74.6	0.52	0.25	23.73	15.26	11.81	
	151	0.41	0.24	15.1	8.79	6.43	
10 lbs. Brine Solution	HVFR	82	0.51	0.30	27.24	17.41	13.44
		151	0.49	0.22	18.26	11.4	8.68
	Xanthan	79	0.19	0.44	12.32	5.85	3.8
		151.6	0.12	0.48	10.18	4.53	2.84
	Emulsion Polymer	83	0.14	0.62	14.39	6.54	4.14
		151	0.09	0.78	14.48	6.26	3.85
Guar	79	0.61	0.21	27.42	19.25	15.68	
	151	0.56	0.12	13.26	8.89	7.05	

This means that the physical activity of polymer is chains directly related with the elastic modulus. The short wavelength by frequency increment made polymer chains more active in the solution and caused the increment of the elastic modulus. The longer polymer chains (higher molecular weight) of HVFR indicated a better elastic modulus in DI water than the other tested fracturing fluids. Figure 5 represents the elastic modulus of friction reducers in 10 lbs. brine at 75, 150, and 250 °F. First of all, it was difficult to properly

interpret the elastic modulus characteristics of friction reducers at 150 and 250 °F because the abundant cations in 10 lbs. brine solution interrupted the hydration of the friction reducers, and furthermore the high temperature made the polymer chains loose. Both factors lowered elastic modulus values. The very low the elastic modulus values at 150 and 250 °F in the 10 lbs. brine solution might be caused by reading errors of the M5600 instrument. Thus, the results would observe only the elastic modulus in the 10 lbs. brine at 75 °F. guar elastic modulus seemed comparable with HVFR because the diol groups of guar let the polymer chains crosslinked with cations (sodium) in 10 lbs. brine solution. The increment of crosslinking density helped the elastic modulus improve.

3.4. PROPPANT SETTLING RATE RESULT

The settling rate was calculated with the fluid height 33.66 cm in a 1,000 ml cylinder and equalize frac sand settlement time (sec.). Figure 6 represents the settling rate of frac sand with various HVFR dosages. The settling rate was reduced with HVFR dosage increment. This result can be explained using Stoke's Law shown in equation (1). The settling velocity and fluid viscosity are in inverse proportion to each other, proving that the relatively higher viscosity of HVFR represents better proppant transportation capability, when compared to other friction reducers, such as xanthan and emulsion polymer. The results show that increasing the dosage of HVFR from 0.5 gpt to 1.25 gpt exhibited a slower settling rate of the proppant by three times from 1.2 cm/s to 0.4 cm/s, respectively.

Stoke's Law for Settling Solids

$$V = \frac{g\left(\left(\frac{\rho_1}{\rho}\right)-1\right)d^2}{18\nu} \quad (1)$$

- V: Settling Velocity of the Solid
- g: acceleration of gravity
- ρ_1 : Mass Density of the Solid
- ρ : Mass Density of the Fluid
- d: Diameter of the Solid (Assuming Spherical)
- ν : Kinematic Viscosity of the Fluid

Table 3. The effect of dosage of HVFRs on proppant settling rate.

Dosage per 1,000 gal (Polymer Concentration)	Settling Rate (cm/s)
0.50 gal	1.17
0.75 gal	0.79
1.00 gal	0.60
1.25 gal	0.44

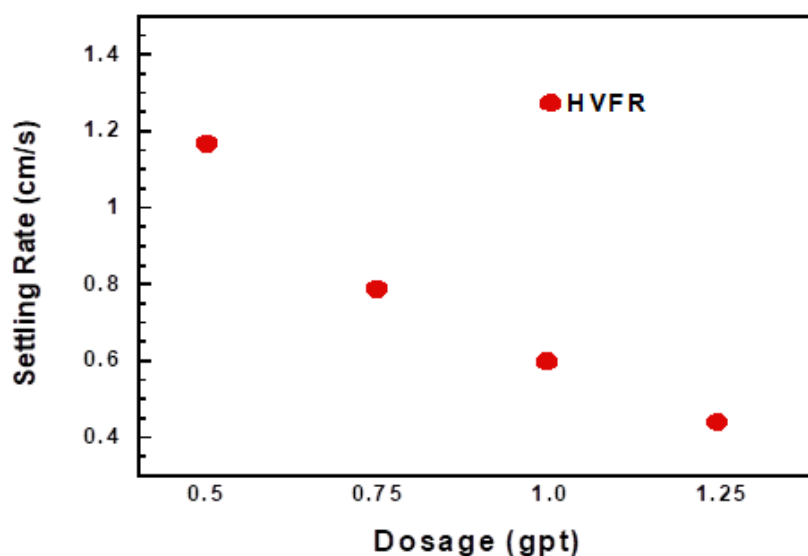


Figure 4. Frac sand settling rate comparison with various HVFR dosage.

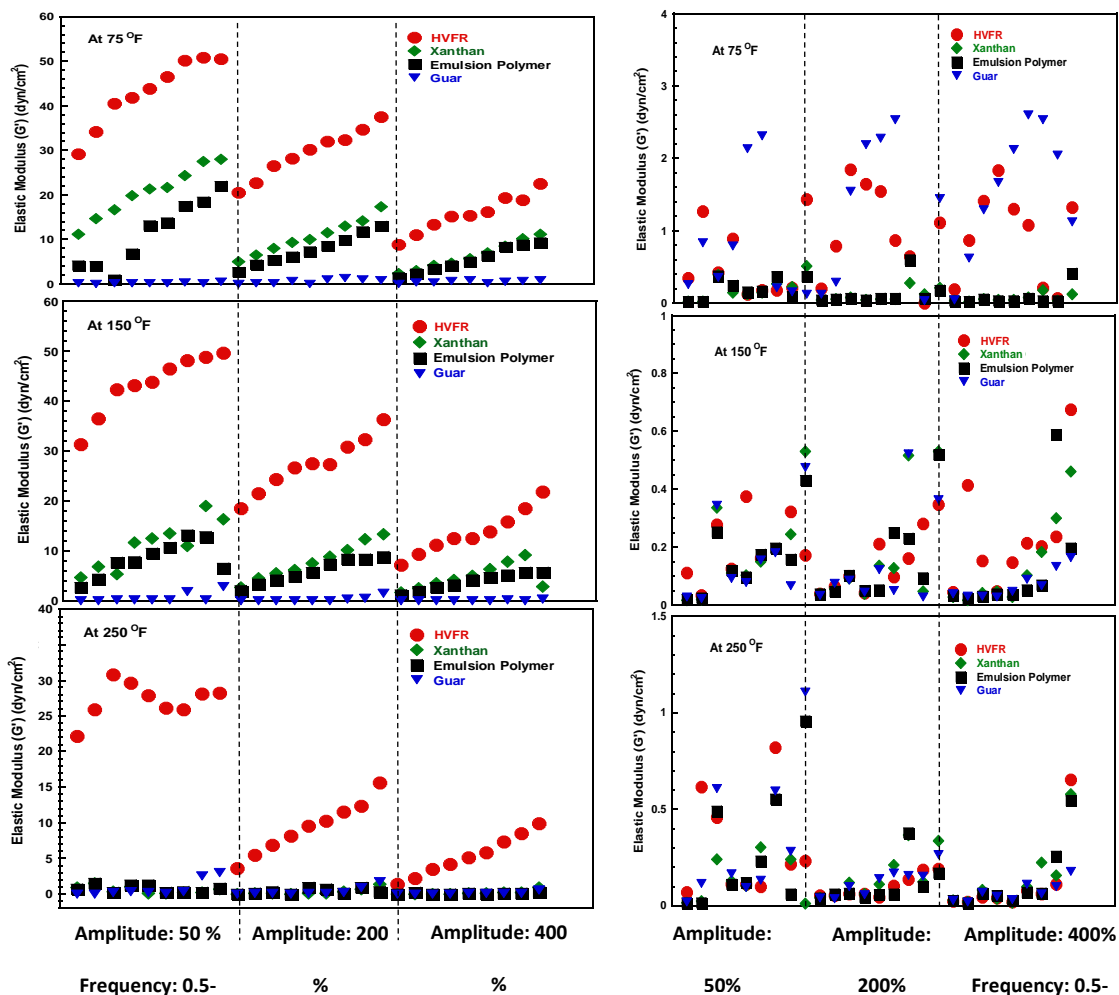


Figure 5. The elastic modulus measurement of HVFR, xanthan, emulsion polymer, and guar at 75, 150, and 250 °F in DI water (left) 10 lbs. brine solution (right).

3.5. HVFR ELASTIC MODULUS CHARACTERISTICS BY AMPLITUDE, FREQUENCY, FLUID TYPE, AND TEMPERATURE

As shown in Figures 7, 8, and 9, the elastic modulus of HVFR could be determined by amplitude, frequency, fluid type, and temperature. In this study, the HVFR dosage was 2 gal per 10 bbl. The elastic modulus of HVFR fracturing fluid was presented with various frequencies and amplitudes in Figure 7. The frequencies and amplitudes affect the polymer chains motion, responding to the elastic modulus of fracturing fluid. As shown in Figure

7, the elastic modulus indicated the highest values at the frequency 4.5 Hz from each amplitude, and lower values were indicated as the amplitude was increased. The higher wavelength raised the elastic modulus as the shear stress was increased, while the higher amplitude reduced the value of elastic modulus as stretching out the polymer chains length ways and losing elastic property in result.

This study will be useful for designing fracturing fluids with optimal proppant transportation conditions. The higher elastic modulus helps proppants suspended in fluid by polymer chains activity. Figure 8 shows the HVFR elastic modulus characteristics by water condition. Plenty of cations in the 10 lbs. brine solution (TDS: 347,000 ppm) hindered the chains' stretching of high molecular weight polymer and resulted in a low elastic modulus. The temperature also affected the elastic modulus of HVFR fracturing fluid as presented in Figure 9. The elastic modulus readings at 250 °F were significantly reduced as the polymer chains become slack.

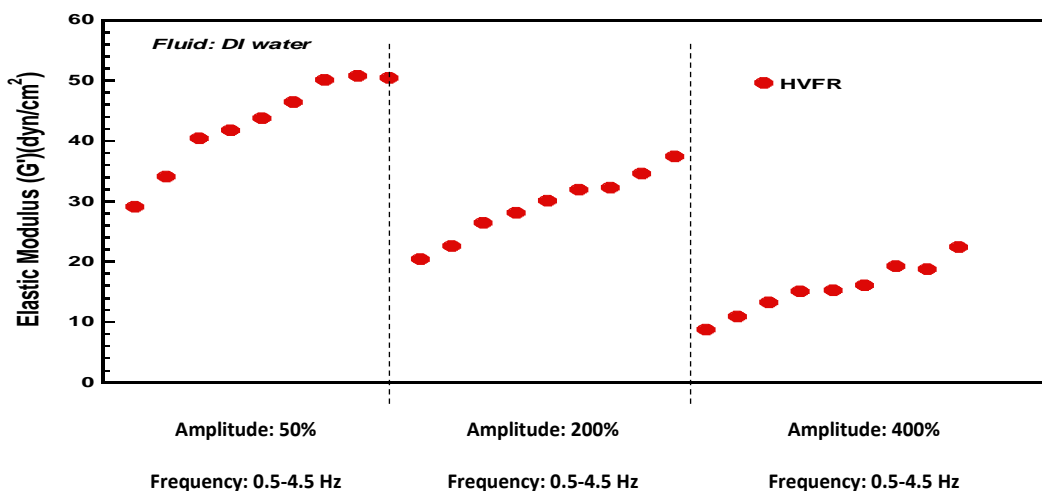


Figure 6. The elastic modulus characteristic of HVFR by amplitude and frequency at room ambient.

3.6. HVFR ELASTIC MODULUS PROFILES IN DI WATER & 10 LBS. BRINE (TDS: 347,000 PPM)

Figure 8 presents elastic modulus G' as a function of frequency (Hz) at 400% amplitude for 2 gal per 10 bbl. of HVFR at two different water qualities, DI water (left) and high-TDS water with 10 lbs. brine (right). Case I, using DI water with HVFR, provides a strong elastic profile and linear relationship by increasing the test frequency the elastic modulus G' increase. In contrast, with case II at high-TDS (340,000 ppm), the elastic modulus increased until the frequency reached 2 Hz. After that, the elastic modulus decreased sharply and came close to the zero dyn/cm^2 .

Generally speaking, water salinity plays a key role in changing the fluid elasticity negatively. To illustrate, at 2 Hz the elastic modulus was 15.15 dyn/cm^2 and 1.83 dyn/cm^2 in both DI water and 10 lbs. brine, respectively. The cations efficiency reduces in high-TDS water due to the presence of high cations like magnesium and calcium causing polymer precipitation. These polyvalent ions in high-TDS environments can cause electrostatic crosslink of the polymer which in tum causes precipitation Aften, W. (2010).

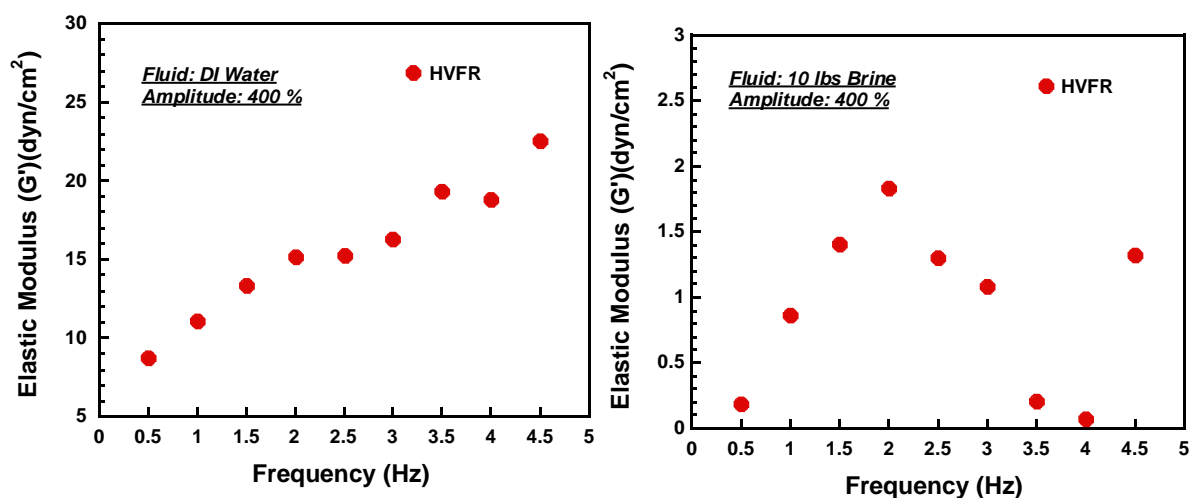


Figure 7. The elastic modulus characteristic of HVFR by fluids (DI Water vs. 10 lbs. brine).

3.7. HVFR ELASTIC MODULUS PROFILES BY TEMPERATURE

Figure 9. shows elastic modulus G' as a function of frequency (Hz) at 400% amplitude for 2 gal per 10 bbl. dosage at different temperatures 75, 150, and 250 °F. At room temperatures 75 and 150 °F, the viscoelastic property was similar, and the HVFR showed that temperatures under 150 °F did not affect the polymer chains physically while exhibited a lower value of G' at high temperature around 250 °F. It also observed that the elastic modulus increased with frequency increments from 0.5 to 4.5 Hz.

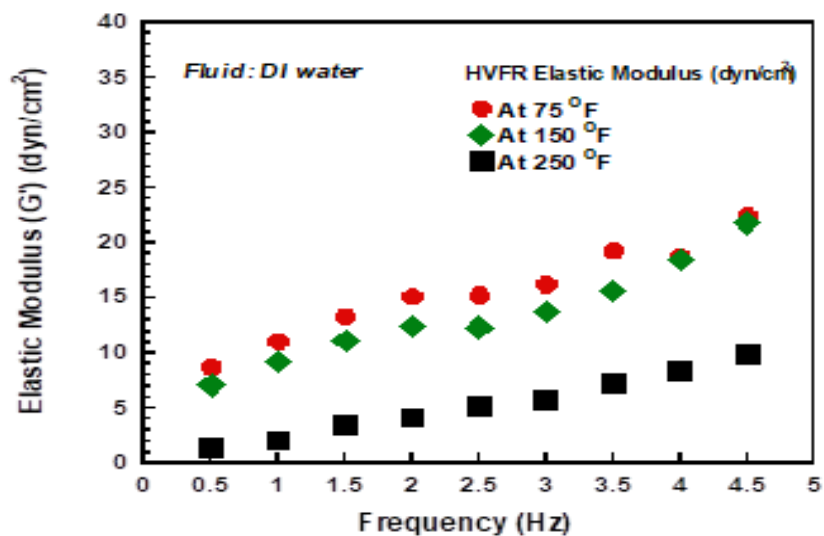


Figure 8. The elastic modulus characteristic of HVFR by temperature.

3.8. FIELD CASE STUDY

A well-C is operated in Wolfcamp Shale. TD (Total Depth) was about 22,000 ft, and TVD (Total Vertical Depth) was approximately 8,900 ft, as shown in Figure 10. The operation pressure range was from 7,000 and 11,000 psi. The fluid type was slickwater, and the proppant size was 40/70 white. The fluid flow rate was between about 60 and 100

bpm. In this frac job, HVFR as well as other chemicals such as acid and gel breaker. were employed. The initial pressure was about 11,000 psi. The dosage of HVFR, from 1.25 gpt to 0.5 gpt, was treated for proppant transportation. According to these results that HVFR could be economically and efficiently used for proppant transportation and pressure reduction at dosage rates as low as 0.5 gpt.

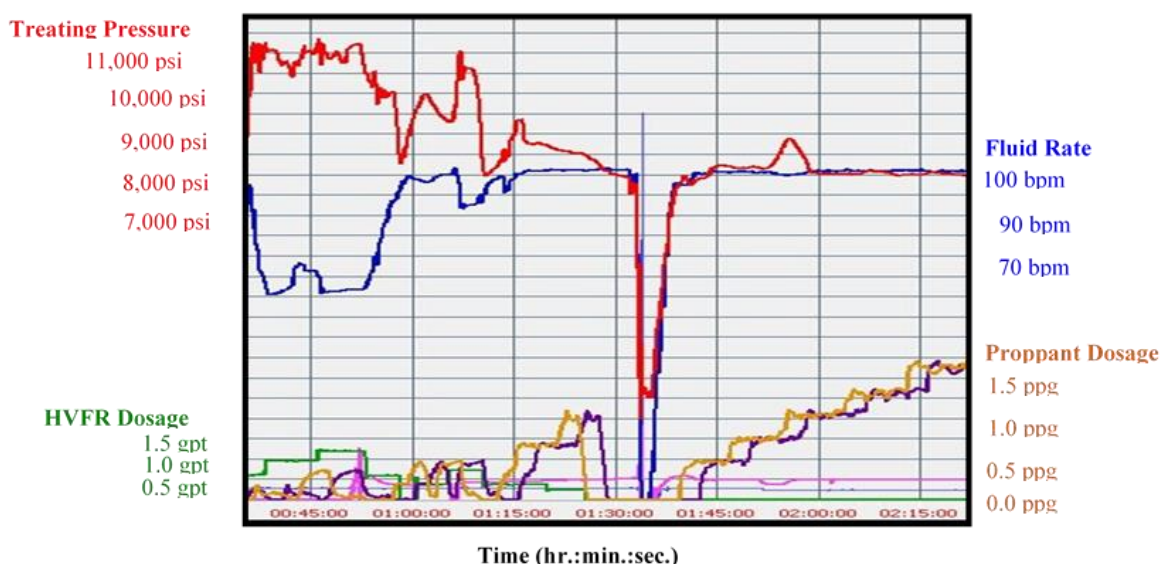


Figure 9. Hydraulic fracture treatment plot from Well-C using HVFRs.

4. DISCUSSION THE POTENTIAL OF FORMATION DAMAGE

Achieving high fracture conductivity is a primary goal of hydraulic fracturing treatment because these conductive channels enable the flow of oil and gas from the formation to the wellbore. Many factors influence the fracture conductivity, such as proppant size and type, fracture closure stress, and fracturing fluid type. HVFR fracturing fluids are rapidly gaining popularity because of their numerous advantages, such as better

proppant carrying capability. In addition, using HVFRs fracturing fluids lowers overall costs due to fewer chemicals (Be Geri, M. et al, 2019a).

Currently, HVFRs have been successfully used as a completion fluid in unconventional formations. However, some concerns remain of the potential formation damage that might occur by using these high molecular weight polyacrylamide-based fluids. Therefore, to address these concerns, experimental investigation prior to this research (SPE-197081) was performed to evaluate the potential of formation damage that might occur due to using HVFRs. To evaluate using HVFR fracture fluids, a conductivity test of an anionic polymer HVFR with a high molecular weight (18 to 26 million (g/mole)) was conducted under closure pressure 2,000 psi and at the reservoir temperature 165°F.

Figure 11. showed the conductivity and permeability of fracturing fluids. There are three types of fracturing fluids: baseline (no HVFR addition), 0.5 gpt, and 2.5 gpt. The pressure and temperature under this test were 2,000 psi and 165 °F, respectively. At 2,000 psi, fluid conductivities and proppant permeabilities of baseline and 0.5 gpt were quite close. In fact, 0.5 gpt fracturing fluid showed better compatibility and permeability than the baseline, even though the HVFR used in this test has a very high molecular weight, positive results concluded that 110% and 94% regained permeability was observed at dosages of 0.5 gpt and 2.5 gpt.

5. CONCLUSIONS

This paper presented the overall understanding of HVFR, xanthan, emulsion polymer, and guar on viscosity and elastic modulus in DI water and harsh brine solutions. Based on the active ingredient weight and volume of friction reducers, HVFR has good characteristics for proppant transportation and pressure reduction from viscosity and elastic modulus results. The relatively higher molecular weight and thermal stability of the synthetic polymer chemical structure supported the desired properties in frac operation.

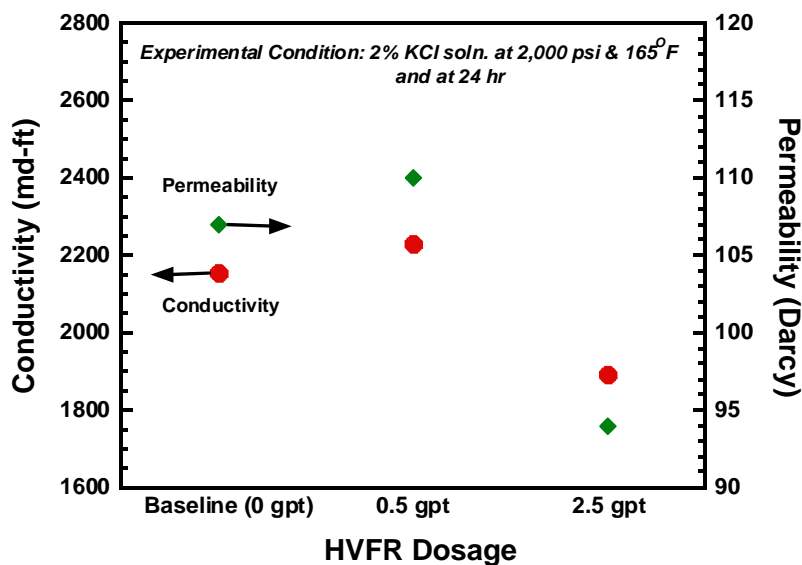


Figure 10. Conductivity and permeability on baseline, 0.5 gpt, and 2.5 gpt at 2,000 psi and 24 hr.

In medium brine and high brine solutions through 2wt% and 10 lbs. brine, HVFR, the n' (flow behavior index) value of HVFR and Guar was higher than emulsion polymer and xanthan. The lower viscosity reduction from low shear rate to high shear rate may improve proppant transport deeper into the fracture. From Stoke's law and the viscosity

profiles of friction reducers, the investigation could prove HVFR has a good proppant transportation capability.

The elastic modulus is also related to the proppant transport characteristic. It is a physical stress affecting fluid properties and proppant transportation by the activity of polymer chains. Higher elastic modulus values represent the capability to transport proppants farther. As a result, this research observed that HVFR has an excellent elastic modulus when compared to other friction reducers.

Based on the results of viscosity profiles and elastic modulus, the research focused on HVFR properties on the effects of amplitude, frequency, fluid type, and temperature. The elastic modulus of HVFR has good heat resistance up to 150 °F, as shown in the viscosity profile. In addition to the viscosity profile and elastic modulus, the permeability and conductivity of HVFR supports the induction of HVFR in frac operations. As shown in one of field cases in this paper, the use of HVFR has been rapidly grown, and the future of utilizing HVFRs looks promising.

REFERENCES

- Acharya, A. R. (1988, November 1). Viscoelasticity of Crosslinked Fracturing Fluids and Proppant Transport. Society of Petroleum Engineers. <https://doi:10.2118/15937-PA>
- Aften, C. (2018, October 5). Analysis of Various High Viscosity Friction Reducers and Brine Ranges Effectiveness on Proppant Transport. Society of Petroleum Engineers. <https://doi:10.2118/191792-18ERM-MS>
- Aften, C. W. (2010, January 1). Study of Friction Reducers For Recycled Stimulation Fluids In Environmentally Sensitive Regions. Society of Petroleum Engineers. <https://doi:10.2118/138984-MS>

- Aggour, T. M., & Economides, M. J. (1999, February 1). Impact of Fluid Selection on High-Permeability Fracturing. Society of Petroleum Engineers. <https://doi:10.2118/54536-PA>
- Asadi, M., Conway, M. W., & Barree, R. D. (2002, January 1). Zero Shear Viscosity Determination of Fracturing Fluids: An Essential Parameter in Proppant Transport Characterizations. Society of Petroleum Engineers. <https://doi:10.2118/73755-MS>
- Ba Geri, M., Imqam, A., & Dunn-Norman, S. (2018, October 5). Proppant Transport Behavior in Inclined Versus Vertical Hydraulic Fractures: An Experimental Study. Society of Petroleum Engineers. <https://doi:10.2118/191813-18ERM-MS>
- Ba Geri, M., Imqam, A., & Suhail, M. (2019, March 15 a). Investigate Proppant Transport with Varying Perforation Density and its Impact on Proppant Dune Development Inside Hydraulic Fractures. Society of Petroleum Engineers. <https://doi:10.2118/195018-MS>
- Ba Geri, M., Imqam, A., & Flori, R. (2019, April 8 b). A Critical Review of Using High Viscosity Friction Reducers as Fracturing Fluids for Hydraulic Fracturing Applications. Society of Petroleum Engineers. <https://doi:10.2118/195191-MS>
- Ba Geri, M., Imqam, A., Bogdan, A., & Shen, L. (2019 c, April 8). Investigate the Rheological Behavior of High Viscosity Friction Reducer Fracture Fluid and Its Impact on Proppant Static Settling Velocity. Society of Petroleum Engineers. <https://doi:10.2118/195227-MS>
- Ellafi, A., M. Ba Geri, B. Bubach, and H. Jabbari (2019, June 23). Formation Evaluation and Hydraulic Fracture Modeling of Unconventional Reservoirs: Sab'atayn Basin Case Study. American Rock Mechanics Association.
- Geri, M. B., Flori, R., & Sherif, H. (2019, July 25). Comprehensive Study of Elasticity and Shear-Viscosity Effects on Proppant Transport Using HFVRs on High-TDS Produced Water. Unconventional Resources Technology Conference. doi:10.15530/urtec-2019-99
- Gomaa, A. M., Gupta, D. V. S., & Carman, P. (2015, April 13). Viscoelastic Behavior and Proppant Transport Properties of a New High-Temperature Viscoelastic Surfactant-Based Fracturing Fluid. Society of Petroleum Engineers. <https://doi:10.2118/173745-MS>
- Harris, P. C., Morgan, R. G., & Heath, S. J. (2005, January 1). Measurement of Proppant Transport of Frac Fluids. Society of Petroleum Engineers. <https://doi:10.2118/95287-MS>

- Harris, P. C., Walters, H. G., & Bryant, J. (2009, November 1). Prediction of Proppant Transport From Rheological Data. Society of Petroleum Engineers. <https://doi:10.2118/115298-PA>
- Hu, Y. T., Chung, H., & Maxey, J. E. (2015, February 3). What is More Important for Proppant Transport, Viscosity or Elasticity? Society of Petroleum Engineers. <https://doi:10.2118/173339-MS>
- Li, L., Sun, H., Qu, Q., Le, H. V., Ault, M., Zhou, J., ... Smith, D. (2014, October 27). High-Temperature Fracturing Fluids Prepared with Extremely High-TDS and Hard Produced Water. Society of Petroleum Engineers. <https://doi:10.2118/170607-MS>
- Li, S., & Zhang, D. (2019, April 1). How Effective Is Carbon Dioxide as an Alternative Fracturing Fluid? Society of Petroleum Engineers. <https://doi:10.2118/194198-PA>
- Samuel, M., Polson, D., Graham, D., Kordziel, W., Waite, T., Waters, G., ... Downey, R. (2000, January 1). Viscoelastic Surfactant Fracturing Fluids: Applications in Low Permeability Reservoirs. Society of Petroleum Engineers. <https://doi:10.2118/60322-MS>
- Shah, S. N. (1993, May 1). Rheological Characterization of Hydraulic Fracturing Slurries. Society of Petroleum Engineers. <https://doi:10.2118/22839-PA>
- Shrivastava, K., & Sharma, M. M. (2018, January 23). Proppant Transport in Complex Fracture Networks. Society of Petroleum Engineers. <https://doi:10.2118/189895-MS>
- Srinivasan, K., Ajisafe, F., Alimahomed, F., Panjaitan, M., Makarychev-Mikhailov, S., & Mackay, B. (2018, August 28). Is There Anything Called Too Much Proppant? Society of Petroleum Engineers. <https://doi:10.2118/191800-MS>
- Walters, H. G., Stegent, N. A., & Harris, P. C. (2009, January 1). New Frac Fluid Provides Excellent Proppant Transport and High Conductivity. Society of Petroleum Engineers. <https://doi:10.2118/119380-MS>
- Whitfield, S. (2017, June 1). Permian, Bakken Operators Face Produced Water Challenges. Society of Petroleum Engineers. <https://doi:10.2118/0617-0048-JPT>

VI. A COMPREHENSIVE REVIEW OF FORMATION DAMAGE CAUSED BY HIGH-VISCOSITY FRICTION REDUCERS: WOLFCAMP CASE STUDY

Mohammed Ba Geri¹, Abdulaziz Ellafi², Ralph Flori¹, Jerry Noles³, and Sangjoon Kim³

1: Department of Petroleum Engineering, Missouri University of Science and Technology, Rolla, MO 65409

2: Department of Petroleum Engineering, University of North Dakota, Grand Forks, ND 58202

3: CoilChem LLC, Washington, Oklahoma

ABSTRACT

The success of using the hydraulic fracture treatment can be evaluated by measuring fracture conductivity and regained permeability. However, selecting the most suitable fracture fluid system plays an essential role in minimizing or eliminating formation damage. To address potential formation damage that may occur during fracturing treatment, this research presents a comprehensive review of a good number of published papers that are carefully reviewed and summarized. These works include experimental research, case studies, and simulation work on recent improvements on using HVFR to carry proppant and capture the optimum design in fracturing operations. This paper also provides formation damage mechanisms such as chemical, mechanical, biological, and thermal mechanisms. Moreover, the research explains the fracture damage categories including the damage inside the fracture and damage inside the reservoir. The advantages of using HVFRs are also fully explained. Experimental rheological characterization was studied to investigate the viscoelastic property of HVFRs on proppant transport. In addition,

successful implication of utilizing HVFRs in the Wolfcamp formation, in the Permian Basin was discussed.

The research findings were analyzed to reach conclusions on how HVFRs can be an alternative fracture fluid system within many unconventional reservoirs. Compared to the traditional hydraulic fracture fluid system, the research shows the many potential advantages that HVFR fluids offer, including superior proppant transport capability, almost 100% retained conductivity, around 30% cost reduction, and logistics such as minimizing chemical usage by 50% and the ability to store operation equipment on location, reduce water consumption by 30%, and achieve environmental benefits. Finally, this comprehensive review addresses up-to-date of using HVFRs challenges and emphasizes necessities for using high viscosity friction reducers as alternative fracture fluids.

1. INTRODUCTION

Selecting optimal fracturing fluids plays a key role in successful hydraulic fracturing treatment. The primary goal of the hydraulic fracturing process is to achieve high fracture conductivity, because these conductive channels enable the flow of oil and gas from the formation to the wellbore. The fracture damages can negatively impact the effectiveness of the stimulation process. Several numerical studies confirmed that hydraulic damage could decrease the well productivity by up to 50% Han, (2014). Conventional fracturing fluids, such as guar-based fluids, build a filter cake on the surface of the shale matrix. Therefore, the potential of formation damage after using viscous fracturing fluids increases because the formed filter cake blocks the pore-throat of low

permeability rocks (Wang et al., 2010). In addition, utilising viscous fracturing fluids has the potential of decreasing the fracture conductivity due to a higher residual polymer. Many factors influence the fracture conductivity, such as proppant size and type, fracture closure stress, and fracturing fluid type (Ba Geri et al., 2019d).

Many investigations have been conducted concerning fracture damage evaluation. Bennion et al., (1999) summarized some issues and solutions associated with low permeability gas reservoirs during the stimulation and production process. The research concluded that improper fluid selection is one of the major mechanisms that cause formation damage. Reinicke et al., (2010) conducted an experimental study to investigate the mechanical damage that occurred at the hydraulic fracture face. In some cases, reservoir fluids are not compatible with fracturing fluids due to its chemical complicity (Aggour and Economides, 1999). Farah et al., (2016) performed numerical techniques in order to evaluate the formation damage caused by fracturing-fluid during the fracturing treatment and its influence on the hydrocarbon production and unconventional gas formation. Cooke, C. (1975) studied the impact of several types of fracturing fluids on fracture conductivity and described a theoretical method to evaluate fluid residue on fracture conductivity. Davles and Kulper (1988) studied several factors that affect proppant-pack and fracture conductivity, such as closure stress, multiphase flow, proppant size, proppant type, and fracturing fluids. Norman et al., (1989) evaluated commonly used hydraulic fracturing fluids using a simplified technique and reached the conclusion that the quickest fluids to clean up are flowing foams, uncrosslinked gels, and crosslinked fluids.

Voneiff et al., (1996) performed a simulation study to investigate the impact of unbroken fracturing fluids on the productivity performance of gas wells. The conclusions

of their research were unbroken fracture fluids initial gas production decreased by 80%, fracture clean-up can be delayed by weeks or months, and 30% reduction in gas reserves. Pope et al., (1996) discussed the effects of viscous fingering of using guar-based fracturing fluids on fracture conductivity and concluded that for predicting the retained permeability, known polymer concentration, polymer molecular weight, and temperature are required. Behr et al., (2006) developed a numerical model-initialization in order to evaluate the fracture damage that occurs after closure in tight gas reservoirs. Wang et al., (2008) ran a simulation study in order to understand how polymers in the fractures can affect the cleanup process.

Recently, HVFRs as a completion fluid have been successfully used in unconventional formations (Motiee et al., 2016, Van Domelen, 2017, and Ba Geri et al., 2019b). However, some concerns remain because of the potential formation damage that might occur by using these high molecular weight polyacrylamide-based fluids as completion fluids. Motiee et al., (2016) used high concentrations of friction reducers (HCFR) of 14 gpt. They conducted conductivity experiments under a high-temperature system at 220°F for 25 hours and concluded that using 14gpt of HCFR gives 72% of regained conductivity, while adding 1ppt of breaker increased the regained conductivity up to 80%. Van Domelen (2017) reported a comparison study between 15 lb/Mgal of crosslinked and 3 gpt of viscosity-building friction reducers (VFR) under the same conductivity measurement condition and reached the observation that the final regained conductivity was 106% and 36% of 3gpt of VFR and 15 lb/Mgal of crosslinked, respectively. Galindo (2019) studied the effect of increasing HVFRs viscosity on formation

damage. The results showed that HVFRs might cause formation damage if used without a breaker because of polymer residuals.

Ba Geri et al., 2019a presented a critical review of using HVFRs in lab studies and field operations. The investigation provided a full understanding of using HVFRs as an alternative fracture fluid. The study notes that limited work has been done to evaluate the potential of formation damage that could occur when using HVFRs during fracturing treatment. This paper provides a comprehensive study of the effects of utilizing HVFRs on fracture conductivity and regained permeability. Three cases were implemented to study the effect of formation damage caused by using HVFRs fracturing fluids. The Baseline (without HVFR) in 2% KCl solution was investigated in Case I (base case), while the effect of increasing the HVFRs dosage by 0.5 gpt and 2.5 gpt was investigated in Case II and Case III. In both cases, the sieve size distribution was performed before and after the test. Successful field implementation of using HVFRs was also discussed.

2. FORMATION DAMAGE MECHANISMS

Formation damage can be described as “the impairment of the invisible, by the inevitable and uncontrollable, resulting in an indeterminate reduction of the unquantifiable!” (Bennion, 1999). Creating a highly conductive path in ultra-low permeability unconventional reservoirs is an essential step to allow the hydrocarbons to flow from the reservoirs to the wellbore. To maintain the fracture conductivity, high-viscosity fracture fluids (e.g., guar gum or crosslinked) are required to carry a high concentration of proppant (Yuan et al., 2015). These viscous fluids should be degraded

after the fracture treatment for an easy clean-up process. The Well productivity performance is reduced due to formation damage and usually, an expensive treatment is required to remove fracture damage. Formation damage can be classified into four main mechanisms Figure 1: chemical, mechanical, biological, and thermal. These mechanisms inhibit the flow of fluid formation from reservoirs into the fracture network and consequently impair hydrocarbon production rates and well productivity (Civan, 2000, Nasr-El-Din, 2003 and Wang et al., 2008).

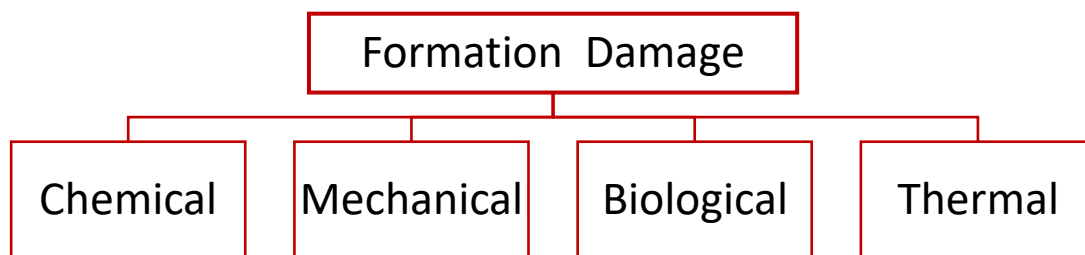


Figure 1. Classification of the common formation damage mechanisms (Civan, 2000).

In general, fracture damage can be classified into two categories as shown in the Table 1:

Table 1. Fracture damage categories (Wang et al., 2010).

Damage inside the fracture	Damage inside the reservoir	Other factors affect clean up
Fracture plugging with chemicals and polymers Fracture-face damage Proppant crushing Proppant embedment	Fluid leakoff Clay swelling Relative permeability change Capillary effects	Gel residue, breaker Fracture-fluid viscosity Viscous fingering Formation temperature Fracture conductivity Reservoir heterogeneity Fracture geometry

It is important to minimize or eliminate formation damage as this plays a key role in increasing well productivity. In unconventional reservoirs, well performance is a strong function of fracture conductivity and permeability of the region near the wellbore. Therefore, many researchers focus their studies to develop techniques to minimize or prevent formation damage. This paper will provide a better understanding of the distinct changes of the mechanical characterization on the HVFRs that could be used as guidance for fracture engineers to design and select more effective high viscous friction reducers. By doing so, the promising results of using HVFRs can minimize formation damage and maximize well productivity, and the ultimate operator goal will be achieved.

3. WHY HIGH VISCOSITY FRICTION REDUCERS?

The primary function of friction reducers is changing turbulent flow to laminar flow, which can reduce frictional loss that occurs while pumping fracturing fluids by up to 80%. Recently, high-viscosity friction reducers (HVFRs) have gained popularity as drilling and hydraulic fracturing fluids because the HVFRs exhibit numerous advantages such as the following (Ba Geri et al., 2019a &b):

- Reduced pipe friction during fracturing treatments
- High regain conductivities compared to linear and crosslinked gels
- Lower operational cost
 - Uses less water compared to conventional slickwater treatments
 - Consumes 33-48% less chemicals than conventional treatments

- Requires less equipment on location
- Requires fewer number of tank trucks in the field
- More fracture complexity using a less viscous fluid system
- Better hydrocarbon production results compare to or greater than other fluids.
- Improved flexibility to design treatments that balance technical, economic, and operational goals
- Reduced freshwater, proppant, and equipment requirements compared with conventional fluid systems
- Minimized environmental footprint with selection of engineered additives
- Simplified operations by reduced screen out risks.

4. EXPERIMENTAL DESCRIPTION

4.1. EXPERIMENTAL MATERIALS

4.1.1. Experimental Materials. Three different samples, baseline (w/o HVFR), 0.5 gpt (0.5 gal of HVFR per 1,000 gal), and 2.5 gpt (2.5 gal of HVFR per 1,000 gal), were selected to prepare typical hydraulic fracturing fluids. The HVFR is anionic polymer, and the molecular weight is 18 to 23 million. The conductivity and permeability test were conducted in 2% KCl solution at 165 °F and at a closure stress of 2,000 psi to prepare the fracturing fluid at lab temperature.

4.1.2. Proppant. The proppant size that was selected for this study was between mesh size 30 and 50. Tables. 2, 3, and 4 represent the sieve analysis of proppant used for

the test with the baseline, 0.5 gpt, and 2.5 gpt. The sieve size distribution was performed before and after the test.

Table 2. Proppant sieve analysis for baseline.

Mesh Size	Length (mm)	Baseline	
		Pre Sieve (%)	Post Sieve (%)
30	0.600	0.2	0.0
35	0.500	27.5	26.6
40	0.425	49.6	47.2
45	0.355	19.9	23.2
50	0.300	2.8	3.0
Total		100.0	100.0
Median Particle Diameter (MPD, mm)		0.463	0.458

Table 3. Proppant sieve analysis for 0.5 gpt.

Mesh Size	Length (mm)	Baseline	
		Pre Sieve (%)	Post Sieve (%)
30	0.600	0.2	0.2
35	0.500	27.5	26.5
40	0.425	49.6	47.8
45	0.355	19.9	22.5
50	0.300	2.8	2.9
Total		100.0	99.9
Median Particle Diameter (MPD, mm)		0.463	0.459

Table 4. Proppant sieve analysis for 2.5 gpt.

Mesh Size	Length (mm)	Baseline	
		Pre Sieve (%)	Post Sieve (%)
30	0.600	0.2	1.8
35	0.500	27.5	28.7
40	0.425	49.6	48.7
45	0.355	19.9	18.3
50	0.300	2.8	2.6
Total		100.0	100.1
Median Particle Diameter (MPD, mm)		0.463	0.458

5. MEASUREMENTS OF RHEOLOGICAL PROPERTY

5.1. SHEAR VISCOSITY CHARACTERIZATION (K, N)

Based on the standard practice in the hydraulic fracturing industry, the most typical shear rates that were measured while pumping the fluid slurry into the fractures are within the range 10 s^{-1} to 170 s^{-1} as well as 511 s^{-1} to determine fluid apparent viscosity. In lab studies the common shear rate was either 40 s^{-1} or 100 s^{-1} (Hu et al., 2015, Goma et al., 2015, Ba Geri et al., 2019c&f). This study investigated three different fracture fluid shear rates: 40 s^{-1} , 100 s^{-1} , and 170 s^{-1} .

5.2. SHEAR ELASTICITY CHARACTERIZATION (ELASTIC MODULUS, G')

Several methods can be used to measure the elastic properties of viscoelastic fluid, such as the viscoelastic characterization of the fracturing fluids, N1, relaxation time, dynamic oscillatory frequency test, and the amplitude sweep test. This study investigated the viscoelasticity behavior of the tested fluid by testing the dynamic oscillatory frequency through M5600 (Grace Instrument).

5.3. FRACTURE CONDUCTIVITY EXPERIMENT PROCEDURE

Conductivity cells were loaded with proppants with 2.0 lb/ft^2 loading between Ohio Sandstone Cores. $1,000 \text{ psi}$ closure stress was initially applied for 12-24 hours, and then the pressure was increased to $2,000 \text{ psi}$ for 50 hr. The conductivity and permeability of the samples were measured at 0, 24, and 50 hr. Equations (1) and (2) represent conductivity and permeability, respectively.

Conductivity:
$$kW_f = \frac{26.78\mu Q}{\Delta P} \quad (1)$$

Permeability:
$$k = \frac{321.4\mu Q}{\Delta P W_f} \quad (2)$$

where:

k: Proppant Pack Permeability (Darcy)

kW_f : Proppant Pack Conductivity (Millidarcy-feet)

μ : Viscosity of Liquid (cp)

Q: Flow Rate ($cm^3/min.$)

P: Differential Pressure (psi)

W_f : Proppant Pack Width (in)

6. RESULTS AND ANALYSIS

6.1. RHEOLOGICAL CHARACTERIZATION OF THE HVFRS

6.1.1. Viscosity Profile Measurement. Figure 2 shows the HVFR viscosity profile in fresh water. The range of pH and TDS in this water was 7-8 and 300-450 ppm, respectively. Divalent cations, such as Ca^{2+} and Mg^{2+} , were under 10 ppm. The HVFR solution was vigorously stirred for 30 minutes, and then each solution's viscosity was measured at shear rates 40, 100, and $170 s^{-1}$ through the M5600 rheometer (Grace Instrument) at room ambient. As shown in Figure 2, the viscosity has been proportionally increased with the HVFR dosage and represents the shear thinning property. For instance, at a loading of 3 gpt, the results for HVFR showed that HVFR has high viscosity (31 cp) at a lower shear rate of $0.40 s^{-1}$ compared to the viscosity of high shear rate of $0.170 s^{-1}$

showed a much lower viscosity of around 14 cp. The second observation was that at the same shear rate (e.g. 40 s^{-1}), increasing the HVFR dosage from 1 gpt to 3 gpt leads to an increase in the viscosity profile from around 8 cp to 31 cp, respectively.

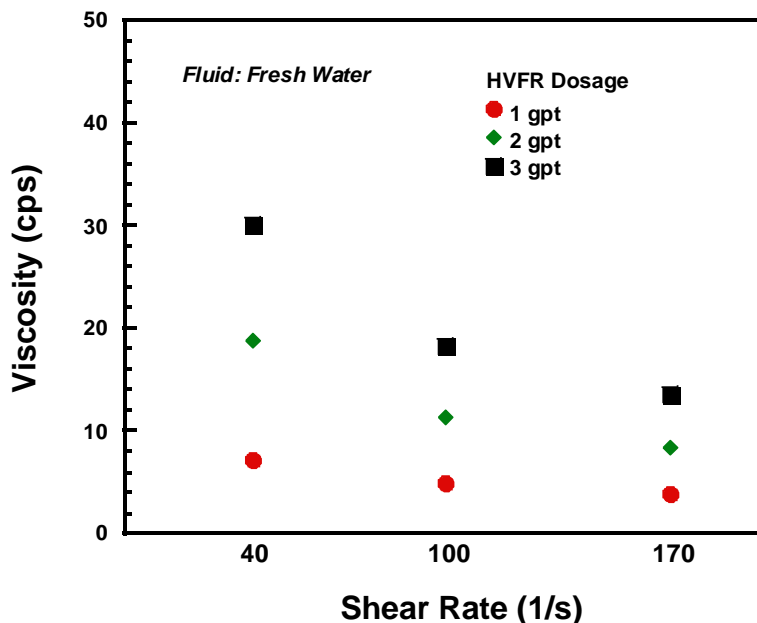


Figure 2. HVFR viscosity profile with various dosage in fresh water.

6.1.2. Elasticity Profile Measurement. The viscoelastic properties of HVFR were measured through the M5600 (Grace Instrument). The dosage ratio was 0.5, 1.0, 2.0, and 3.0 gal of HVFR per 1,000 in fresh water. Prior to the viscoelastic test, each sample was stirred to be completely dispersed in fluids for 30 minutes. In this experiment, the frequency was set at 0.5 to 3.0 Hz with 0.5 Hz increments, and the amplitude was 200 %. The viscoelastic properties were measured at room ambient. Figure 3 represents the elastic modulus (G') of HVFR in fresh water. The elastic modulus of the HVFR solution was increased with the increase of the HVFR dosage.

To illustrate, at a low dosage of HVFR (less than 1 gpt), the elastic modulus is almost zero, while increasing the dosage up to 3 gpt provides a strong elasticity profile above 5 dyn/cm². In addition, the elastic modulus of HVFR was increased with the test frequency. For example, G' increased from 1 dyn/cm² to almost 6 dyn/cm² by increasing the frequency from 0.5 Hz to 3 Hz, respectively.

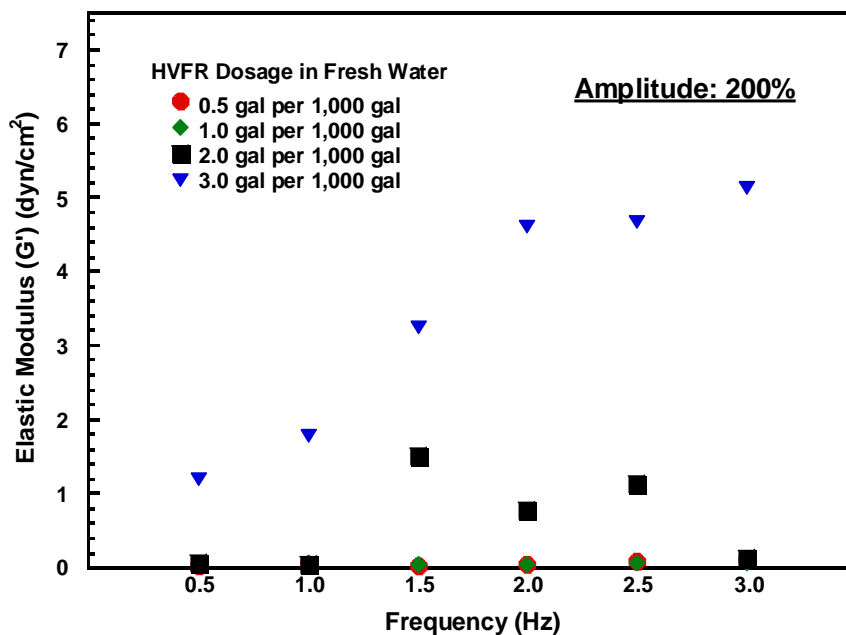


Figure 3. HVFR elastic property with various dosage in fresh water.

6.2. CONDUCTIVITY AND PERMEABILITY MEASUREMENT ON BASELINE, 0.5 GPT, AND 2.5 GPT.

Figure 4 represents the conductivity and permeability of the baseline, 0.5 gpt, and 2.5 gpt, depending on pressure and time. The measurement of the sample baseline means the reading of fluid conductivity and proppant permeability without HVFR. As adding 0.5 gal and 2.5 gal of HVFR per 1,000 gal of 2% KCl solution, the effect of HVFR was investigated. As shown in figure 1 (A-1,000 psi at 24 hr), the 0.5 gpt and 2.5 gpt samples

regained conductivity and permeability at about 95% and 93%, respectively, compared with baseline samples. At 2,000 psi in Figure 4 (B), the fluid conductivity and proppant permeability of 0.5 gpt showed quite close with the characteristic of baseline. As time goes in Figures 4 (C) and (D), shows that at 2,000 psi 0.5 gpt of HVFR contributed to improve the conductivity and permeability.

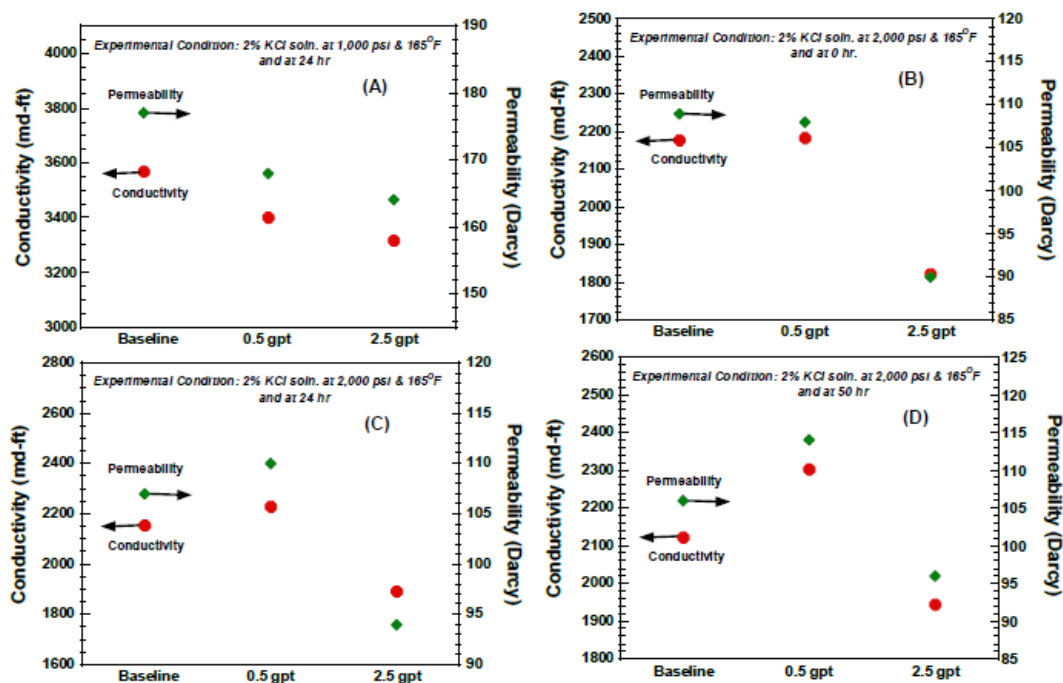


Figure 4. Conductivity and permeability on baseline, 0.5 gpt, and 2.5 gpt by pressure and time.

Table 4 represents the regain percentage of conductivity and permeability on samples, 0.5gpt and 2.5 gpt. The conductivity and permeability of 0.5 gpt at 2,000 psi for 24 & 50 hr. were great. 103 and 108 % on regaining permeability were more than what expected. In addition, the conductivity and permeability of 2.5 gpt look fine. The overall

regained percentage of 2.5 gpt was 83 to 93% in this conditional environment. The polymer chains in 2.5 gpt might interfere with conductivity and permeability.

Table 5. The regain percentage of 0.5 gpt and 2.5 gpt.

Stress, psi	Time (hr) @ stress	Conductivity (md-ft)/ Permeability (Darcy)			% Regain (Permeability)	
		Baseline	0.5 gpt	2.5 gpt	0.5 gpt	2.5 gpt
1,000	24	3568/177	3401/168	3317/164	95	93
2,000	0	2177/109	2183/108	1821/90	99	83
2,000	24	2153/107	2228/110	1890/94	103	88
3,000	50	2122/106	2304/114	1944/96	108	91

6.3. CASE STUDY: WOLFCAMP FORMATION, REEVES COUNTY, TX.

6.3.1. Geological Background. A well-H was located in the Wolfcamp formation in West Texas. The well depth was about 10,000 feet along the basin axis, and the lateral section was approximately 8,300 feet. The net pay thickness of Wolfcamp is about 1,000 feet to over 4,000 feet, and the average porosity is 7%. The maximum pressure was 9,800 psi, and the backside pressure was 2,000 psi. In this job, slick was employed as the base treatment fluid.

6.3.2. Fracture Design and Execution. Figure 5 shows a plot of the individual-stage fracturing treatment. In the early stages of the treatment, the pressure reached close to 9,600 psi which could be an indication of creating more fractured area while during the remainder of the process, the pressure was within the range of 7,200 psi and 8,600 psi. The proppant concentration was increased gradually from 0.5 ppg to 1.5 ppg with increasing the dosage of HVFRs from 0.50 gpt to 1 gpt. The fracture treatment was placed as the fracture design expectation. In the field trial, the low dosage of HVFRs (e.g., 1 gpt)

provided promising production results as well as reduction on the cost related to using HVFR.

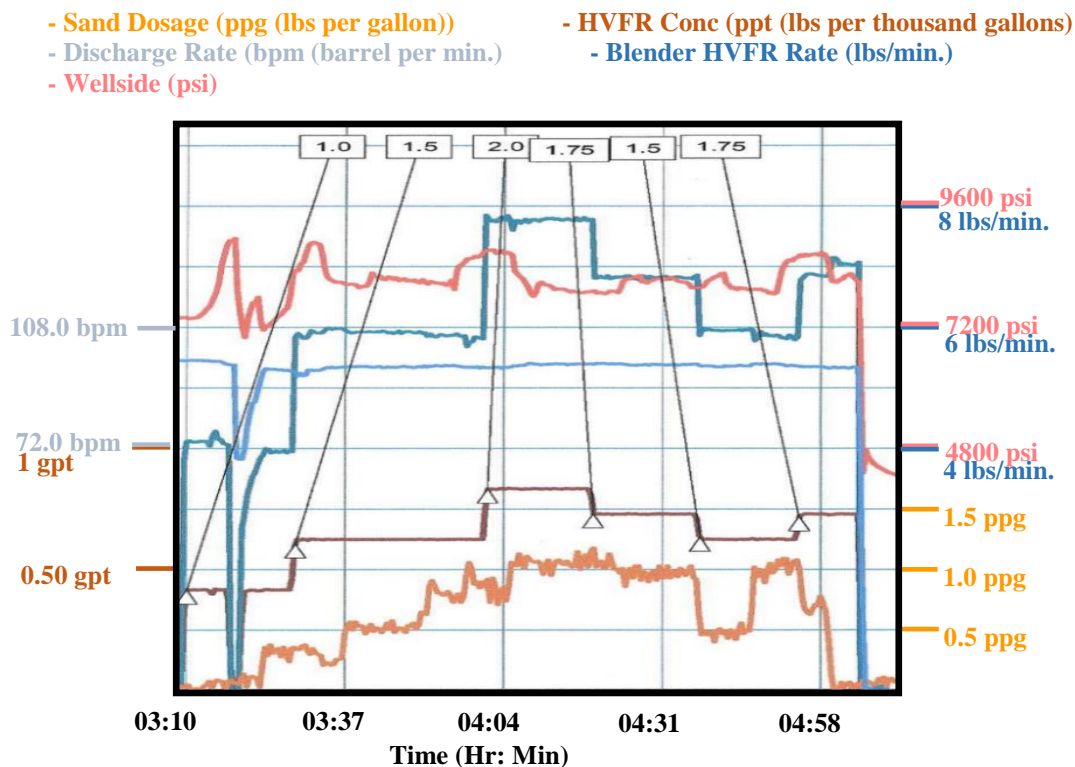


Figure 5. Hydraulic fracture treatment plot from Well-H using HVFRs.

Figure 6 represents real time data from Wolfcamp Well-H. Desirable pressure responded at the prop dosage 0.25 ppg, which entered the formation with 0.3 gpt. During operation, the dosage range of HVFR was increased from 0.3 gpt to 1 gpt. The upper pressure reached 9,400 psi; however, most of the operation was conducted between 7,200 psi and 8,600 psi. The prop amount was approximately 19,000 lbs per stage, and 100% of

the prop was placed in the formation. Compared to the cost of linear gel, using HVFR provided about 25-30% cost reduction.

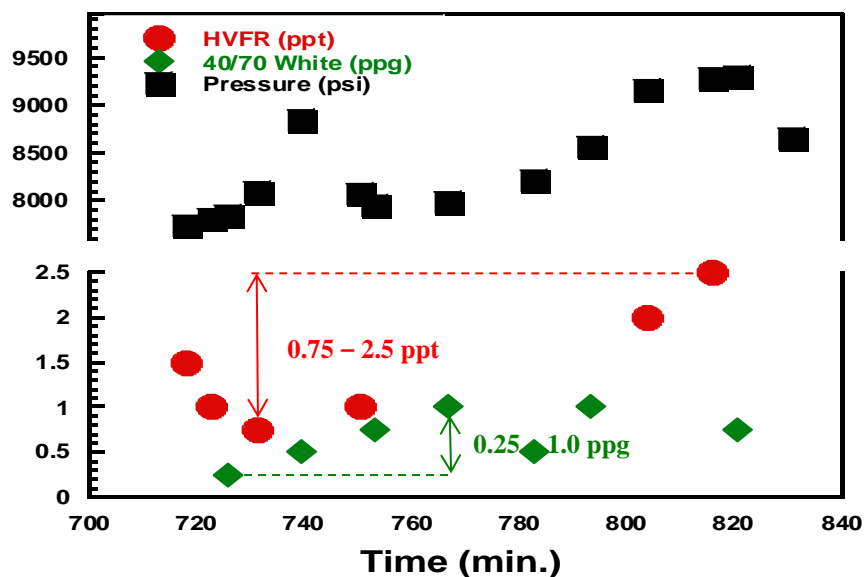


Figure 6. HVFR dosage real time data.

7. CONCLUSIONS

This paper provides a comprehensive review of formation damage caused by using fracture fluids. The formation damage mechanisms (e.g. chemical, mechanical, biological, thermal) and fracture damage categories were explained. After that, experimental work investigated the viscoelastic properties of HVFRs, and the potential of formation damage caused by using a new fracture fluid system (HVFRs) was determined. Finally, a field case study was discussed, including the advantages of utilizing HVFRs as an alternative fracture fluid system to the conventional fracture fluids such as linear gel. HVFRs were used

Successfully in the Wolfcamp formation causing production improvement and 25-30% cost reduction.

The viscoelastic property of high molecular weight (18 to 23 million) of HVFRs shows promising results on fracture conductivity and regained permeability. Through the conductivity and permeability test it was found that 0.5 gpt of HVFR did not affect the conductivity and permeability during the frac operation. Even the dosage of 0.5 gpt helped to improve fluid conductivity and proppant permeability with up to 108 % of regain at 2,000 psi and 165 °F for 50 hr, which is a remarkable finding. The high dosage of 2.5 gpt in the frac operation may initially hinder the conductivity and permeability due to polymer chains. However, the conductivity and permeability have gradually improved to 91% of regain as time goes on.

REFERENCES

- Aggour, T. M., & Economides, M. J. (1999, February 1). Impact of Fluid Selection on High-Permeability Fracturing. Society of Petroleum Engineers. <https://doi:10.2118/54536-PA>
- Ba Geri, M., Imqam, A., & Dunn-Norman, S. (2018, October 5). Proppant Transport Behavior in Inclined Versus Vertical Hydraulic Fractures: An Experimental Study. Society of Petroleum Engineers. doi:10.2118/191813-18ERM-MS
- Ba Geri, M., Imqam, A., & Suhail, M. (2019, March 15). Investigate Proppant Transport with Varying Perforation Density and its Impact on Proppant Dune Development Inside Hydraulic Fractures. Society of Petroleum Engineers. doi:10.2118/195018-MS
- Ba Geri, M., Imqam, A., & Flori, R. (2019a, April 8). A Critical Review of Using High Viscosity Friction Reducers as Fracturing Fluids for Hydraulic Fracturing Applications. Society of Petroleum Engineers. <https://doi:10.2118/195191-MS>

- Ba Geri, M., Imqam, A., Bogdan, A., & Shen, L. (2019b, April 8). Investigate the Rheological Behavior of High Viscosity Friction Reducer Fracture Fluid and Its Impact on Proppant Static Settling Velocity. Society of Petroleum Engineers. <https://doi:10.2118/195227-MS>
- Ba Geri, M., R. Flori, A. Imqam, L. Shen, & A. Bogdan. (2019c, June). Static Proppant Settling Velocity Characteristics in High Viscosity Friction Reducers Fluids for Unconfined and Confined Fractures. American Rock Mechanics Association.
- Ba Geri, M., Ellafi, A., Flori, R., Noles, J., & Kim, S. (2019f, October). Viscoelastic Characterization Effect of High-Viscosity Friction Reducers and Proppant Transport Performance in High-TDS Environment. Society of Petroleum Engineers. <https://doi:10.2018/196014-MS>
- Behr, A., Mtchedlishvili, G., Friedel, T., & Haefner, F. K. A. (2006, May 1). Consideration of Damaged Zone in a Tight Gas Reservoir Model with a Hydraulically Fractured Well. Society of Petroleum Engineers. <https://doi:10.2118/82298-PA>
- Bennion, D. B., Thomas, F. B., & Bietz, R. F. (1996, January 1). Low Permeability Gas Reservoirs: Problems, Opportunities and Solutions for Drilling, Completion, Stimulation and Production. Society of Petroleum Engineers. <https://doi:10.2118/35577-MS>
- Civan, Faruk, Reservoir Formation Damage: Fundamentals, Modeling, Assessment, and Mitigation. 2000
- Cooke, C. E. (1975, October 1). Effect of Fracturing Fluids on Fracture Conductivity. Society of Petroleum Engineers. <https://doi:10.2118/5114-PA>
- Davies, D. R., & Kuiper, T. O. H. (1988, May 1). Fracture Conductivity in Hydraulic Fracture Stimulation. Society of Petroleum Engineers. <https://doi:10.2118/17655-PA>
- Farah, N., Ding, D.-Y., & Wu, Y.-S. (2017, August). Simulation of the Impact of Fracturing-Fluid-Induced Formation Damage in Shale Gas Reservoirs. Society of Petroleum Engineers. <https://doi:10.2118/173264-PA>
- Galindo, T. (2019, January 29). Can Proppant Transport be Negatively Affected by Too Much Viscosity? Society of Petroleum Engineers. <https://doi:10.2118/194317-MS>
- Geri, M. B., Flori, R., & Sherif, H. (2019, July 25). Comprehensive Study of Elasticity and Shear-Viscosity Effects on Proppant Transport Using HFVRs on High-TDS Produced Water. Unconventional Resources Technology Conference. doi:10.15530/urtec-2019-99

- Geri, M. B., Ellafi, A., Ofori, B., Flori, R., & Sherif, H. (2019, July 31). Successful Implementation of High Viscosity Friction Reducers from Laboratory to Field Scale: Middle Bakken Case Study. Unconventional Resources Technology Conference. doi:10.15530/urtec-2019-447
- Gomaa, A. M., Gupta, D. V. S. V., & Carman, P. S. (2015, February 3). Proppant Transport? Viscosity Is Not All It's Cracked Up to Be. Society of Petroleum Engineers. <https://doi:10.2118/173323-MS>
- Han, Jiahang (2014). Hydraulic Fracture Damage Analysis in Tight Gas Reservoirs. PhD Dissertation.
- Hu, Y. T., Chung, H., & Maxey, J. E. (2015, February 3). What is More Important for Proppant Transport, Viscosity or Elasticity? Society of Petroleum Engineers. <https://doi:10.2118/173339-MS>
- Motiee, M., Johnson, M., Ward, B., Gradl, C., McKimmy, M., & Meeheib, J. (2016, February 1). High Concentration Polyacrylamide-Based Friction Reducer Used as a Direct Substitute for Guar-Based Borate Crosslinked Fluid in Fracturing Operations. Society of Petroleum Engineers. <https://doi:10.2118/179154-MS>
- Nasr-El-Din, H. A. (2003, January 1). New Mechanisms of Formation Damage: Lab Studies and Case Histories. Society of Petroleum Engineers. <https://doi:10.2118/82253-MS>
- Norman, L. R., Hollenbeak, K. H., & Harris, P. C. (1989, January 1). Fracture Conductivity Impairment Removal. Society of Petroleum Engineers. <https://doi:10.2118/19732-MS>
- Pope, D. S., Leung, L.W., Gulbis, J., & Constien, V. G. (1996, November 1). Effects of Viscous Fingering on Fracture Conductivity. Society of Petroleum Engineers. <https://doi:10.2118/28511-PA>
- Van Domelen, M., Cutrer, W., Collins, S., & Ruegamer, M. (2017, March 27). Applications of Viscosity-Building Friction Reducers as Fracturing Fluids. Society of Petroleum Engineers. <https://doi:10.2118/185084-MS>
- Voneiff, G. W., Robinson, B. M., & Holditch, S. A. (1996, November 1). The Effects of Unbroken Fracture Fluid on Gas Well Performance. Society of Petroleum Engineers. <https://doi:10.2118/26664-PA>
- Wang, Y., Holditch, S. A., & McVay, D. A. (2008, January 1). Simulation of Gel Damage on Fracture-Fluid Cleanup and Long-Term Recovery in Tight-Gas Reservoirs. Society of Petroleum Engineers. <https://doi:10.2118/117444-MS>

- Wang, J. Y., Holditch, S., & McVay, D. (2010, September 1). Modeling Fracture-Fluid Cleanup in Tight-Gas Wells. Society of Petroleum Engineers. <https://doi:10.2118/119624-PA>
- Yuan, B., Su, Y., Moghanloo, R.G., Rui, Z., Wang, W., Shang, Y., 2015. A new analytical multi-linear solution for gas flow toward fractured horizontal wells with different fracture intensity. J. Nat. Gas Sci. Eng. 23, 227e238

SECTION

3. CONCLUSIONS

This project evaluates the rheological characterization of HVFRs and investigates the compatibility of HVFRs with the Permian and Bakken produced water. Correlateing the friction reductions measurment on high-TDS produced water was also studied in produced water and fresh water as well. The obtained results from this experimental investigation provides new insights into the pressure reduction and proppant transport theories that leads to the developing conclusions as follows:

- HVFR indicated high viscosity values and heat resistant property among friction reducer samples.
- Based on viscosity values and well temperature by depth, HVFR has great proppant suspension and transportation capacity.
- HVFR showed a great elastic property helping proppant transportation.
- The high viscosity reading and elastic property of HVFR turned into a good fit in frac operation.
- Also, HVFR has other properties, such as high molecular weight, thermal stability, high regained conductivity, and permeability in frac operation, comparing other friction reducers.
- The Future of utilizing HVFR looks promising from a field test.

REFERENCES

- Acharya, A.R. 1988. Viscoelasticity of Crosslinked Fracturing Fluids and Proppant Transport. SPE Production Engineering 3: 483-488. SPE-15937-PA. <http://dx.doi.org/10.2118/15937-PA>.
- Adrian, R.J. 2005. Twenty Years of Particle Image Velocimetry. Experiments in Fluids 39 (2): 159-169. <http://dx.doi.org/10.1007/s00348-005-0991-7>.
- Ba Geri, M., Flori, R., Ellafi, A., Noles, J., Essman, J., Kim, S., & Alkamil, E. H. K. (2019, November 11). Correlated Friction Reduction and Viscoelastic Characterization of Utilizing the Permian Produced Water with HVFRs during Hydraulic Fracturing. Society of Petroleum Engineers. doi:10.2118/197748-MS
- Ellafi, A., Jabbari, H., Ba Geri, M., & Alkamil, E. (2019, November 11). Can HVFRs Increase the Oil Recovery in Hydraulic Fractures Applications? Society of Petroleum Engineers. doi:10.2118/197744-MS

VITA

Mohammed Salem Ba Geri was born in Hadramout, Yemen. He received his bachelor's degree in Petroleum Engineering from Hadramout University of Science and Technology, Yemen in 2007. He was awarded a fully funded scholarship from Hadramout Establishment for Human Development (HEHD) to obtain his master's degree in Saudi Arabia 2010.

Mohammed worked for one year at University of Salford Manchester from 2013 to 2014. Then he worked at Ministry of Oil & Minerals in Yemen as a reservoir engineer from 2014 to 2016. He was awarded a fully funded scholarship from Hadramout Establishment for Human Development (HEHD) to obtain his PhD degree in USA in 2017. He received a PhD in Petroleum Engineering from Missouri University of Science and Technology, Rolla, MO, in December 2019.

Ba Geri was a member of Society of Petroleum Engineers (SPE). He served as a volunteer with the SPE since 2010. The field of his research: evaluate high viscosity friction reducers on proppant transport and formation damage. His area of interest: stimulations/hydraulic fracturing, well completions, unconventional reservoirs, and production engineering. He had several research papers in proppant transport, high viscosity friction reducer's evaluation, unconventional shale reservoirs, and tight gas.